MND-P-3003

THIS DOCUMENT CONSISTS OF 130 PAGES

NO. 40 OF 100 COPIES, SERIES A

RADIOISOTOPE FUELED AUXILIARY POWER UNIT

QUARTERLY PROGRESS REPORT

NUMBER 6

APRIL 1958-JULY 1958

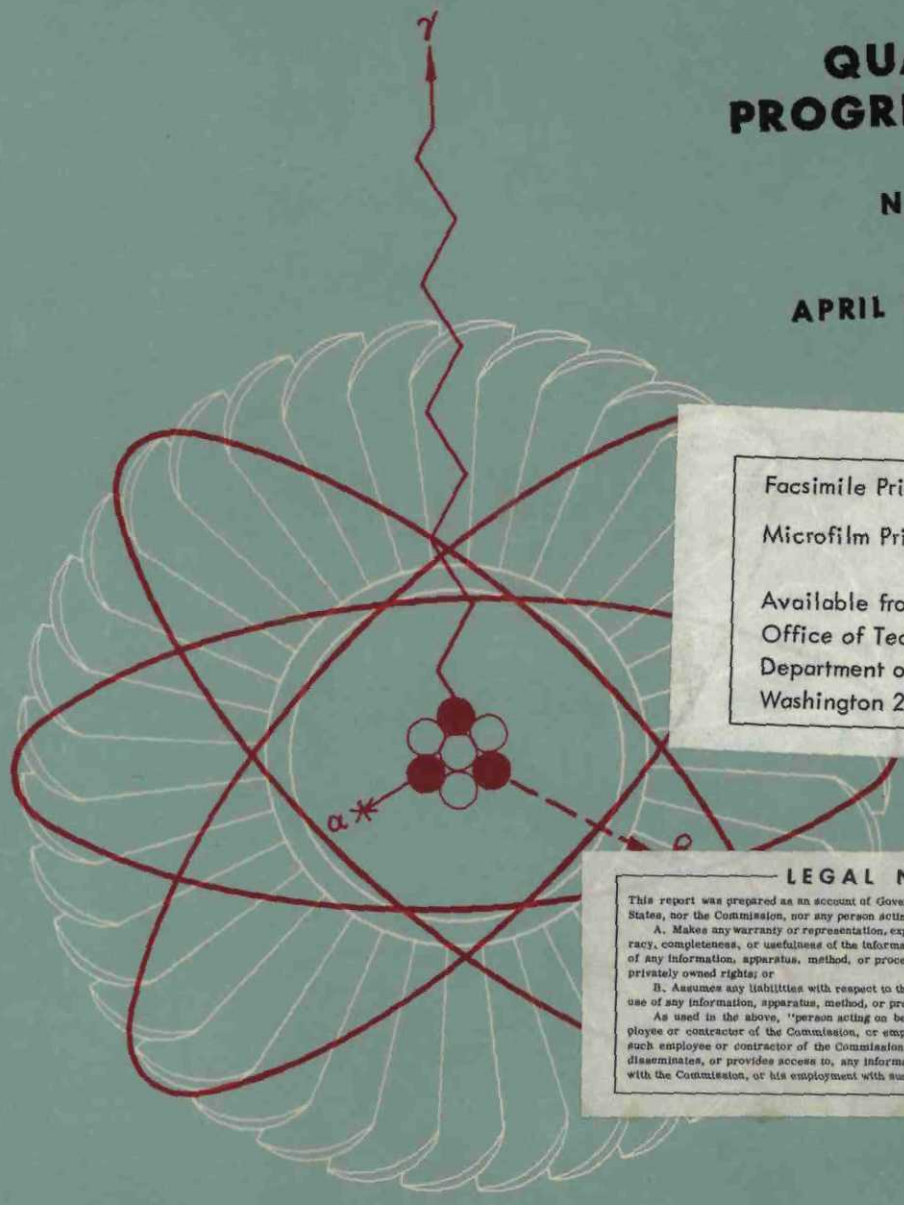

MARTIN

DISCLAIMER

SECRET

NOTICE: This document contains information affecting the National Defense of the United States within the meaning of the Espionage Laws, Title 18, U.S.C., Sections 793 and 794. Its transmission or the revelation of its contents in any manner to an Unauthorized Person is prohibited by Law.

DEFENSE INFORMATION

This document contains information affecting the National Defense of the United States within the meaning of the Espionage Laws, Title 18, U.S.C., Sections 793 and 794, the transmission or violation of which in any manner to an unauthorized person is *prohibited by law.*

SECRET

~~SECRET~~

UNCLASSIFIED

"~~Special Distribution~~"

This report is prepared under contract AT(30 3) 217 with the United States Atomic Energy Commission

RADIOISOTOPE FUELED AUXILIARY POWER UNIT

QUARTERLY PROGRESS REPORT NUMBER 6

APRIL 1958 - JULY 1958

APPROVED BY Kenneth P. Johnson
Project Engineer

Classification changed to UNCLASSIFIED
by authority of Asst. Chief, Declassification Branch
J.C.R. Denow 12-4-62.

Research & Development

C-83

MND-P-3003

1

DEFENSE INFORMATION

This document contains information affecting the National Defense of the United States within the meaning of the Espionage Laws, Title 18, U.S.C., Sections 793 and 794, the transmission or violation of which in any manner to an unauthorized person is prohibited by law.

MARTIN
BALTIMORE

UNCLASSIFIED

~~SECRET~~

LEGAL NOTICE

This report was prepared as an account of Government sponsored work. Neither the United States, nor the Commission, nor any person acting on behalf of the Commission:

A. Makes any warranty or representation, express or implied, with respect to the accuracy, completeness, or usefulness of the information contained in this report, or that the use of any information, apparatus, method, or process disclosed in this report may not infringe privately owned rights; or

B. Assumes any liabilities with respect to the use of, or for damages resulting from the use of any information, apparatus, method, or process disclosed in this report.

As used in the above, "person acting on behalf of the Commission" includes any employee or contractor of the Commission to the extent that such employee or contractor prepares, handles or distributes, or provides access to, any information pursuant to his employment or contract with the Commission.

FOREWORD

This sixth quarterly progress report covers the development work under way on the SNAP-I program. It is submitted by The Martin Company in compliance with Contract AT(30-3)-217 to cover the period from 1 April to 30 June, 1958.

Under a subcontract to The Martin Company, Thompson Products, Incorporated, Cleveland, Ohio, has been carrying forward the development of power conversion equipment as outlined herein.

DISTRIBUTION LIST FOR 3215

		Copy No.
1.	Air Force Ballistic Missile Division Commander, Air Force Ballistic Missile Division Hq., Air Research and Development Command, USAF P. O. Box 262 Inglewood, California For: Major George Austin	1
2.	Air Research and Development Command Commander, Air Research and Development Command Andrews Air Force Base Washington 25, D. C. Attn: RDTAPS, Capt. W. G. Alexander	2
3.	Army Ballistic Missile Agency Commanding General Army Ballistic Missile Agency Redstone Arsenal, Alabama Attn: ORDAB-c	3,4
4.	Atomic Energy Commission, Washington U. S. Atomic Energy Commission Technical Reports Library Washington 25, D. C. Attn: Mrs. J. M. O'Leary	
	For: Lt. Col. G. M. Anderson, DRD	5
	Capt. John P. Wittry, DRD	6
	Lt. Col. Robert D. Cross, DRD	7
	R. G. Oehl, DRD	8
	Edward F. Miller, PROD	9
	Technical Reports Library	10
5.	Atomics International Atomics International Division of North American Aviation, Inc. P. O. Box 309 Canoga Park, California Attn: Dr. Chauncey Starr For: J. Wetch	11
6.	Bureau of Aeronautics Chief, Bureau of Aeronautics Washington 25, D. C. Attn: C. L. Gerhardt, NP	12

Copy No.

7. Bureau of Ordnance
Chief, Bureau of Ordnance
Dept. of the Navy, Room 4110 Main Navy Bldg.
Washington 25, D. C.
Attn: Mrs. Maryle R. Schmidt or Laura G. Myers (To be opened by addressee only)
For: Ren 13
SP 14

8. Bureau of Ships 15
Chief, Bureau of Ships
Code 1500
Department of the Navy
Washington 25, D. C.
Attn: Melvin L. Ball

9. Canoga Park Area Office 16
U. S. Atomic Energy Commission
Canoga Park Area Office
P. O. Box 591
Canoga Park, California
Attn: A. P. Pollman, Area Manager

10. Chicago Operations Office 17,18
U. S. Atomic Energy Commission
Chicago Operations Office
P. O. Box 59
Lemont, Illinois
Attn: A. I. Mulyck
For: T. A. Nemzek
Mr. Klein

11. Chief of Naval Operations 19
Office of the Chief of Naval Operations
Department of the Navy
Washington 25, D. C.

12. Department of the Army 20
Atomic Division
Office of Chief of Research and Development
Department of the Army
Washington 25, D. C.

13. Diamond Ordnance Fuse Laboratories 21,22,23
Commanding Officer
Diamond Ordnance Fuse Laboratories
Washington 25, D. C.
Attn: ORDTL 06.33, Mrs. M. A. Hawkins

Copy No.

14. Hanford Operations Office — 24
U. S. Atomic Energy Commission
Hanford Operations Office
P. O. Box 550
Richland, Washington
Attn: Technical Information Library

15. Lockheed Aircraft Corporation — 25,26
Asst. AF Plant Representative
Missile Systems Division
Lockheed Aircraft Corporation
P. O. Box 504
Sunnyvale, California
For: John H. Carter

16. Mound Laboratory — 27
Monsanto Chemical Company
Mound Laboratory
P. O. Box 32
Miamisburg, Ohio
Attn: Library and Records Center
For: Mr. Roberson

17. National Advisory Committee For Aeronautics, Ames — 28
National Advisory Committee for Aeronautics
Ames Aeronautical Laboratory
Moffett Field, California
Attn: Smith J. de France, Director

18. National Advisory Committee For Aeronautics, Langley — 29
National Advisory Committee for Aeronautics
Langley Aeronautical Laboratory
Langley Field, Virginia
Attn: Henry J. E. Reid, Director

19. National Advisory Committee For Aeronautics, Lewis — 30
National Advisory Committee for Aeronautics
Lewis Flight Propulsion Laboratory
21000 Brookpark Road
Cleveland 35, Ohio
Attn: George Mandel

Copy No.

20. Naval Ordnance Laboratory — 31,32,33
Commander, U. S. Naval Ordnance Laboratory
White Oak, Silver Spring, Maryland
Attn: Eva Lieberman, Librarian

21. Naval Research Laboratory — 34
Director, Naval Research Laboratory, Code 1572
Washington 25, D. C.
Attn: Mrs. Katherine H. Cass

22. New York Operations Office — 35
U. S. Atomic Energy Commission
New York Operations Office
70 Columbus Avenue
New York 23, New York
Attn: Document Custodian

23. Oak Ridge National Laboratory — 36
Union Carbide Nuclear Company
X-10, Laboratory Records Department
P. O. Box X
Oak Ridge, Tennessee
Attn: Eugene Lamb

24. Office Of Naval Research — 37
Office of Naval Research
Department of the Navy, Code 735
Washington 25, D. C.
Attn: E. E. Sullivan
For: Code 429

25. Project Rand — 38
Director, USAF Project Rand
Via AF Liaison Office
The Rand Corporation
1700 Main Street
Santa Monica, California
Attn: F. R. Collbohm
For: Dr. John Huth

26. Rome Air Development Center — 39
Commander, Rome Air Development Center
Griffiss Air Force Base, New York
Attn: RCSG, J. L. Briggs

		Copy No.
27.	Technical Information Service Extension U. S. Atomic Energy Commission Reference Branch Technical Information Service Extension P. O. Box 62 Oak Ridge, Tennessee	40 through 64
28.	Thompson Products, Inc. Thompson Products, Inc. Staff Research and Development New Devices P. O. Box 1610 Cleveland 4, Ohio Attn: C. G. Martin	65,66,67
29.	University of California Radiation Laboratory University of California Radiation Laboratory Technical Information Division P. O. Box 808 Livermore, California Attn: Clovis G. Craig For: Dr. Hayden Gordon	68
30.	Wright Air Development Center Commander, Wright Air Development Center Wright-Patterson Air Force Base, Ohio Attn: WCACT For: Capt. Clarence N. Munson, WCLPS G. W. Sherman, WCLEE WCOSI	69 70 71,72

CONTENTS

CONTENTS (Cont'd)

CONTENTS (Cont'd)

ILLUSTRATIONS

ILLUSTRATIONS (Cont'd)

TABLES

SUMMARY

During the quarter ending June 30, developmental effort has continued on components and general system design of the SNAP I Auxiliary Power Unit. Tests were run on the boiler and components in the power conversion system. Results are summarized and organized by task as presently defined by contract to the USAEC.

TASK I - OVER-ALL SYSTEM DESIGN

As a result of coordination with Lockheed and a review of ground handling procedures connected with SNAP-I, a modular concept has evolved. In essence, this concept is one of fabricating the SNAP-I in one complete package which can be readily attached to the WS-117L vehicle structure. This permits testing of the SNAP-I as a complete module prior to assembly into the WS-117L and reduces installation problems.

The Martin Company was requested to participate, as a part of the facilities committee, in recommending a site at Camp Cooke. Recommendations were made and a report prepared.

An integrity test program subjecting bare fuel elements at 1500 degrees Fahrenheit to burning and explosive conditions simulating launch pad aborts was concluded with positive results during this period.

TASK II - BOILER DEVELOPMENT PROGRAM

Heat transfer experiments were conducted on a full-scale boiler mock-up to check the adequacy of the boiler design in producing mercury vapor at the design point. In order to prevent slugging through the boiler, it was necessary, as a result of these experiments, to redesign the boiler coil to provide separation of liquid and the vapor. Experiments were again conducted with positive results. (Mercury vapor was produced at a flow rate of two pounds per minute and a temperature of 1350 degrees Fahrenheit.)

TASK III - FUEL ELEMENT DEVELOPMENT PROGRAM

Development work continued on determining the sintering properties of the CeO_2 with impurities as reported in the latest experimental results from ORNL. It has been necessary to provide more room in the fuel element because of a higher level of impurity present than had originally been anticipated by ORNL. The diameter of the fuel element was changed from 3 1/2 inches to 4 1/8 inches. This change in fuel element design will provide for the worst case because it is anticipated that the impurity level will be reduced by ORNL during the course of the program.

TASK IV - MATERIALS CORROSION PROGRAM

Dynamic mercury corrosion tests were conducted during this period on Croloy 5 Si and Croloy 5 Ti. These materials were selected because they are used in stationary power plants with mercury as a working fluid. The loops failed after 150 hours of operation, which indicates that it will be necessary to expand the materials development effort in order to provide a satisfactory APU design. Static lead corrosion tests continued on CeO_2 pellets, brazed joints, and flame sprayed coatings. New inputs from ORNL indicate that much of the CeO_2 work will have to be redone. Positive results are being obtained in establishing compatibility between inhibited lead, brazed joints, and molybdenum coatings.

TASK V - POWER CONVERSION SYSTEM

Turbine

Preliminary runs were made in mercury on the first turbine alternator test package during the month of June. A bearing failure made it necessary to stop the test.

Pump

Many centrifugal pump types were tested during this past quarter. A jet-boosted centrifugal pump attained the design performance required (15 pounds flow per minute, 270 psia discharge pressure, 1.86 psia inlet pressure). The efficiency of this pump was approximately 20 per cent.

Controls

During this quarter, extensive breadboard testing of control components was conducted, and the results of the these tests have been factored into the design of prototype components. Investigations of start and stop procedures were also conducted.

Alternator

A radial gap alternator was designed, fabricated, and tested. The alternator under test was uncanned and merely gave data on electrical characteristics.

Bearings

Several configurations of the hydrosphere bearing were tested and indications are that a nongrooved socket configuration is most desirable for maximum radial load capacity.

Materials Evaluation

One-hundred-hour tests were conducted on 1010 steel and Type 446 stainless steel. These tests were made in isothermal loops at a temperature of 750 degrees Fahrenheit and showed little evidence of corrosion.

TASK VI - GROUND TEST

Design work is under way to prepare a facility for testing the APU module. Equipment requirements have been determined and orders placed for equipment wherever possible.

TASK VII - SNAP III

During this period a conceptual design for the SNAP III Unit was delineated and coordinated with Westinghouse and contract arrangements completed. SNAP III will be an APU having a one-watt power output and employing a thermoelectric power conversion system. A demonstration model will be ready early in the calendar year 1959. This model may be fueled with Po-210.

I. TASK I - OVER-ALL SYSTEM DESIGN PROGRAM

A. SNAP-I SYSTEM INTEGRATION

A new concept for the handling and testing of SNAP-I has been proposed. The basic principle in this new concept is that the entire SNAP-I system will be constructed as an integral module that becomes a part of the WS-117L vehicle. There are only four points of structural attachment between the SNAP-I module and the vehicle.

After assembly at The Martin Company the module is tested, shipped, stored, and integrated into the vehicle as a single entity. It is then possible to join the SNAP-I components together under laboratory conditions and thus minimize the possibility of contamination of the working fluid loop. Complete system checking prior to shipment and use is also feasible by means of the modular concept. In general, the advantage of the SNAP-I modular concept is that it moves assembly and test procedures from the field into the laboratory and plant.

One view of a preliminary design of the SNAP-I module integrated into a preliminary vehicle design is shown in Fig. 1 . The vehicle integration is proceeding in a somewhat unique manner. Lockheed Missile Systems Division (LMSD), the vehicle prime contractor, has furnished The Martin Company a drawing with the outlines of the predominant features of the aft portion of a vehicle that will employ the SNAP-I system. (LMSD has stated that the vehicle to employ SNAP-I will have to be especially designed for that purpose, and that this design will progress as the SNAP-I integration proceeds.) Martin designers then fitted the SNAP-I module into this vehicle, and proposed some vehicle changes in order to accomplish this.

The integration drawing (a part of which is shown in Fig. 1) was then forwarded to LMSD for comment. The LMSD designers prepared a drawing including counter-proposals for vehicle changes suggested by Martin, as well as additional aspects of vehicle design and proposed changes in the SNAP-I module design. Martin design personnel will evaluate the LMSD proposals and changes, make counter-proposals, include advanced SNAP-I design details and forward a drawing, incorporating these ideas, to LMSD. This process will continue until the integrated design is satisfactory to both organizations.

A pre-flight testing plan for the SNAP-I module at the flight site has been proposed and will be coordinated with LMSD. This is the first step in achieving agreement on a factory-to-flight sequence and launch site facilities.

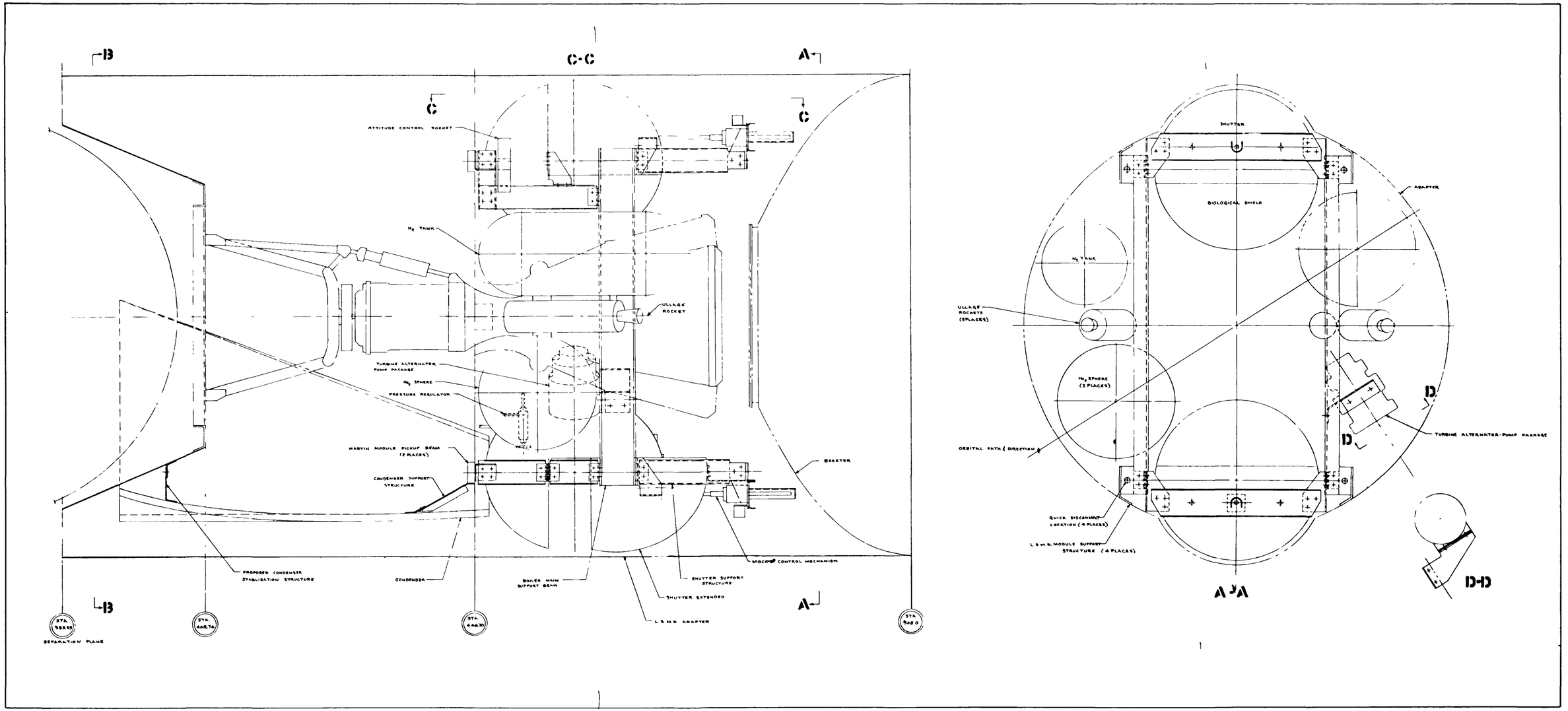

Fig. 1. SNAP I Integration - Module Concept - Modification-2

It has been learned that the Atlas booster cannot structurally support the combined load of the fueled WS-117L vehicle and the SNAP-I module with its biological mercury installed. It appears that the biological mercury will have to be drained from the shield before the vehicle fuel is loaded. This will cause increased dosage at the film pack due to the longer time available for gamma-ray air scatter. LMSD is investigating this problem.

1. Proposed Pre-Flight Testing of SNAP-I Module at Flight Site

The use of SNAP-I requires Lockheed to consider the testing of their auxiliary power system (APS) in two separate parts. They are:

1. SNAP-I - including heat source, power conversion component (to 2000 cycles per second, single phase) and associated components;

2. Power Converter Equipment (PCE) - including transformers, rectifiers, batteries, inverters, load switching devices, etc.

Preliminary testing of SNAP-I at the assembly site and the power converter equipment (PCE) at Lockheed (or the flight site) should be accomplished separately. This means that a simulator for the PCE and a controllable 2000-cycle per second, single phase generator will be needed at these locations. These two portions of the APS can be mated electrically during the test of the SNAP-I module at the flight site. Further testing of vehicle components or payload requiring vehicle auxiliary power prior to flight can be accomplished by use of the previously mentioned generator.

The final APS test must be accomplished prior to flight time, after the mercury is drained from the biological shield. This can be a programmed automatic go-no-go test similar to that described in Section IV-3 of LMSD-2870.

The test of the SNAP-I module prior to launch pad operation should be accomplished in a shielded chamber several days before flight. The choice of using a PCE simulator or the actual flight PCE units is up to LMSD. If the PCE flight units are to be used they should be checked out before this time, and they need not be in the shielded chamber since only electrical connections are required. If special cooling is required for the chamber, the exact needs will be determined after the Martin Ground Test. It is anticipated that the following tests of the SNAP-I module will be accomplished by Lockheed personnel with the assistance of Martin engineers and those of their subcontractors:

1. Time required to drain mercury;

2. Time required for boilers to come up to temperature;

3. Measure unshielded dose rate at one or more points for each boiler;

4. Start-up time
After start-up, measure following parameters of electrical output under simulated vehicle load (transformer, rectifier, load resistor) or actual flight PCE:

   a. Voltage at input to transformer,
   b. Current in generator circuit,
   c. Frequency in generator circuit, including harmonic content,
   d. Introduce load variations and record change in (a) (b) and (c);

5. Tape record vibration at module pick-up points;

6. Record the following during all tests:

   a. Shutter position,
   b. Boiler outlet temperature (using sensing and amplifying units in shutter control mechanism),
   c. Condenser temperature (several points),
   d. Subcooler temperature,
   e. Temperature of outer shell of biological shield,
   f. Temperature at vehicle pick-up location.

B. OPERATIONAL HAZARDS

1. Launch Site Recommendation

The Lockheed Missile Systems Division requested The Martin Company, as part of the Facilities Committee, to appraise three specific launch sites at Camp Cooke in regard to APU considerations. A recommendation was made after evaluating the following factors:

Locations of Sites. - Site 1 is located in the northwest corner of the Camp Cooke Military Reservation. Site 2 is located in the west-central portion of Camp Cooke. Site 3 is located in the south-central area of the Camp Cooke Military Reservation;

Seismological Criteria. - Each site was evaluated in terms of foundation material, nearby faults, and past seismic history. Several known past seismic disturbances of significance occurred in proximity to Sites 2 and 3. It was recommended that a known fault south of Site 3 be investigated;

Meteorological Criteria. - Meteorological factors were weighed lightly since they would have only a minor effect upon the APU, and it is apparent that they do not fluctuate significantly from site to site;

Hydrological Criteria. - The hydrologic criteria considered were the proximity of sites to ground water reservoirs, surface reservoirs, and watershed areas;

Geological Criteria. - Geological factors, in particular rock hardness, topography, and stratography were considered. These factors were related to the recovery of the APU following vehicle launch abort and impact;

Range Safety. - Range safety is influenced by the time increment that the vehicle is over or adjacent to the coastal area;

Population Criteria. - Base and off-base population density and distribution were considered;

Public Transportation. The proximity of the Southern Pacific Railroad and off-site public transportation routes was considered.

The sites were rated by a system utilizing these criteria, weighing the relative value of each criterion, and integrating the value of individual sites for each criterion. On this basis, Site 3 was recommended as the most favorable site in regard to the APU.

2. Re-Entry Evaluation Study

A re-entry evaluation study was initiated to determine the post-orbit environment of the APU, and in particular the conditions of impact. The secondary purpose of the study is to establish parameters for rocket sled and plasma jet testing. Specifically the study is to yield the following information:

Velocity Spectrum. - The velocity spectrum of the SNAP-I during re-entry and including impact is being estimated for various entrance flight path angles. Aerodynamic drag factors and terminal velocities are being estimated;

Aerodynamic Heating. - The effects of aerodynamic heating upon the component including component temperatures, stagnation points, heat input, and heat loss are being estimated. The component temperature at impact is being predicted;

Evaluation. - The combined effects of velocity, aerodynamic heating and drag, and mechanical forces acting upon SNAP-I are being analyzed. A prediction of the portions of the component surviving re-entry and present at impact is being made.

An IBM 704 Program is utilized in the study in order to relate the multiplicity of variables involved.

3. Core Integrity Test Program

Model Missile Tests. - This testing program was carried out under contract with the Broadview Research Corporation, Burlingame, California, between May 5 and June 30, 1958. A final report by Broadview analyzing the results of this program is being prepared.

The objective of this program is to determine core integrity under conditions existing during an Atlas booster launch failure. Such integrity was determined by observing the effects upon scale model test assemblies and their protective coatings when they were exposed to scale model missile failures. The following is a preliminary description of the test performed on the grounds of Beale Air Force Base, California.

a. 1/18 Model Missile Tests

1. With 1/2 Scale Model Cores

The model missile containing simulated fuel loading of liquid oxygen and kerosene was set up. At the same time the model core was held at 1500 degrees Fahrenheit in an electric furnace. Successively, the fuel bags were ripped, the core was transferred into the fuel mixture, and the mixture was detonated.

Ten tests were performed. The test variables were protective coating types, amount of pretest core damage, and detonation time.

(a) Chromalloy coated cores - Two cores were tested with undamaged coatings.

(b) Colmonoy coated cores - Four cores were tested with undamaged coatings.

(c) Colmonoy coated cores - Two cores were tested. The pretest damage on each one was light.

(d) Colmonoy coated cores - Two cores were tested. The pretest damage on each one was heavy.

One undamaged Colmonoy coated core was tested in two separate missile failures. Cores were pre-damaged in a manner to simulate coating failures that might be caused from launch pad impact.

None of the cores sustained significant physical or chemical damage from the exploding liquid oxygen-kerosene mixture. The surfaces exposed by pre-test damage showed some rapid oxidation which stopped soon after the detonation. It appeared that this reaction was arrested by a coating of molybdenum oxide which smothered the reacting surface.

2. With 1/3 Scale Model Cores

Two undamaged 1/3 scale cores were tested by the same experimental procedure. No significant physical or chemical damage was present on either core following the detonation.

3. With 1/6 Scale Model Cores

Two model missile failure tests were accomplished. The procedure was changed so that each test contained three undamaged cores. On the first detonation all three cores were found with no significant physical or chemical deformation. In the second failure only two cores were found, both were undamaged. The third core was ejected from the fireball and was not found.

b. 1/10 Model Missile Cores

1. With 1/3 Scale Model Cores

One 1/10 model missile failure test was accomplished. It contained two undamaged Colmonoy coated cores. Neither core sustained any significant physical or chemical damage.

2. With 1/2 Scale Model Cores

Two 1/10 model missile failures were accomplished. One detonation included one undamaged core and one heavily damaged core. The other missile failure included two undamaged cores. All cores were coated with Colmonoy.

None of the cores sustained significant damage. The damaged surface exposing molybdenum metal exhibited rapid oxidation immediately following the detonation which was quickly arrested by molybdenum oxide formation.

Molybdenum-Liquid Oxygen Tests. - The reaction between liquid oxygen and hot elemental molybdenum is obscure. During the month of June the Broadview Research Corporation initiated a test program under a Martin subcontract to investigate this reaction.

Specifically, the experiments consist of the following four parts:

a. Molybdenum Wire-Liquid Oxygen Reaction

In this experiment electrically heated molybdenum is immersed in liquid oxygen at three given temperatures between 1400 and and 2100 degrees Fahrenheit.

b. Colmonoy Coated Molybdenum Strip-Liquid Oxygen Reaction

In this experiment reactions between coated molybdenum strips and liquid oxygen are performed. The strips are electrically heated. Test specimen temperatures and coating damage are varied.

c. Colmonoy Coated Molybdenum Test Assembly-Liquid Oxygen Reaction

Experiments are performed by immersing hot test assemblies in liquid oxygen. Damaged and intact coatings are tested.

d. Molybdenum Test Assembly-Liquid Oxygen Reaction

In this experiment five uncoated molybdenum test assemblies are immersed in liquid oxygen at selected assembly temperatures between 1400 and 2100 degrees Fahrenheit.

C. SYSTEM SHIELDING

Preliminary computations were made to determine the vehicle shielding required if the material were to be placed in the vicinity of the boiler. In order to limit the dosage to 50 roentgens at the film pack after 60 days, about five inches of tungsten are required on top of each molybdenum block and 1 1/4 inches around the sides.

Two sets of calculations were made as the result of requests at the SNAP Coordination Committee meeting. The results are shown in Figs. 2 and 3.

Figure 2 shows dose rates versus distance from the launching vehicle. The values are for two half-power boilers with the biological shield mercury removed, and include the effect of self-absorption in the source, air absorption and air scattering.

Figure 3 gives a comparison of dose rates and weight of a single half-power boiler containing 5×10^5 curies with different outer container sizes for the biological shield. The shield is filled with mercury. The dose rates are at a distance of two feet from the center of the outer container (roughly one foot from the surface) and for each 15 degrees of arc. Each succeeding container is one-half inch larger than the preceding. The chart includes data for a new boiler design (designated Rev. 1). This new design was necessitated by new specific activity data received from Oak Ridge National Laboratory. The separated fission products will contain more impurities than were originally anticipated. Consequently, the boiler had to be made slightly larger, reducing the thickness of biological shield available in the total volume.

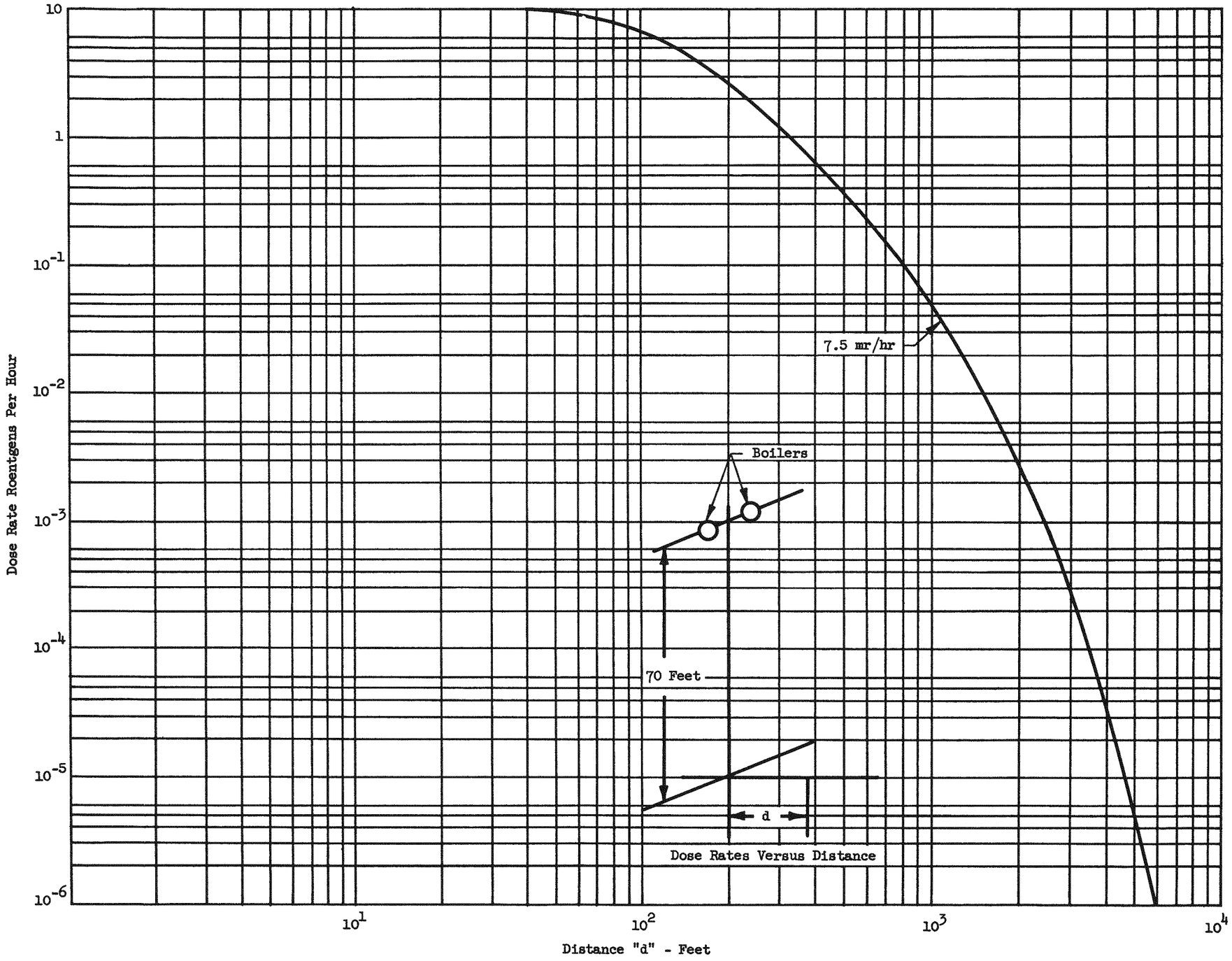

Fig. 2. Dose Rate versus Distance from Launching Vehicle

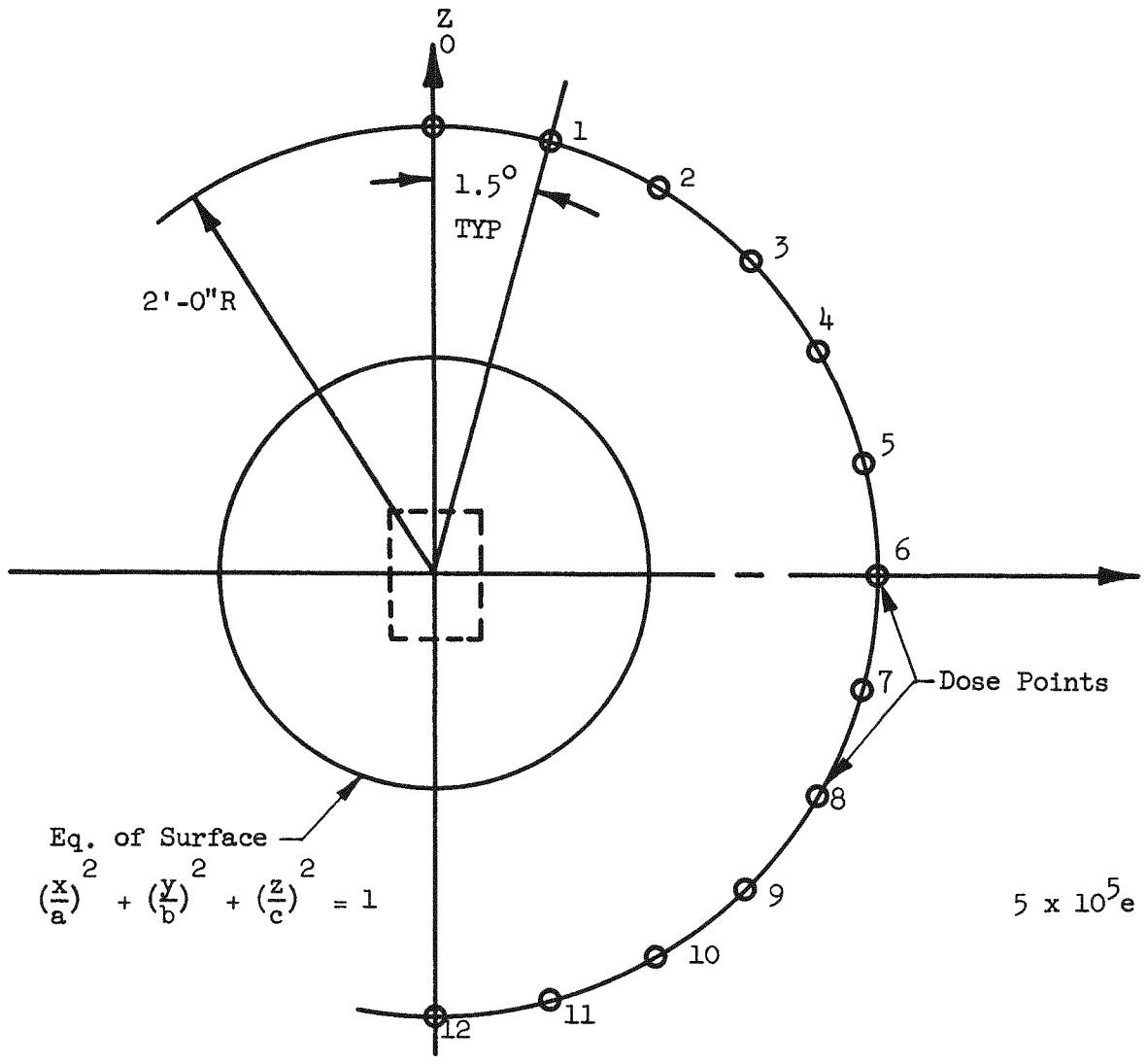

Surface Constants					Present Design Surface					
a	10"		10.5"		11"		11.5"		12"	
b	10"		10.5"		11"		11.5"		12"	
c	11"		11.5"		12"		12.5"		13"	
Calculated Weight With Mercury (Pounds)	Orig. 2230	Rev.1 2222	Orig. 2575	Rev.1 2566	Orig. 2953	Rev.1 2943	Orig. 3365	Rev.1 3356	Orig. 3814	Rev.1 3805
Dose Point					Dose Rates R/HR					
0	0.211	0.235	0.100	0.112	0.048	0.053	0.023	0.025	0.011	0.012
1	0.239	0.277	0.113	0.132	0.054	0.063	0.026	0.030	0.012	0.014
2	0.328	0.411	0.155	0.195	0.074	0.093	0.036	0.044	0.017	0.021
3	0.399	0.539	0.190	0.256	0.090	0.122	0.043	0.058	0.021	0.028
4	0.367	0.531	0.175	0.052	0.083	0.120	0.033	0.057	0.018	0.027
5	0.305	0.459	0.114	0.218	0.069	0.104	0.033	0.049	0.016	0.024
6	0.275	0.417	0.131	0.198	0.063	0.094	0.030	0.045	0.018	0.021
7	0.278	0.419	0.132	0.199	0.063	0.095	0.030	0.045	0.015	0.022
8	0.308	0.449	0.147	0.214	0.070	0.102	0.033	0.048	0.016	0.023
9	0.332	0.448	0.158	0.213	0.075	0.101	0.036	0.048	0.017	0.023
10	0.274	0.343	0.131	0.163	0.062	0.077	0.030	0.037	0.013	0.017
11	0.190	0.220	0.090	0.104	0.043	0.050	0.021	0.024	0.010	0.011
12	0.164	0.182	0.078	0.087	0.037	0.041	0.017	0.020	0.009	0.0094

Fig. 3. Comparison of Dose Rates from Original Boiler and Boiler Revision No. 1

II. TASK II - BOILER DEVELOPMENT PROGRAM

Task II covers the design, fabrication, test, and operation of the half-power boiler. Progress during this quarter has been directed toward the operation of the full-power boiler mock-up test loop, plus the redesign of this loop for later operations with the half-power boiler. In addition, a new half-power boiler was being fabricated for future testing in the mock-up test loop. Further details concerning the progress of these items are presented in this chapter.

A. HEAT TRANSFER MOCK-UP TEST

Full-power boiler mock-up experiments were conducted during April and May. These tests consisted of circulating mercury through the electrically heated full-power boiler mock-up to produce superheated mercury vapor at various flow rates. Some difficulties were encountered in obtaining the proper design conditions with the 25-foot length of boiler coil, and the tests were terminated in May after operating for 360 hours. The maximum mercury superheat realized was 1120 degrees Fahrenheit at 210 psia; whereas the design point is 1350 degrees Fahrenheit at 210 psia.

From the operating experience and data gained, the following conclusions could be drawn:

1. Additional heat transfer area was required to attain design conditions (1.87 pounds per minute at 1350 degrees Fahrenheit and 210 psia). This was due to the fact that mercury film boiling coefficients were lower than predicted from the available literature;

2. Type 316 stainless steel tubing is not a suitable boiler coil material due to the reduced heat transfer efficiency caused by the accumulation of corrosion products on the heat transfer surface.

Mercury film boiling coefficients are lower than those of boiling water due to the difference in the film boiling mechanism. In a boiling mercury system there is a sharp phase separation, while with water it is quite common to have two-phase flow. This phase separation is due to the inherent stability of mercury vapor bubbles. Thus, it is possible in a forced flow boiling mercury system for the mercury bubbles to creep along the heat transfer surface, squeezing the liquid away from the wall as they rise. The percentage of the heat transfer area effectively

insulated in this manner is quite large, and the result is a very low heat transfer coefficient. This effect gives rise to a very high temperature difference between the mercury bulk temperature and the heat transfer surface temperature as evidenced by boiler test data.

These deficiencies were alleviated in the second series of tests and the techniques employed are enumerated.

Phase 2 of the Full Power Boiler Mock-Up Test was initiated in June, 1958. During the interim period between Phases 1 and 2, the following modifications to the boiler mock-up test loop were accomplished:

1. Additional heat transfer area was obtained by installing 50 feet of boiler coil in the lead bath annulus surrounding the sodium heater of the full-power boiler;

2. The condenser was bypassed and the sub-cooler functioned as both a condenser and sub-cooler;

3. A wire spiral wrapped around a 0.109 inch outside diameter hypodermic tube 51 feet long was installed in the 3/8 inch boiler coil;

4. A thermocouple for measuring mercury bulk temperatures was placed within the 0.109 inch outside diameter hypodermic tube of the spiral wound assembly.

The increased heat transfer area and coefficient from these modifications provided considerable flexibility in the investigation of various parameters. It was possible to investigate the superheat attainable from flow rates in the range from 50 per cent below to 50 per cent above the design condition of 1.87 pounds per minute. Superheats in excess of the design condition (1350 degrees Fahrenheit) were attained at all flow rates with an appropriate adjustment of the power input. Test results produced 1445-degree Fahrenheit superheated mercury at 210 psia with a 5.2 kilowatt power input.

Mechanical means, in the form of the spiral wound assembly, were employed to increase the boiling heat transfer coefficient. This insert improves the wetting condition at the wall by directing liquid mercury against the tube wall and by producing greater turbulence in the boiling area. The effectiveness of this method was borne out by Phase 2 data, which (unlike Phase 1) showed the tube wall temperature only slightly above the mercury bulk temperature. Mercury bulk temperatures in the superheat region were measured accurately by inserting a thermocouple within the 0.109 inch hypodermic tube to a point 38 feet from the boiler inlet. When employed in this manner, the conduction and radiation corrections were reduced to a negligible amount.

B. TEST LOOP REDESIGN

While tests were being conducted on the full-power boiler mock-up, a new half-power boiler mock-up was being fabricated for future extensive testing in the mercury test loop. Since the first results of the full-power test boiler were unsatisfactory, it became necessary to change the coil design in the new half-power boiler to be similar to the successful model. The redesigned coil consists of 3/8 inch outside diameter tubing of AISI Type 316 stainless steel containing a wire spring of 0.051 inch diameter passing along the tubing inner wall for purposes of flow control. Floating within and following the convolutions of the coil is a tube of AISI Type 316 stainless steel having an outside diameter of 0.109 inch and a wall of 0.012 inch used for thermocouple probing. This coil design has been incorporated into the new half-power boiler mock-up and delivery was delayed until the first of August.

C. MERCURY HEAT TRANSFER TEST

Because of the lack of basic heat transfer data or empirical correlations for forced convection film boiling of mercury in the high mercury boiling and superheat range, it has become necessary to formulate a mercury heat transfer testing program. Ultimate objectives of this program are:

1. Forced convection film boiling heat transfer correlation;
2. Forced convection heat transfer correlation for a helical coil system;
3. Reliable pressure drop data for a boiling mercury system;
4. General corrosion information on the use of Type 347 stainless steel in a boiling and condensing mercury system.

The test loop will be composed of a test section, test section housing, condenser-subcooler, pump, pressurizer, flowmeter and preheater, and will be housed in a closed container that is equipped with an exhaust system. (See schematic, Fig. 4).

1. Test Section

The test section consists of 3/8 inch outside diameter helically wound Type 347 stainless steel coil. The coil has 32 turns on a four-inch diameter circle with two thermocouples placed every one and one-half turns. At each recording point, thermocouples will be installed both inside the tube and in the tube wall to measure temperatures of both the flowing mercury and the wall at the same point. This will permit the calculation of local heat transfer coefficients throughout the test section.

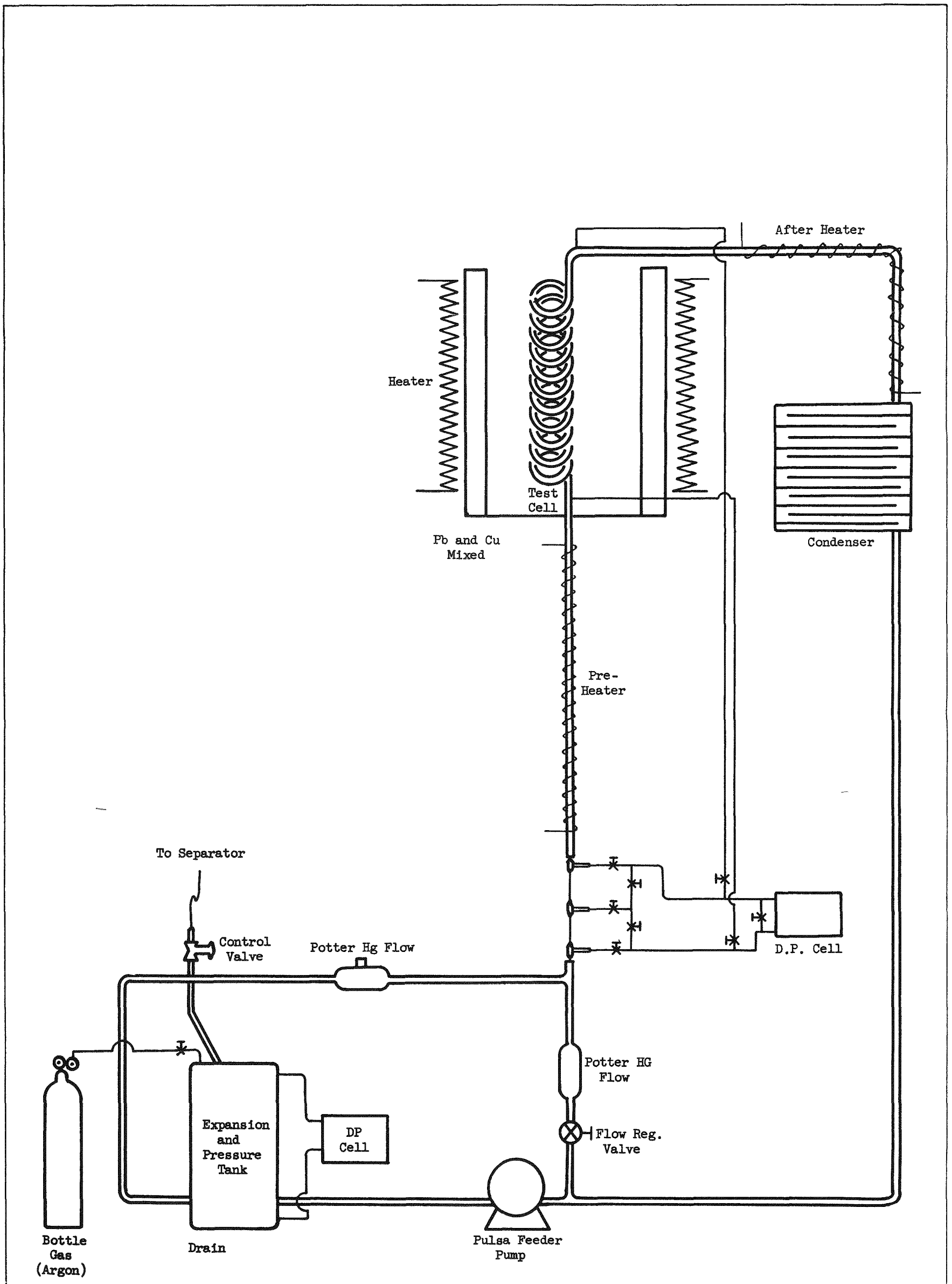

Fig. 4. Schematic for Basic Heat Transfer Test Loop

2. Test Section Housing

The housing will consist of a 14-inch section of nominal 12-inch Schedule 120 stainless steel (Type 316) pipe equipped with three helically wound immersion heaters.

3. Condenser-Subcooler

Condensing of mercury vapor and subcooling of the liquid will be accomplished in a helical 3/8 inch outside diameter coil on a 12-inch diameter circle. Heat will be transferred by radiation and natural convection to two heat sinks, one located inside the condenser-subcooler coil at a half-inch spacing, and the second located with the same spacing outside the condenser-subcooler helical coil.

4. Pump

The fluid mercury will be pumped with a positive displacement pump which will cover a range of 0.3 to 2.9 gallons per hour.

5. Pressurizer

The mercury discharging from the pump will flow into a pressurizer tank. This tank will serve to pressurize the loop with argon gas, and will provide an expansion chamber for smoothing out the pulsating action of the pump. A bleed-off type of over-pressurization system will be used to control the pressure at the test section inlet.

6. Flowmeter

The loop flow will be sensed with a Potter turbine-type flowmeter and will be recorded on a strip chart recorder. A range of flows of from 0.3 to 3 gallons per hour will be covered.

All design drawings have been released for manufacturing and all necessary equipment, such as tubing, fittings, and instrumentation were procured. Assembly of the heat transfer loop should be complete by the end of next quarter.

D. HEAT TRANSFER ANALYSES

1. IBM-704 Machine Code

The analytical work on the new boiler concept has consisted of developing a FORTRAN program for the IBM-704 computer. The ultimate

objective is the development of a program that will produce a complete radial and axial temperature distribution in the molybdenum fuel block for simplified models of both the half-power and full-power boilers. This program investigates six radial regions with varying heat conduction properties with 79 axial sources. The quantities calculated and printed out are fluid velocity, fluid temperatures, qualities, molybdenum temperatures, tube wall temperatures and forced convection, and boiling and superheat heat transfer coefficients. Three problems employing somewhat simplified models, but which are superior to those employed to date, have been run satisfactorily.

E. THERMAL SHUTTER CONTROL EQUIPMENT

Most of the controls effort for this quarter was on the temperature control servo amplifier and thermal shutter control mechanism. The breadboard amplifier was checked out electrically, mated with the thermal shutter control mechanism, and tested under load.

The amplifier input was a Wheatstone bridge used to simulate a resistance thermometer. The motor operated as expected, reversing and showing proportional speed control as the variable arm of the input bridge was swept through its values. A 46-pound weight was lifted at approximately three inches per minute. This is considerably more than the expected shutter weight, so there is no doubt as to the mechanical ability of the system.

The printed circuit model was designed and constructed concurrently with the breadboard test work. It was checked out, met its design specifications, and vibration testing was initiated. Since the printed model is extremely rugged, no serious difficulties are expected.

F. ISOTOPE HALF-POWER BOILER DESIGN

Manufacturing drawings for the first isotope half-power boiler are 90 per cent complete. However, during a coordination visit to Oak Ridge National Laboratory, it was learned that insufficient space was being provided for the isotope fuel pellets. A revised fuel element assembly was designed and, pending coordination with ORNL, will be incorporated into the initial isotope boiler design. Release to Manufacturing is expected during the next quarter.

III. TASK III - FUEL ELEMENT DEVELOPMENT PROGRAM

This task covers the fabrication, assembly, and test of the complete half-power radioisotope fuel block. Progress during the past quarter has been made on fuel pellets, oxidation-resistant coatings, and molybdenum braze materials. Visits were made to Oak Ridge National Laboratory to coordinate the fuel fabrication process, and to determine Company responsibilities for various operations. Information concerning this progress is presented in this chapter.

A. CeO_2 FUEL PELLETS

Fabrication and testing of CeO_2 based bodies were continued during this period. The studies consisted of:

1. Variation of compacting pressure as a means of controlling dimensions of fuel pellets;
2. Effect of change in chemical processing of CeO_2;
3. Corrosion testing of CeO_2 fuel compositions (reported in Task IV report).

A study was made of the effect of varying the compacting pressure of a CeO_2 body on the compacted and sintered properties of the pellet. For this study a 96.25 per cent CeO_2, 1.25 per cent Nd_2O_3, 2 per cent TiO_2 and 0.5 per cent $CaCO_3$ body composition was selected as a representative composition having good sintering and corrosion properties. Table 1 lists the results of the variation of compacting pressure.

From the data listed in Table 1 it can be seen that it is possible to vary the compacting pressure to a large degree without changing the sintered density of the pellet. However, this only applies in the case of a material which displays good sintering characteristics or a material to which is added an aid to improve the sinterability of poor material. The data presented in Table 1 also denote how the shrinkage and final dimension of the pellet may be controlled without changing the compacting die size, and without the necessity of grinding the pellets to a final dimension. As the CeO_2 pellet fabrication process does not permit the use of an organic binder, there may be a tendency for pellets to laminate when compacted at pressures greater than 25 tons per square inch.

TABLE 1

Effect of Compacting Pressure on Shrinkage and Density

Samples (Compacting Pressure) (tons per square inch)	Compacting Ratio	Density (per cent theoretical) Green	Sintered	Per Cent Shrinkage Diameter	Height
5	1:2.5	49.8	96.6	20.3	20.2
10	1:2.7	53.6	96.3	18.3	18.4
15	1:3.0	56.9	97.0	16.5	16.6
20	1:3.1	57.6	97.3	16.4	16.2
25	1:3.1	59.3	96.9	15.5	15.3
30	1:3.3	60.5	97.3	15.0	14.9
35	1:3.2	61.5	97.2	14.6	14.6
40	1:3.3	62.4	96.9	14.1	14.1
45	1:3.4	63.3	96.7	13.5	13.5
50	1:3.6	63.4	97.2	13.5	13.6

Batch Composition: 97.5 per cent (97.5 per cent CeO_2 + 2.5 weight per cent Nd_2O_3) + 2 per cent TiO_2 + 0.5 per cent $CaCO_3$.

Calculated Theoretical Density: 7.03 grams per cubic centimeter.

It has been shown that certain minor additions of TiO_2 and TiO_2-CaO to the CeO_2 in amounts of less than five per cent are effective in increasing sintered density of the compacted pellets, and are also effective in stabilizing the CeO_2 in the presence of liquid lead. It was felt that a more uniform dispersion of the addition in the CeO_2 could be achieved by the introduction of the TiO_2-CaO in a soluble salt which on thermal decomposition would convert to the oxide; also, it would be advantageous to reduce the amount of handling of the powder in the hot cell.

A study was made by ORNL of adding a 2 per cent TiO_2 - 1/2 per cent CaO stabilization and sintering addition in a solution form to the cerous oxalate before conversion to the ceric oxide. The resultant powder produced by this method appeared to have a non-uniform dispersion of the TiO_2 - CaO mixture, an excessive amount of the oxide mixture, and poor sinterability with normal processing.

B. PROTECTIVE COATINGS ON MOLYBDENUM

Work was initiated during this period on the application of oxidation resistant coatings on molybdenum by the flame spray method.

The coating process involves three basic operations:

1. The surface of the article to be sprayed is prepared by rounding all edges and corners and blasting with a steel grit to insure a good mechanical bond between the coating and the base metal before and after fusion;

2. The coating alloy is then applied by flame spraying the alloy in the form of a powder with a spray weld pistol. The coatings after spraying are approximately 0.012 to 0.015 inch thick which will densify on fusion to 0.008 to 0.010 inch thick;

3. The flame sprayed coating is then given a furnace fusion treatment at 2000 to 2200 degrees Fahrenheit for two hours in high purity hydrogen. This treatment fuses the sprayed coating and develops a metallurgical bond between the coating and base metal.

The coated specimens are then tested at 1800 degrees Fahrenheit in air to check for defects in the coatings which would expose bare molybdenum areas and allow oxidation of the molybdenum.

The oxidation protection coatings are subjected to molten lead corrosion at 1500 degrees Fahrenheit for 500 hours to determine the ability of the coatings to resist corrosion attack by the lead as either a solution, reaction or disintegration of the coating.

The coating materials given in Table 2 are being studied for application as oxidation protective coatings on molybdenum.

TABLE 2

Oxidation Resistant Coatings for Molybdenum

Coating	No.	Composition	Oxidation* Weight Change (per cent)	Lead** Corrosion Resistance	Remarks
Colmonoy	4	85 Ni, 8 Cr, 4 Si, 2 B	+0.04	Fair	Good impact resistance
	4A	No.4 + 10 per cent Mo	+0.02	In test	
	4B	No.4 + 20 per cent Mo	+0.05	In test	
	4C	No.4 + 30 per cent Mo	+0.05	In test	
Colmonoy	5	79 Ni, 12 Cr, 4 Si, 2 B	+0.07	Fair	Good impact resistance
	5A	No. 5 + 10 per cent Mo	+0.02	In test	
	5B	No.5 + 20 per cent Mo	+0.03	In test	
	5C	No.5 + 30 per cent Mo	+0.04	In test	
Colmonoy	6	72 Ni, 15 Cr, 4 Si, 3 B	+0.16	Fair	
	6A	No.6 + 10 per cent Mo	+0.03	In test	
	6B	No.6 + 20 per cent Mo	+0.13	In test	
	6C	No. 6 + 30 per cent Mo	+0.02	In test	Good impact resistance
Al + Cr-Si		20 Al, 45 Cr, 32 Si	+0.03	Reaction with lead	Low impact resistance
Al alloy 13		13 Si, 87 Al	+0.04		Low impact resistance
Chromized		Cr	+0.02	In test	
W-Z Chromized		Cr alloy	+0.01	In test	Low impact resistance

* Per cent weight change after 10-hour exposure to air at 1832 degrees Fahrenheit.

** Molten lead corrosion at 1500 degrees Fahrenheit for 500 hours.

The chromized coating is applied to the molybdenum by a gaseous pack process in which the surface of the article to be chromized is placed in contact with a volatile chromium halide in a hydrogen atmosphere. The reaction at high temperatures between the three constituents, molybdenum, hydrogen and chromium halide, results in the deposition of a film of chromium on the surface of the molybdenum. The chromized coating as shown in Fig. 5 is the layer of chromium which appears to be continuous, nonporous, and well bonded to the substrata.

Tests are now being conducted on the corrosion resistance of the chromized coating in molten lead at 1500 degrees Fahrenheit. If the chromized coating is unaffected by the lead, it is planned to utilize this coating as a basic oxidation protective layer to inhibit oxidation of molybdenum during the loading of the fuel pellets and final sealing of fuel holes. As the chromizing coating process is applicable to all surfaces including threaded sections, blind holes, and inaccessible areas, it will be possible to completely chromize the molybdenum block immediately after machining.

Figure 6 shows a section of a molybdenum piece which has been chromized and a flame spray coating of Colmonoy No. 5 alloy applied to the chromized surface. After the fusion treatment, the flame spray coating appears to wet the chromized surface and is well bonded to the chromized coating. It is planned to apply a flame spray coating which will be able to withstand a high impact load over the chromized surface to give primary oxidation protection for the molybdenum. The coatings that will be studied for this application are modified Colmonoy alloys, Al-Si, Al-Cr-Si, and Colmonoy - stainless steel mixtures.

In addition to the requirements of the oxidation protective coatings that they be corrosion resistant to lead for an extended period, it also appears necessary that the coating be resistant to a molten lead oxide for a short period. As the coating surface is not a smooth ground surface, a small amount of lead will adhere to the surface of the specimen after removal from the lead bath. In testing the oxidation resistance of the coating immediately after removal from the lead container the oxidation protective coating is subject to attack by a highly corrosive melt of lead oxide (PbO) in air.

It is therefore planned to subject the coatings to an additional test in which the coating will be in contact with lead in air at 1500 to 1800 degrees Fahrenheit to determine the resistance of the coating to the lead oxide.

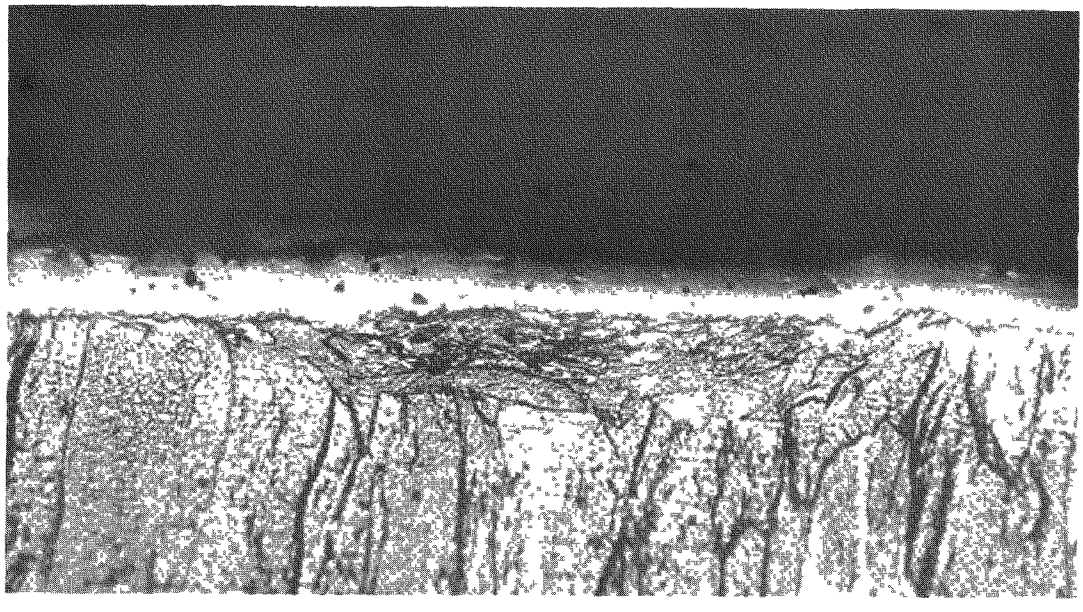

Magnification 300X

Fig. 5. Chromized Coating on Molybdenum

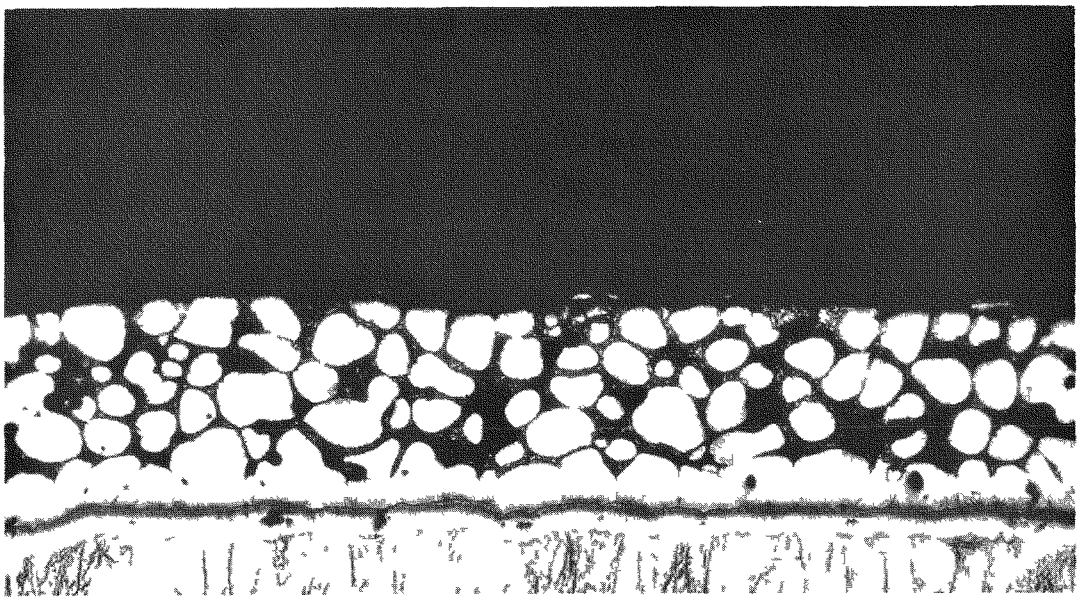

Magnification 150X

Fig. 6. Colmonoy Number 5 Coating on Chromized Molybdenum Surface

C. BRAZED MOLYBDENUM CLOSURES

The stainless steel brazing alloys have shown good wettability on molybdenum surfaces and acceptable brazed molybdenum joints have been made in the laboratory.

Brazed molybdenum joints that have been corrosion tested in molten lead have maintained strong bonds after 500 hours exposure to the molten lead at 1500 degrees Fahrenheit. It appears that the brazed sections which present a minimum amount of exposed brazed surface to the lead are almost unaffected by the lead. However, the same brazing alloys will be corroded by the lead when a large surface area is exposed.

Initial attempts were made to braze molybdenum threaded joints by painting the threads with the brazing compound before assembly. These joints, although bonded, showed large unbonded areas without any braze material in the gap between the threads. Continued studies on the brazing of threaded molybdenum joints showed that those joints made with an excess of braze alloy allowed to infiltrate into threads were superior to brazes made by the conventional methods. The brazed joint shown in Fig. 7 was made by forming the brazing alloy into a bushing by compacting in a die at approximately five tons per square inch. The molybdenum threaded parts were assembled and the compacted bushing was placed on the molybdenum assembly in contact with the upper thread. The pieces were then heated in an argon atmosphere at 2000 to 2050 degrees Fahrenheit to allow the brazing alloy to melt and infiltrate into the gap between the threads, and bond to the molybdenum.

A number of simulated fuel assemblies were made by this method using CeO_2 pellets, lead thermal bond,and molybdenum-containing tube and plug.[2] The fuel pellets were inserted into the molybdenum tube and a lead slug was placed on top of the pellets. The assembly was then heated in argon to 2000 degrees Fahrenheit to allow the lead to melt and flow into the annulus between the CeO_2 pellets and the molybdenum tube. The molybdenum plug was then threaded into the top of the tube and a compacted bushing of the brazing alloy placed on top of the assembly, which melted and flowed into the threaded joint. The entire operation was accomplished at 2000 degrees Fahrenheit in an argon atmosphere. Figure 8 shows a section of the fuel assembly made by the described procedure.

D. OAK RIDGE NATIONAL LABORATORY EXPERIMENTS

During this period, ORNL separated approximately 800 curies of Cerium-144 from old fission product wastes from Arco, Idaho. This

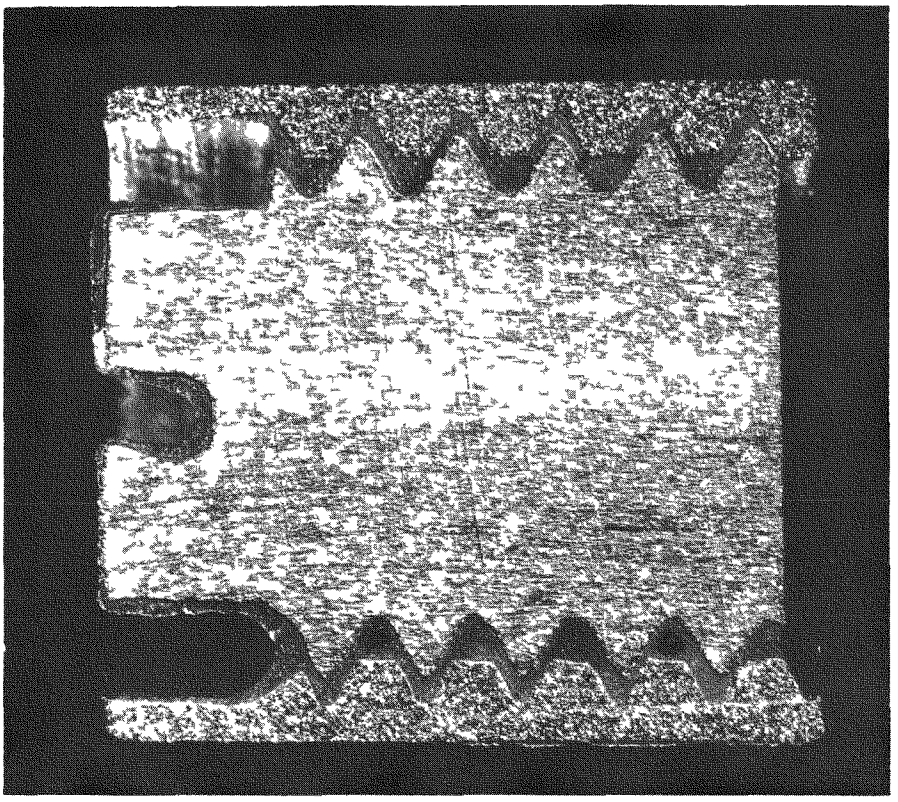

Magnification 7X

Fig. 7. Section of Brazed Molybdenum Threaded Joint

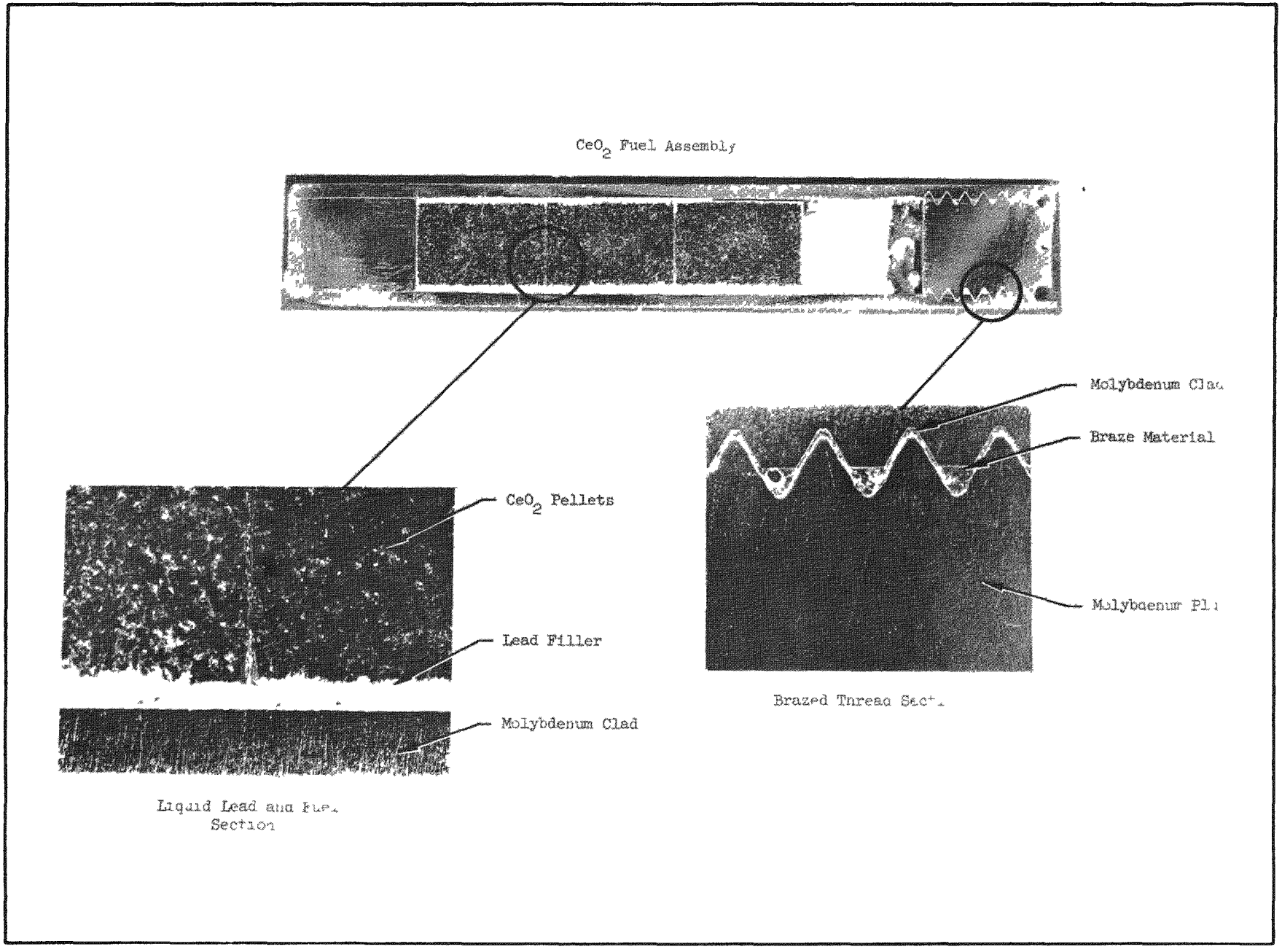

Fig. 8. Fuel Assembly Section

separation was made on a laboratory scale to check out the separation process and also to perform hot pelleting operations to produce sample fuel pellets for the SNAP program. The results of these experiments are reported in "Cerium-144 Fission Product Source Fabrication", by E. Lamb and T. A. Butler, dated July 11, 1958. The data include specific activity, weight and volume measurements, heat output, shrinkage, and radiation output. Figure 9 illustrates the sample pellets fabricated at ORNL.

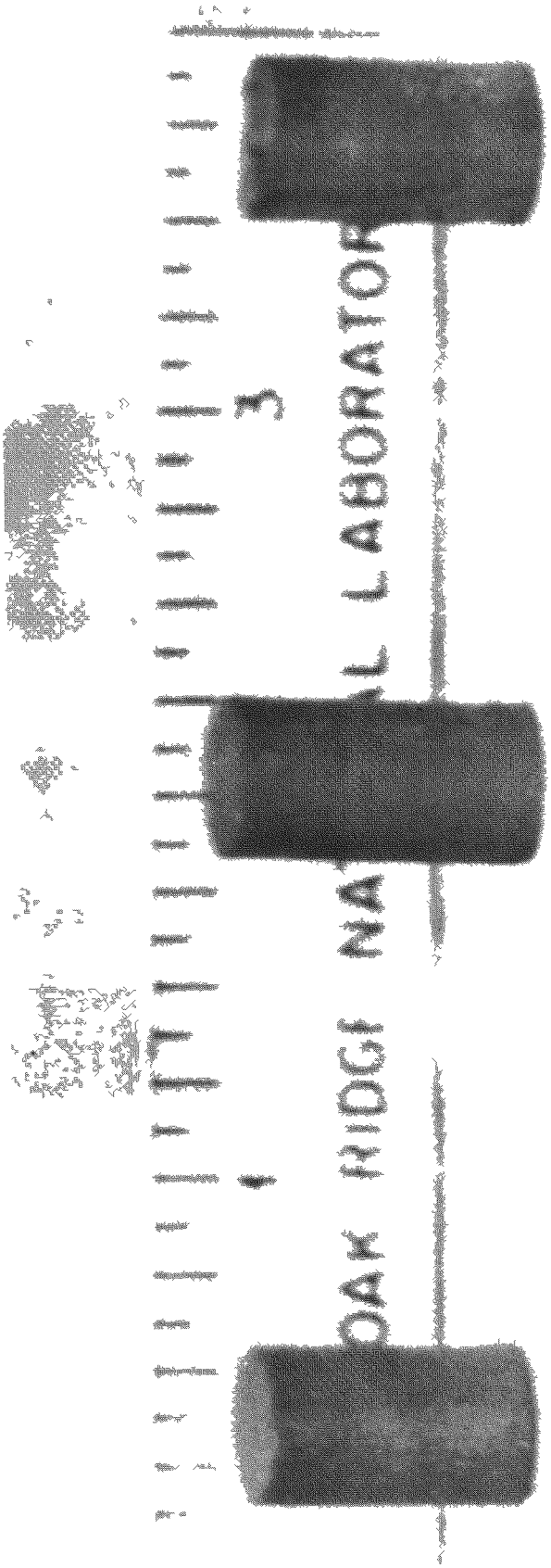

Fig. 9. Sample Pellets Fabricated at ORNL

IV. TASK IV - MATERIALS CORROSION PROGRAM

This task covers the selection of materials required for the various sub-assemblies of the two half-power boilers. Considered in the program are the various construction materials, and the way they are affected when in contact with liquid metals. Progress during the past quarter has been concentrated on the reaction rates of various metals and ceramics in contact with liquid lead, mercury vapor, and liquid mercury. Further details concerning these experiments are presented in this chapter.

A. DYNAMIC MERCURY TESTING

Major modifications were made to the dynamic mercury test loops before they could be properly operated. The Croloy 5 Ti loop was operated first, and further modifications were found necessary after the initial test run. The heat generated in the steel cabinet was so great that the insulation on the wiring and the pitch in a transformer melted. The unit was shut down, rewired with high temperature glass insulated wire, and the transformer was placed outside the cabinet to keep it cool. After these modifications, the unit was placed in operation. The Croloy 5 Si loop was similarly rewired and placed in operation.

The Croloy 5 Ti loop ruptured after approximately 150 hours of high temperature operation. Metallographic study of loop specimens is not yet complete, but it is believed that the rupture can be attributed to two factors:

1. The boiler tubing at the point of rupture was 1/2 inch inside diameter with the same wall thickness as the 1/4 inch inside diameter tubing. This larger diameter reduced the allowable working stress which was already near the limit;

2. Boiler corrosion reduced the wall thickness at the boiler exit until the tube ruptured. There was a considerable quantity of black powder, apparently soluble alloy constituents, which precipitated out of the cool mercury and was distributed in the return leg of the loop. Heat transfer in the boiler also became noticeably worse as operating time increased. All evidence points to a high corrosion rate of the hot dynamic mercury on Croloy 5 Ti. This material has been dropped from consideration and all of the Croloy group may be eliminated after further study.

523

Materials are being procured and assembled for a Carpenter 20CB test loop. Design changes were made in the Carpenter loop to alleviate the difficulties encountered in the Croloy loops.

Large scale mercury reprocessing equipment was put into operation. This purification equipment consists of an oxifier of 150-pound mercury capacity, a gold seal filter which will remove dirt oxide, dust, oil and water from 250 pounds of mercury in ten minutes, and a vacuum still which will deliver 5 to 7 1/2 pounds of purified mercury per hour.

B. STATIC LEAD TESTING

1. Refilling Boiler Mock-Up

A large lead purifier was prepared to deoxidize 25 pounds of lead per run. After the unit was wired and insulated a test was made, and it was determined that a current of four amperes would produce the desired temperature of 900 degrees Fahrenheit. Ninety pounds of lead were then purified for the boiler.

2. Lead Corrosion Tests

The lead corrosion test procedure for cerium dioxide fuel pellets was modified to simulate actual conditions that will ultimately exist. This involved the preparation of molybdenum crucibles and the discontinuance of the use of graphite in the testing area. Thirty lead corrosion tests of cerium dioxide pellets were completed. The cerium dioxide pellets do not show any change in appearance but there is usually some cracking or chipping of the samples at the completion of the lead tests. Because of this tendency and because of some results which might be erratic, it is impossible to definitely correlate the test results. Tentative correlation of these static lead test results indicates that cerium dioxide samples containing titanium dioxide as a constituent withstand the 500-hour, 1500 degrees Fahrenheit lead test better than samples which contain calcium fluoride or calcium carbonate. Additional tests will be carefully run on samples of the composition which have given the best results. Lead will also be heated in a vycor container to see if there is any visible reason for mechanical failure of the samples at 1500 degrees Fahrenheit in lead.

Fifty lead corrosion tests were completed on brazed molybdenum joints. Sandwich test sections of molybdenum brazed with Nicrobraz and Coast Metal alloys give better resistance to lead corrosion than single molybdenum coupons coated with the alloys. Nicrobraz 30 and Nicrobraz 150 give slightly better results than the other alloys. Six brazed molybdenum screw samples were also tested. Nicrobraz 30 and Nicrobraz 150 also gave the best results for the screw samples.

Nine tests were completed on Colmonoy oxidation resistant coatings. No definite conclusions can be drawn from these initial tests. However, molybdenum crucibles were used for holding the samples and the samples showed greater attack where they were in contact with the crucibles. In actual use these coated molybdenum block materials will be in contact with stainless steel. Therefore, stainless steel crucibles will be fabricated for future testing of these oxidation resistant coatings.

C. RESULTS

The results of the lead corrosion tests (500 hours at 1500 degrees Fahrenheit) are given in Tables 3, 4, and 5.

TABLE 3

Lead Tests on Cerium Dioxide Fuel Pellets

Sample		Composition and Density		Results
5	AC 1	Density 100% 98.75% CeO_2 1.25% Nd_2O_3	98.75% mixture with 1.25% TiO_2	Small hairline crack around center
9	AF 1	Density 95.8% 98.75% CeO_2 1.25% Nd_2O_3	98.75% mixture with 1.25% TiO_2	One very small chip
11	AG 1	Density 97.8% 98.75% CeO_2 1.25% Nd_2O_3	98.75% mixture with 1.00% TiO_2 and 0.25% $CaCO_3$	No visible defects, 0.6% gain in weight
21	V 1	Density 92.6% 95% CeO_2 5% Nd_2O_3	95% mixture with 5% TiO_2	Chipped on one edge
22	V 3	Density 91.6% 95% CeO_2 5% Nd_2O_3	95% mixture with 5% TiO_2	Small hairline crack about 0.5 inch long
23	V 4	Density 91.1% 95% CeO_2 5% Nd_2O_3	95% mixture with 5% TiO_2	No change in sample
24	W 1	Density 96.8% 97.5% CeO_2 2.5% Nd_2O_3	97.5% mixture with 2.5% CaF_2	Shattered into many pieces

TABLE 4

Lead Tests on Brazed Molybdenum Samples

Specimen	Inhibitors	Weight Change (per cent)	Remarks
2 sandwich	None	+0.36	No change in sample
Nicrobraz 30 run in argon 1/2 hour at 2200 degrees Fahrenheit			
1 single coupon	Zr and Ni	-1.38	Sample looks good
2 single coupon	None	+0.475	Sample looks good
3 single coupon	Zr and Ni	-3.58	Sample has some of coating removed
4 single coupon	Zr and Ni	-4.33	This sample was sand blasted before coating. Coating flaked off during chemical cleaning
5 single coupon	Zr and Ni	-4.66	Sand blasted sample coating flaked off
6 and 9 coupons	None	-2.54	These samples were joined when received and remained joined during the test. Slight flaking of coating.
7 single coupon	Zr and Ni	-2.84	Degreased before coating. Some of brazing alloy removed during test

523 4

TABLE 5

Lead Tests on Oxidation Resistant Coatings for Molybdenum

Specimen	Inhibitors	Weight Change (per cent)	Remarks
1 Colmonoy 4 pellet	Zr and Ni	+0.17	Oxide coating
2 Colmonoy 5 pellet	Zr and Ni	-3.7	Heavy oxide coating
3 Colmonoy 6 pellet	Zr and Ni	-3.1	Heavy oxide coating
4 molybdenum slug coated with Colmonoy 4	Zr and Ni	-2.1	Lead test has removed coating completely from one side of specimen. This spot is 1/4 inch in diameter
5 molybdenum slug coated with Colmonoy 4	Zr and Ni	-1.2	Coating removed as specimen is much smoother than before test
6 molybdenum slug coated with Colmonoy 5	Zr and Ni	-0.8	Smoother surfaces on side and bottom
7 molybdenum slug coated with Colmonoy 5	Zr and Ni	-0.25	Sample looks good except for surface that touched bottom of molybdenum crucible
8 molybdenum slug coated with Colmonoy 6	Zr and Ni	-1.1	All surfaces smooth
9 molybdenum slug coated with Colmonoy 6	Zr and Ni	-1.5	Coating almost completely removed

V. TASK V - POWER CONVERSION SYSTEM PROGRAM

During this report period, component testing was accelerated in an attempt to establish proper component clearances and operating conditions for the Turbine-Alternator Test Package. Turbine-Alternator Test Package fabrication and assembly were completed and package testing was initiated.

A. SYSTEMS ANALYSIS

A preliminary extended life study of the system has been completed and a report written describing the potential life of the system and several possible control schemes for achieving this extended life. Briefly, this study indicated that with the addition of a load control, the system is capable of producing in excess of 250 watts for about six months.

A study was made of the effect of piping arrangement and tolerances, and rotating unit speed variation on vehicle attitude. The results indicate:

1. That piping must be arranged to minimize the effect of angular momentum on attitude stability;

2. That piping tolerances in the order of $\pm$ 1/16 inch will present no attitude control problem;

3. That the allowable speed change for the unit will be governed by attitude control limitations and is approximately $\pm$ 2000 revolutions per minute (depending on the inertia of the rotor).

A study was made of the effect of gyroscopic torques on bearing loads which would be encountered during test of a rotating unit on a centrifugal accelerator. Results of the study indicate that optimum simulation of launch loadings on the unit would be obtained by orienting the axis of the test unit parallel to the axis of the accelerator.

Displays were prepared and the necessary data compiled for presentation at the NAPS coordination meeting in May.

A preliminary study of start and stop techniques has been completed and a report has been written describing a recommended system. This system utilizes alternator motoring, an external mercury supply, externally powered heaters, and a load control.

The problems associated with arranging the power conversion system in the vehicle have been studied and major arrangement requirements have been defined. These include:

1. Orientation of power conversion rotating package to eliminate gyroscopic torques;

2. Arrangements of fluid loops to cancel the mercury angular momentum to eliminate disturbances due to gyroscopic forces and change of system flow rate;

3. Selection of relative condenser and pump positions to insure minimum pressure drops in the pump inlet lines and to insure a positive pump priming head during ground operation and launch;

4. Selection of relative positions of boiler and pressure regulator to eliminate boiler pressure fluctuations due to mercury levels during the launch;

5. Arrangement of a temporary heating system for turbine exhaust line to prevent backflow of mercury condensate during launch.

The requirement, recently emphasized by Lockheed Corporation, of permitting the gas bottle extension mechanism to pass through the circumference of the aft section of the vehicle has caused revisions in system arrangement plans. With this factor it will be necessary to utilize either a split condenser, or a condenser placed on a single side of the vehicle. This question is presently being evaluated.

B. TURBINE

A report of the results of the 400-watt axial flow air impulse turbine and an analysis of the accuracy of the data obtained have been completed. Tests of the air turbine with equiangular bladed wheel, shown in Fig. 10, indicate a maximum adiabatic aerodynamic efficiency of 42.5 per cent, and over-all efficiency of 40 per cent at $U/C_{th} = 0.28$ (total static basis). These results were at design point conditions with inlet pressure at 200 psia, exhaust pressure at 60 psia, and inlet temperature at 150 degrees Fahrenheit. Tests conducted under the same conditions, except for the inlet temperature of 75 degrees Fahrenheit, indicate substantially the same results. These results are not significantly different from those obtained with the asymmetric bladed wheel. The most likely explanation of this result is that separation occurred at the suction side of the trailing edge of the wheel blades, thereby preventing the maximum reduction of tangential gas velocity.

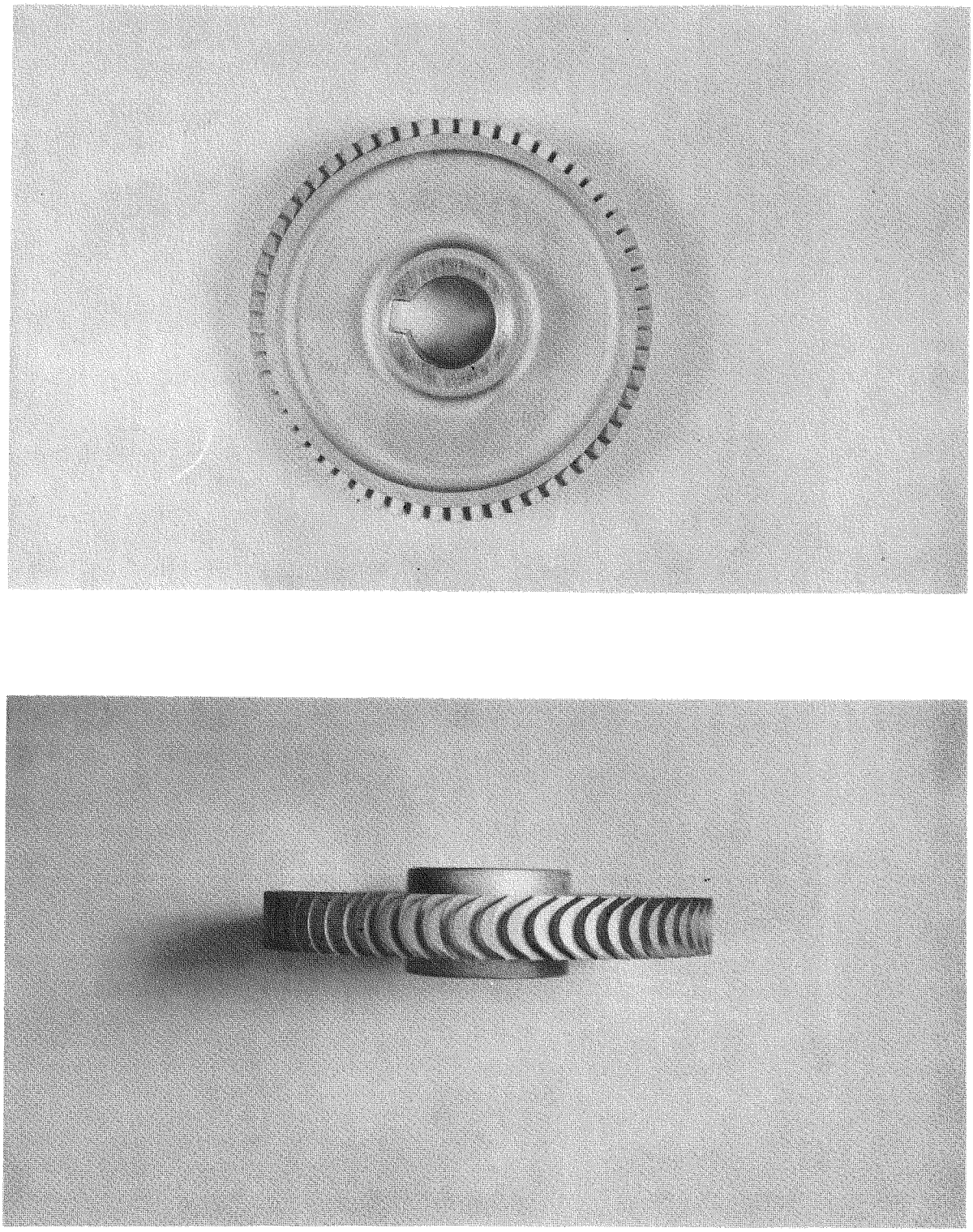

Fig. 10. Equiangular Bladed Air Turbine Wheel

TATP-1 tests during the month of June included one hot run and a nozzle calibration for flow measurement. Because of operational difficulties, a maximum speed of only 7000 revolutions per minute was achieved. A test report will be issued, but this will consist mainly of indicating the exposure to Hg vapor and the fact that no mechanical interference or erosion was evident in the turbine section.

Nozzle calibration is presently incomplete because inlet temperature was limited to 1000 degrees Fahrenheit, due to insufficient line heater capacity and available test cell time. Analysis of those data which were obtained is in process.

A nozzle calibration test procedure, desired information, and method of data reduction have been established. A study to determine the effects of TATP seal clearance on turbine performance was accomplished. In general, an increase of 0.001 inch in the radial clearance of all labyrinth seals in TATP-1 will decrease the turbine efficiency approximately three percentage points. Further running experience with TATP will be required to determine if the 0.003 inch design clearances can be decreased.

Integration of partial admission equations into the IBM program for full admission axial flow turbines is nearly complete. Expected completion of the full program, including checks on the IBM process, is July 11.

Actual disk drag measurements on the equiangular air turbine have been made. Data reduction and analysis are in progress.

A dynamic similarity analysis for air-Hg and argon-Hg turbine operation has been completed for the second and third stages of TATP. This study consisted of attempting to establish the major parameters which influence turbine efficiency, isolating the relative effect of each parameter on performance, and determining the possibility of correlating the effects of parameters of air turbines with mercury turbines.

C. PUMP

Extensive pump tests were conducted in the last quarter of Fiscal 1958. Test results with an 11/16 inch diameter slinger pump indicated good ability to operate at low inlet pressures, but with low efficiency.

Two vaned centrifugal pumps were designed, fabricated and tested. One pump employed vanes on the back face to effect a seal and reduce shaft leakage. These pumps performed well, but still could not meet the low inlet pressure requirements at flow rates in excess of 10 pounds per minute.

Three additional slinger-type pumps were designed and fabricated to allow investigation of the effect of the inlet on slinger performance. Extensive pump analysis work indicated that two stages of pumping would be required to obtain the design performance. Among possible arrangements would be combined slinger and centrifugal pumps and jet centrifugal pumps.

A jet centrifugal pump, combining a jet boost pump with a vaned centrifugal pump, was designed and tested. This pump attained the design performance (15-pound per minute flow, 270 psia discharge pressure, 1.86 psia inlet pressure). Efficiency of this pump was approximately 20 per cent.

Tests of an expanding screw-type (spiral) pump indicated the performance to be lower than for the vaned centrifugal pumps. However, damage to the leading edge of one of the two blades may have appreciably reduced performance of this unit.

A comparison of test results obtained with three of the pumps tested, vaned-centrifugal (centrifugal), vaned-centrifugal and jet (jet-centrifugal), expanding screw (spiral), is shown in Fig.11 . Figure 12 illustrates several of the configurations which were tested.

The vaned centrifugal pump was released to the Prototype Group for incorporation into the Preliminary Prototype unit.

A pump-dynamometer design, to allow accurate evaluation of pump power consumption, was completed.

D. CONTROLS

During April, extensive testing of the breadboard pressure regulator was performed. Results of these tests were applied to the design of the prototype regulator on which fabrication was completed in June.

Static rests were initiated to substantiate the design characteristic of the regulator and the effectiveness of modulation control on the regulator. Figure 13 is a static point plot of Regulated System Pressure versus Alternator Frequency. Figure 14 shows the assembly drawing of the preliminary prototype regulator. Figure 15 is a photograph of the regulator and the high temperature torque motor used for modulation feedback.

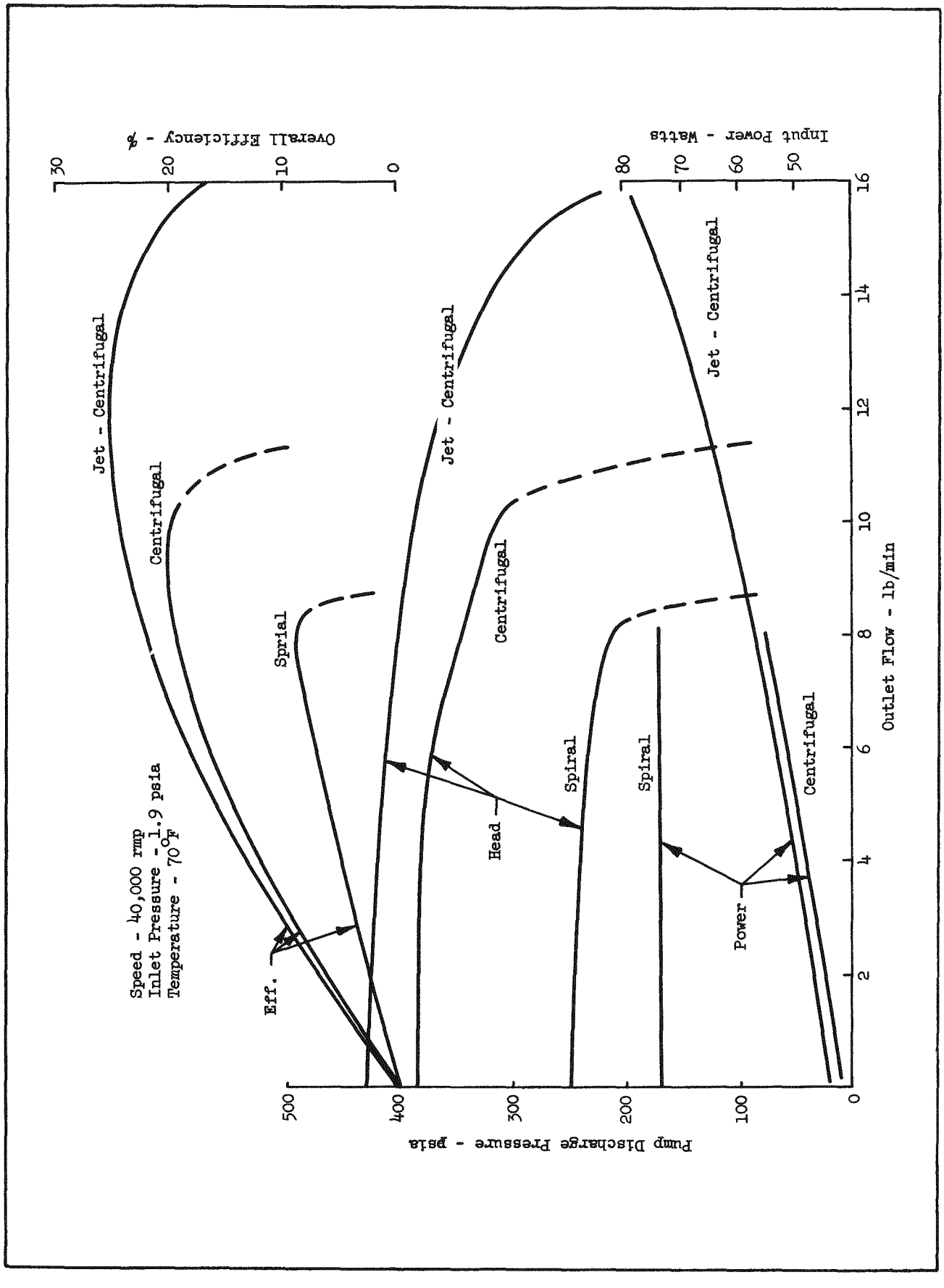

Fig. 11. Pump Characteristic Curves

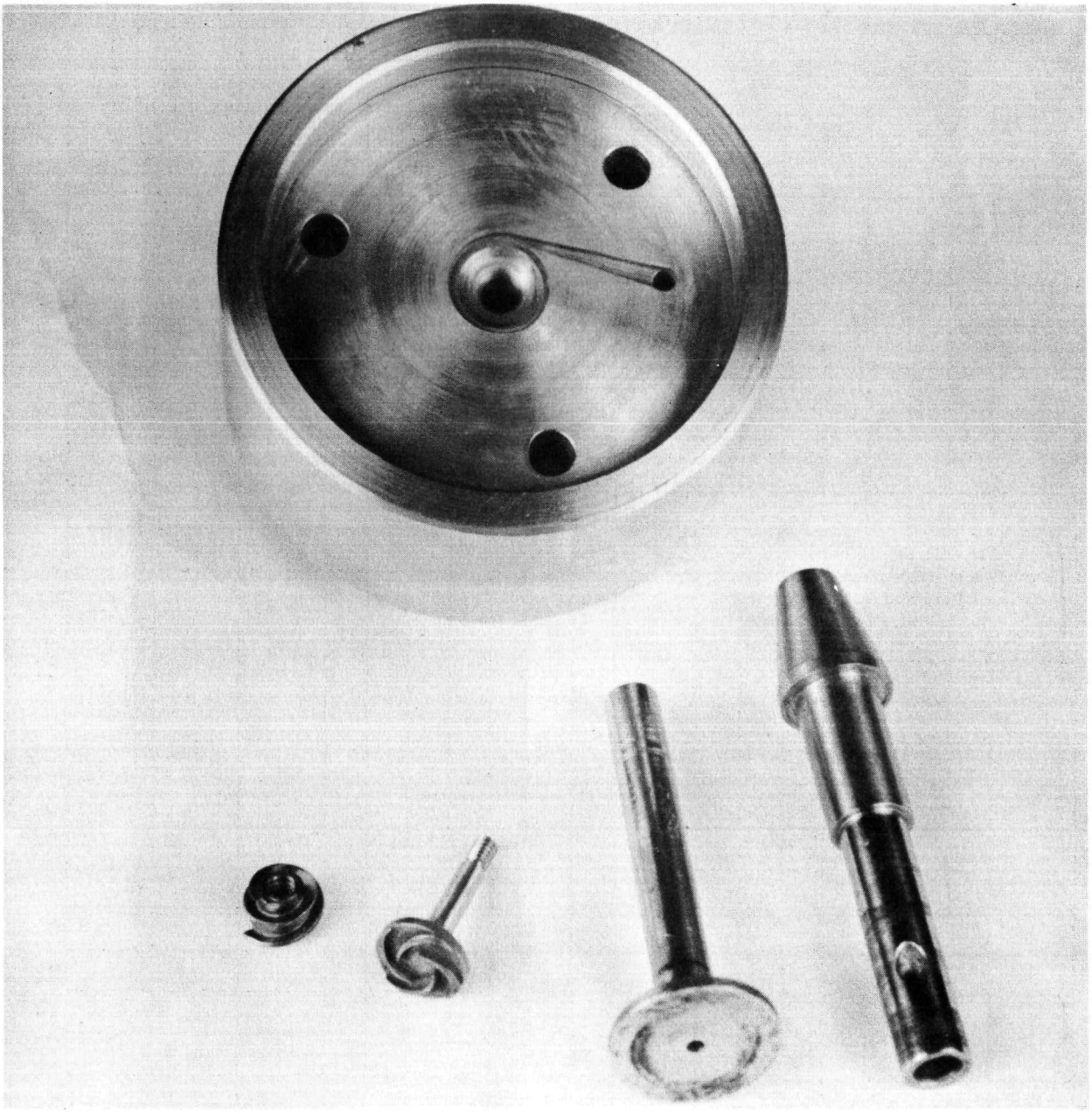

Fig. 12. Pump Configurations

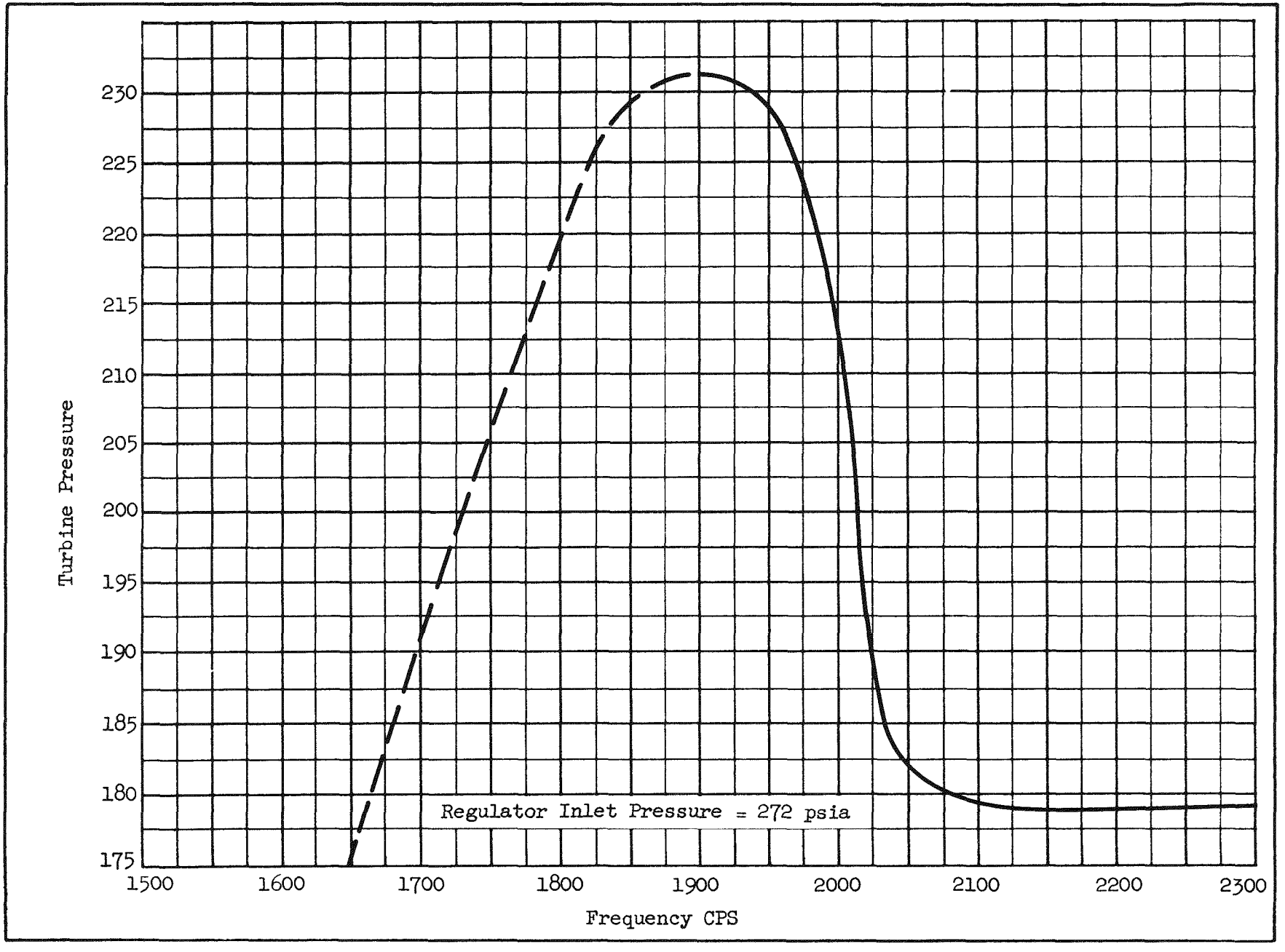

Fig. 13. Integrated Prototype Tests

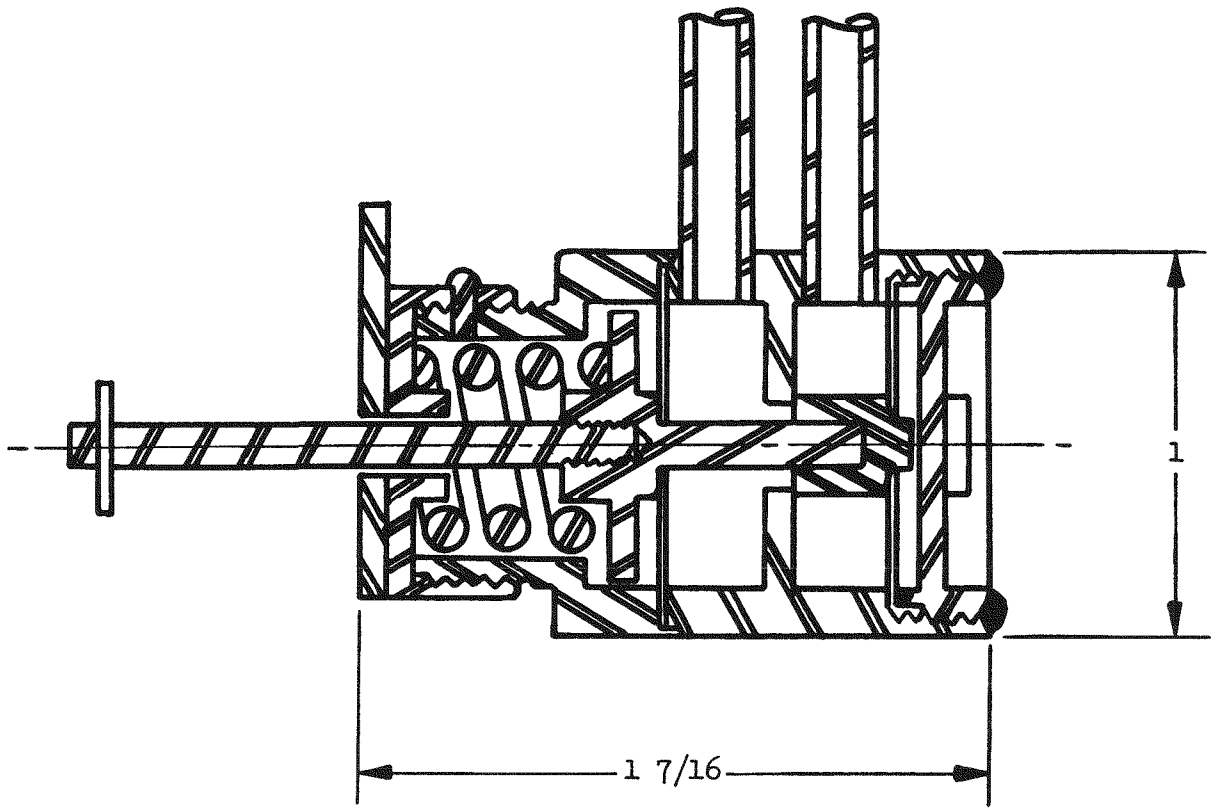

Fig. 14. Mercury Throttle

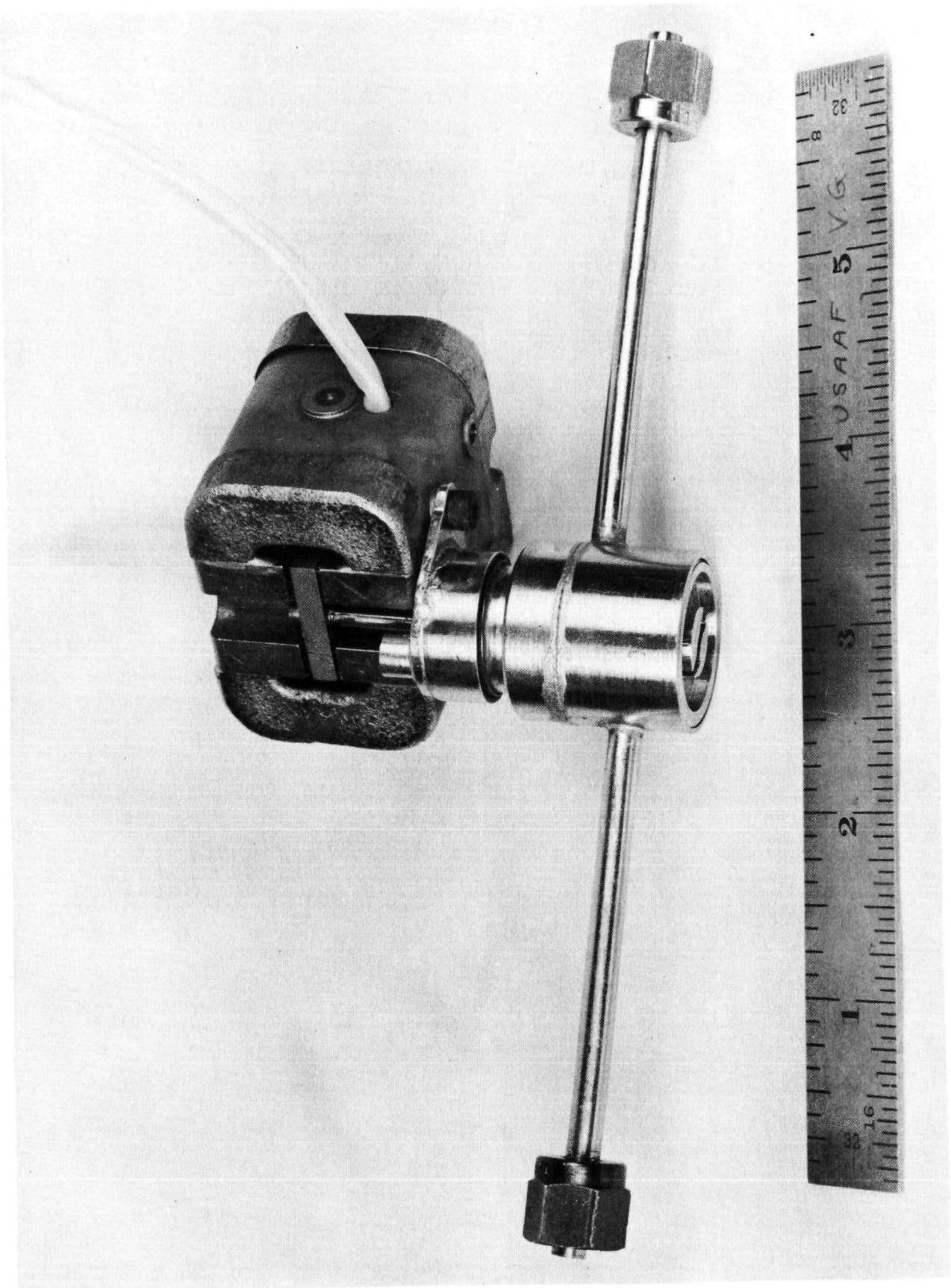

Fig. 15. Pressure Regulator and Torque Motor

The packaging of the functional prototype frequency-discriminator-transistor amplifier was completed in May and tests were conducted in June. The basic schematic diagram and photographs of the package are shown respectively in Figs. 16, 17, and 18. The response characteristic of the frequency discriminator is shown in Fig. 19. Figures 20 and 21 are amplifier gain characteristic curves plotted for various transistor beta values and circuit resistance values as indicated by the basic equivalent circuit of Fig. 22 and the schematic circuit diagram, Fig. 23 . Figure is a plot of torque motor current versus alternator frequency for the frequency-discriminator-transistor amplifier package.

A breadboard-type half-wave magnetic amplifier was constructed and tested. After this circuit was modified to give optimum performance, it was determined from further tests that a half-wave magnetic amplifier is not capable of providing adequate feedback system gain. A full-wave configuration is planned for future testing, and cores for this unit have been ordered and will be wound in August.

Several start-up and shut-down techniques for the SPTP units and extensions of these techniques to the GEPS and flight units have been considered. There are many system component requirements which make multiple start and stop capabilities a difficult task to achieve. After considering these factors in detail, the following conclusions were drawn, based on present component developments and information, and on probable advances in state-of-the-art component developments. It should be understood that though many alternatives exist, the approach suggested in each case is felt to be satisfactory and feasible.

1. It is expected that the bearings will require lubrication at all times. To accomplish this an auxiliary supply is proposed which will provide 200 psia mercury to the bearing sockets, while the same quantity of mercury is removed from the bearing drain lines, thus maintaining total system inventory at a constant level. By means of two simple check valves, this supply can be made to operate only when the shaft-driven pump is operating at reduced speed.

2. It is required that the turbine and alternator cavities be free of liquid prior to and during start-up. This can be accomplished by preheating the cavities and by relying on the labyrinth seals to restrict the flow of mercury into the turbine and alternator cavities. This approach will also reduce the effects of thermal shock and possible condensation of vapor to liquid when the mercury is initially fed to the turbine.

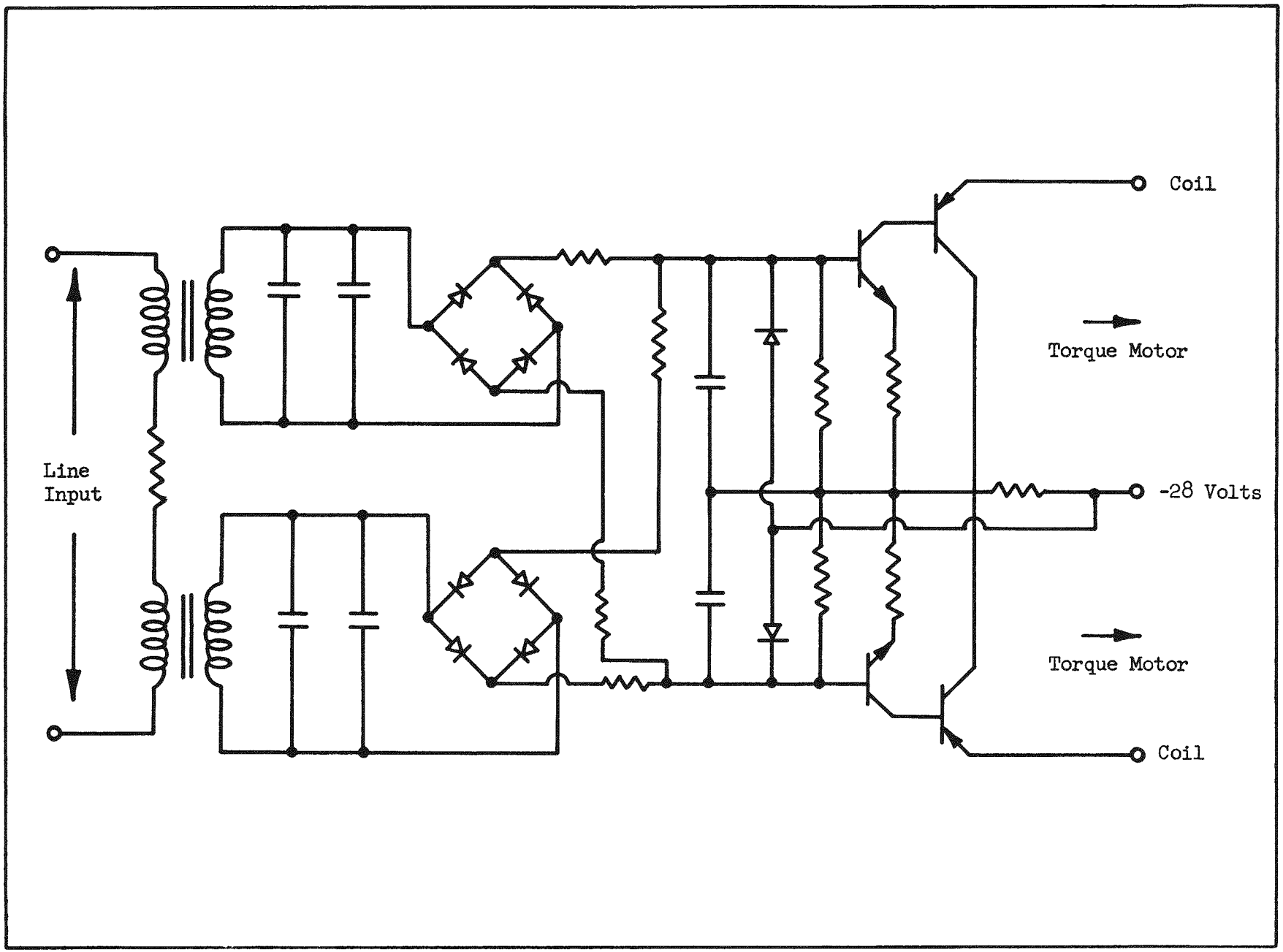

Fig. 16. Discriminator - Amplifier Schematic

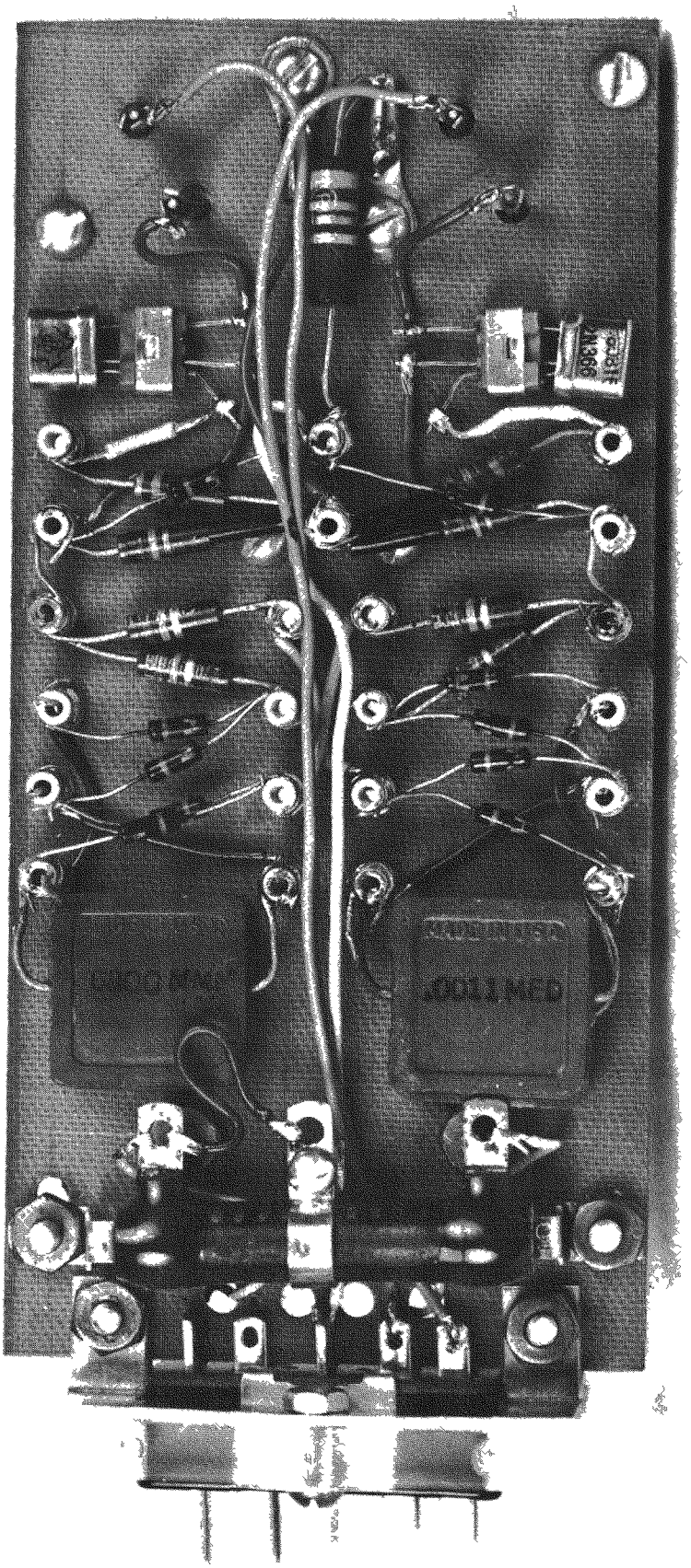

Fig. 17. Frequency Discriminator-Transistor Amplifier Package
Bottom View

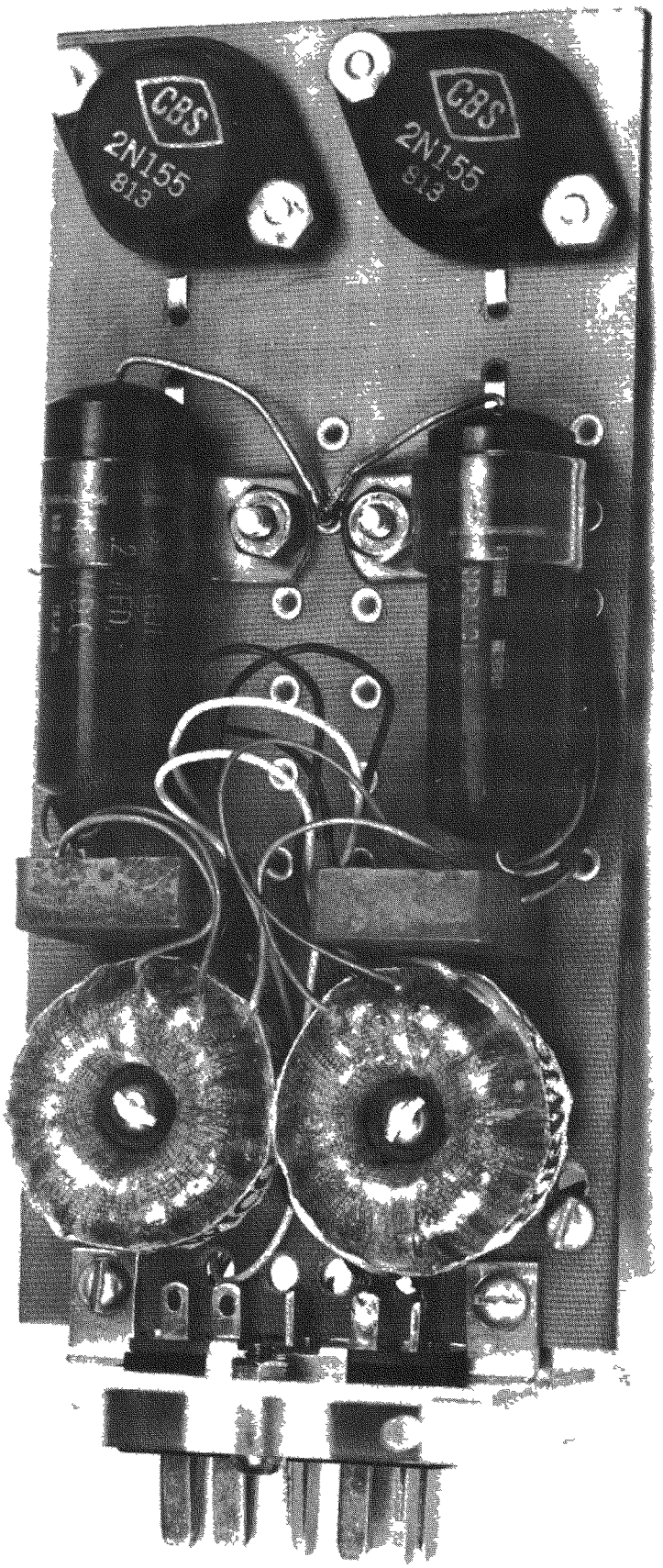

Fig. 18. Frequency Discriminator-Transistor Amplifier Package Top View

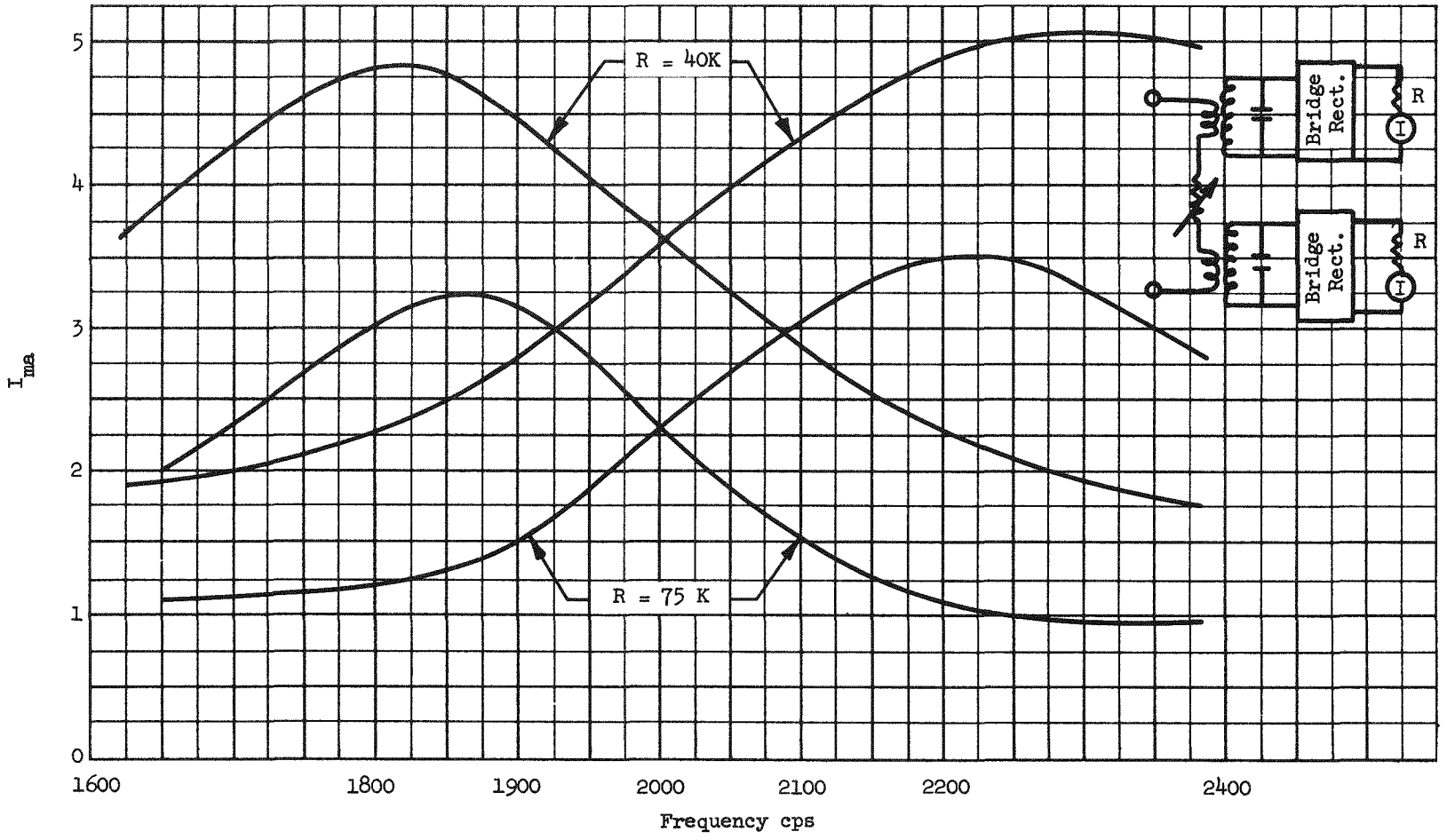

Fig. 19. Current Through Tuned Circuit Loads versus Frequency

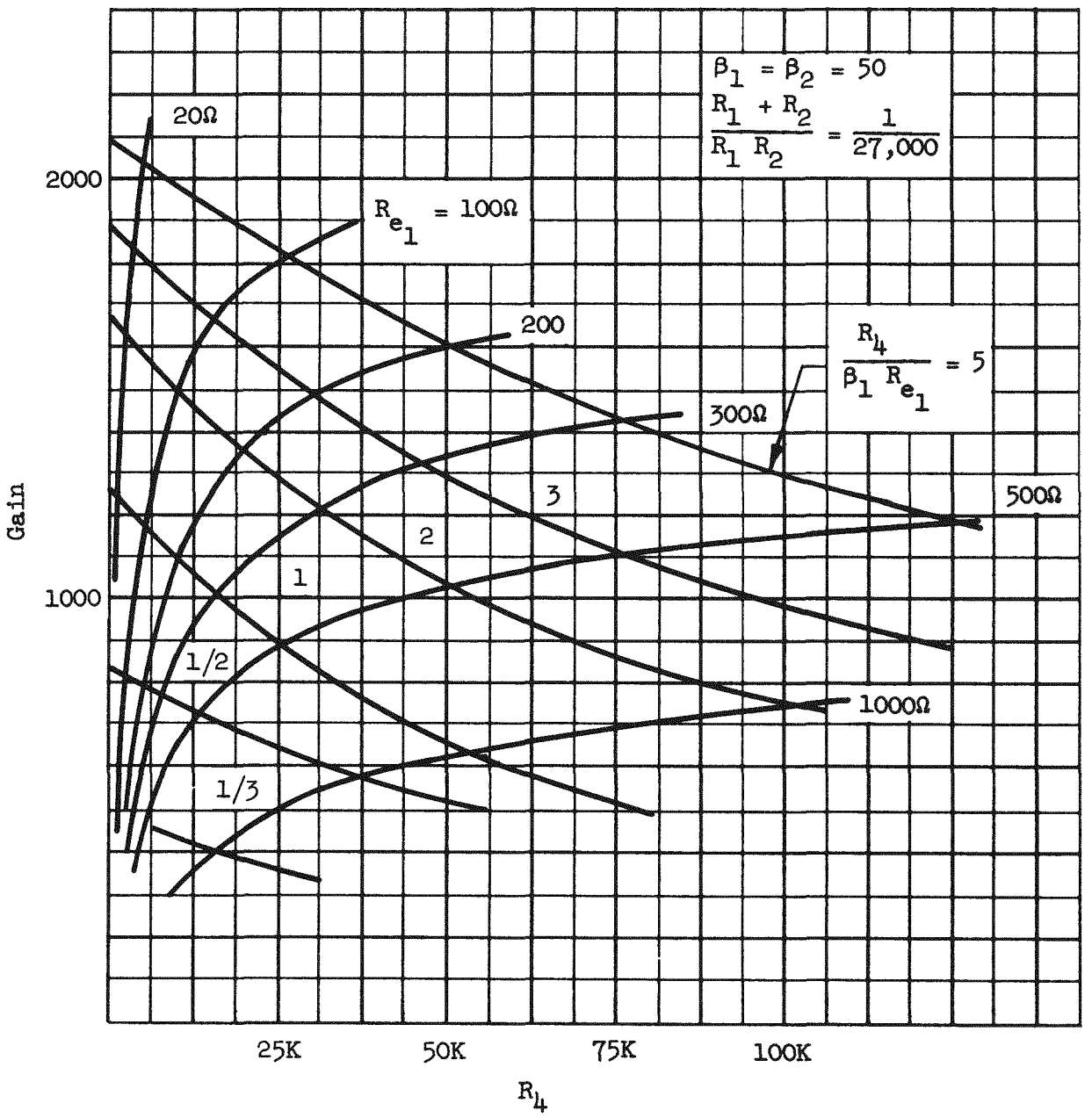

$$\text{Gain} = \frac{1 + \frac{R_1 + R_2}{R_1 R_2}\ \beta_1 R_{e_1}\ \frac{R_4/\beta_1 R_{e_1}}{R_4/\beta_1 R_{e_1}}}{/+\ R_4/\beta_1 R_{e_1}} \quad /+\ R_4/\beta_1 R_{e_1}$$

Fig. 20. Amplifier Gain Characteristic Curves

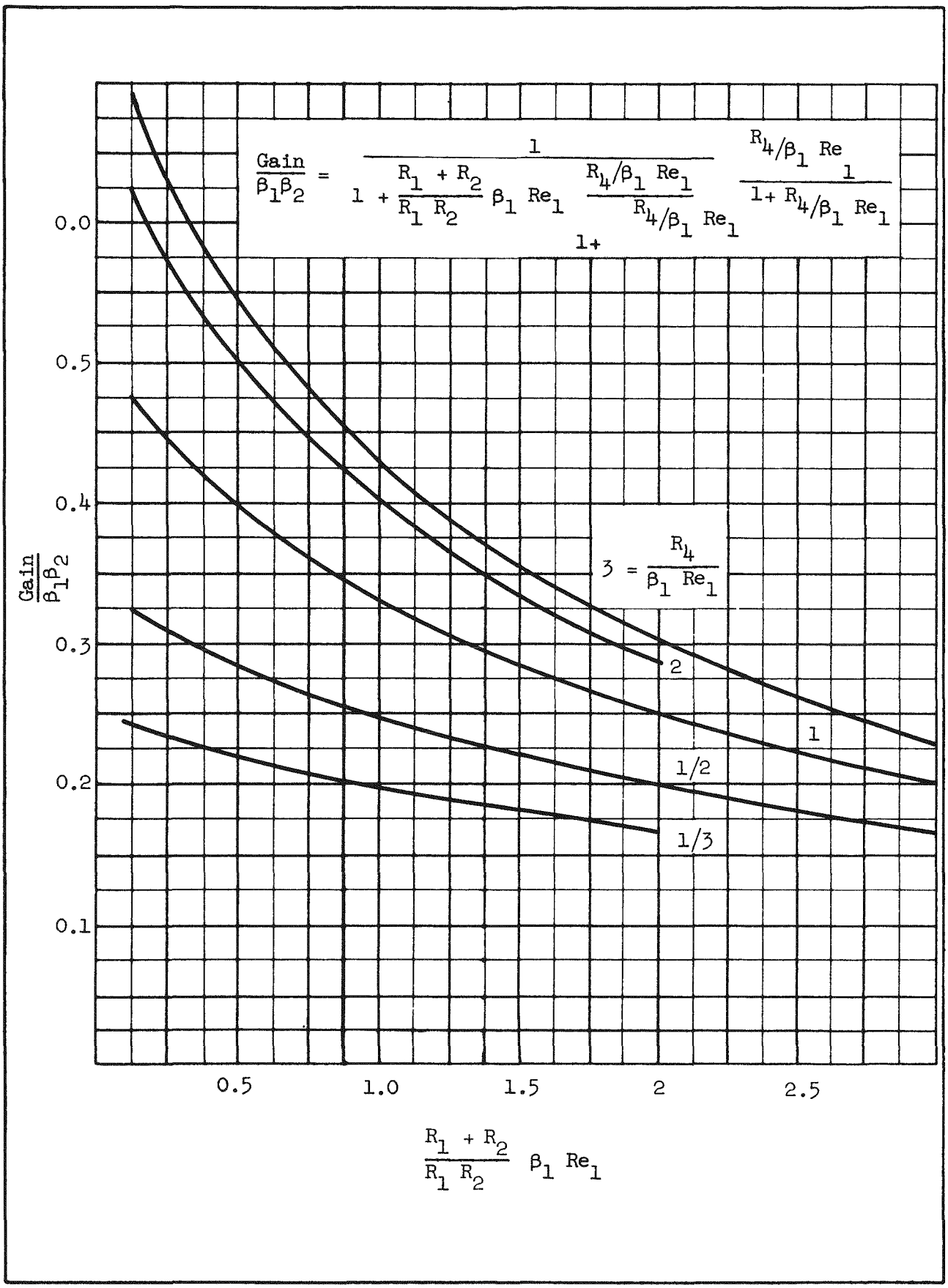

Fig. 21. Amplifier Gain Characteristic Curves

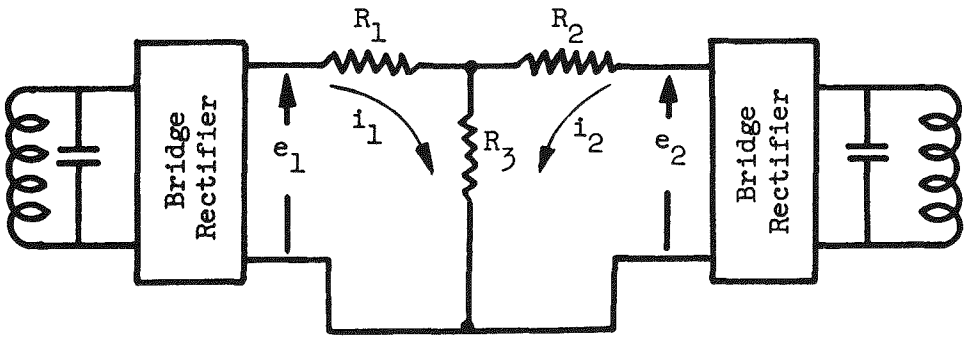

Fig. 22. Equivalent Circuit

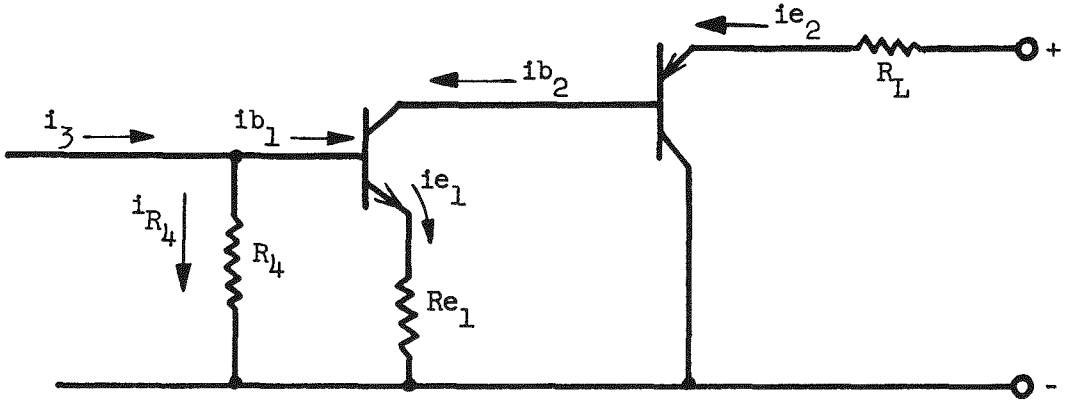

$$\beta_1 = \frac{ie_1}{ib_1} \qquad \beta_2 = \frac{ie_2}{ib_2}$$

$$R_3 = \frac{\beta_1 \, Re_1 \, R_4}{\beta_1 \, Re_1 + R_4} \qquad ie_2 = \beta_1 \, \beta_2 \, ib_1$$

$$ib_1 = \frac{i_3}{1 + \beta_1 \, \frac{Re_1}{R_4}}$$

Fig. 23. Schematic Circuit Diagram

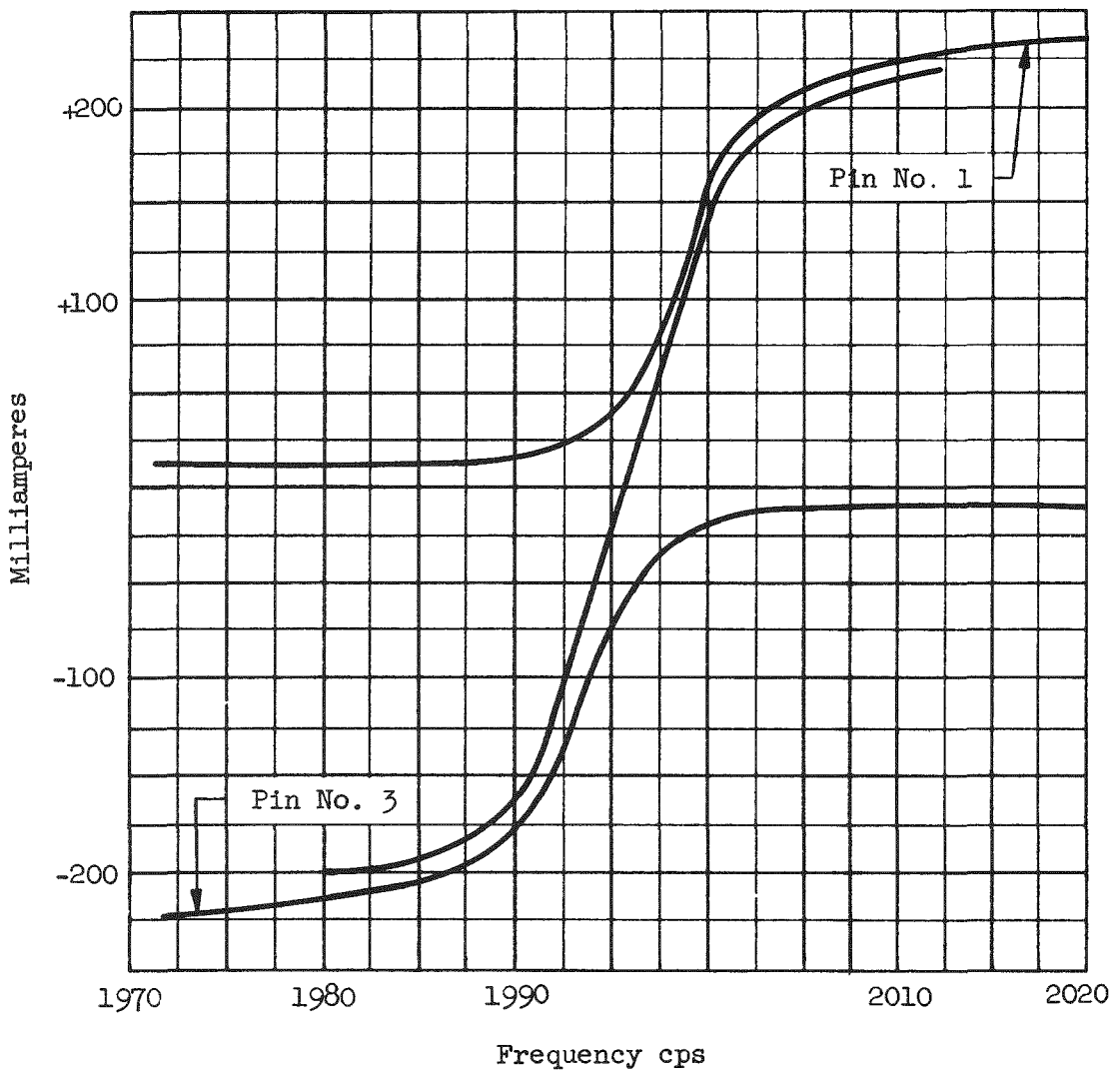

Fig. 24. Output Current versus Frequency

3. Some method of inducing rotation is required. To accomplish this it is desirable to operate the alternator as a motor to accelerate the unit to approximately 30,000 revolutions per minute. This will require a variable frequency power supply to bring the unit up to speed while operating as a synchronous motor. The rate at which acceleration is accomplished may be programmed and controlled by a suitable servo timing system. Alternator motoring will eliminate the need for an external bearing mercury supply if an internal accumulator is employed.

4. It is required that the system pump be under a slight head (2 psia min) at all times. To insure that mercury is available and the cavitation problem is held to a minimum, the pump shaft line of center will be located at least four inches below the liquid level of the system. This will also assist in sustaining pump operation during launch.

5. A suitable electrical load is required along with certain switching devices to control the transition between alternator motoring and generation. The switching will be controlled by a speed-actuated relay which will disconnect the variable frequency generator and switch in a "stabilizing load." The "stabilizing load" can be a series resonant circuit which will tend to provide a power balance within the system at about 40,000 revolutions per minute. The stabilizing load will resist any tendency for the system to run away on acceleration and will be replaced by a constant power load designed by Lockheed once the system reaches a state of reasonable dynamic equilibrium.

E. ALTERNATOR

1. Radial-Gap Alternator

The radial-gap alternator, which is intended to be the Prototype Unit, was designed, fabricated and tested. Figure 25 is a photograph containing the wound stator and the rotor with its retainer sleeve. A curve of voltage regulation versus load at unity power factor is shown in Fig. 26. The total harmonic distortion at no load was less than two per cent; and at rated load and unity power factor, the distortion was less than five per cent. These tests, however, were performed without a protective metal sleeve between the rotor and the stator.

A program was initiated to evaluate materials that may be used in lieu of the metal sleeve presently used to protect the stator windings from the mercury vapor atmosphere within the package. Although most of the materials proved unsatisfactory, several glass compounds showed promising results. This program will continue.

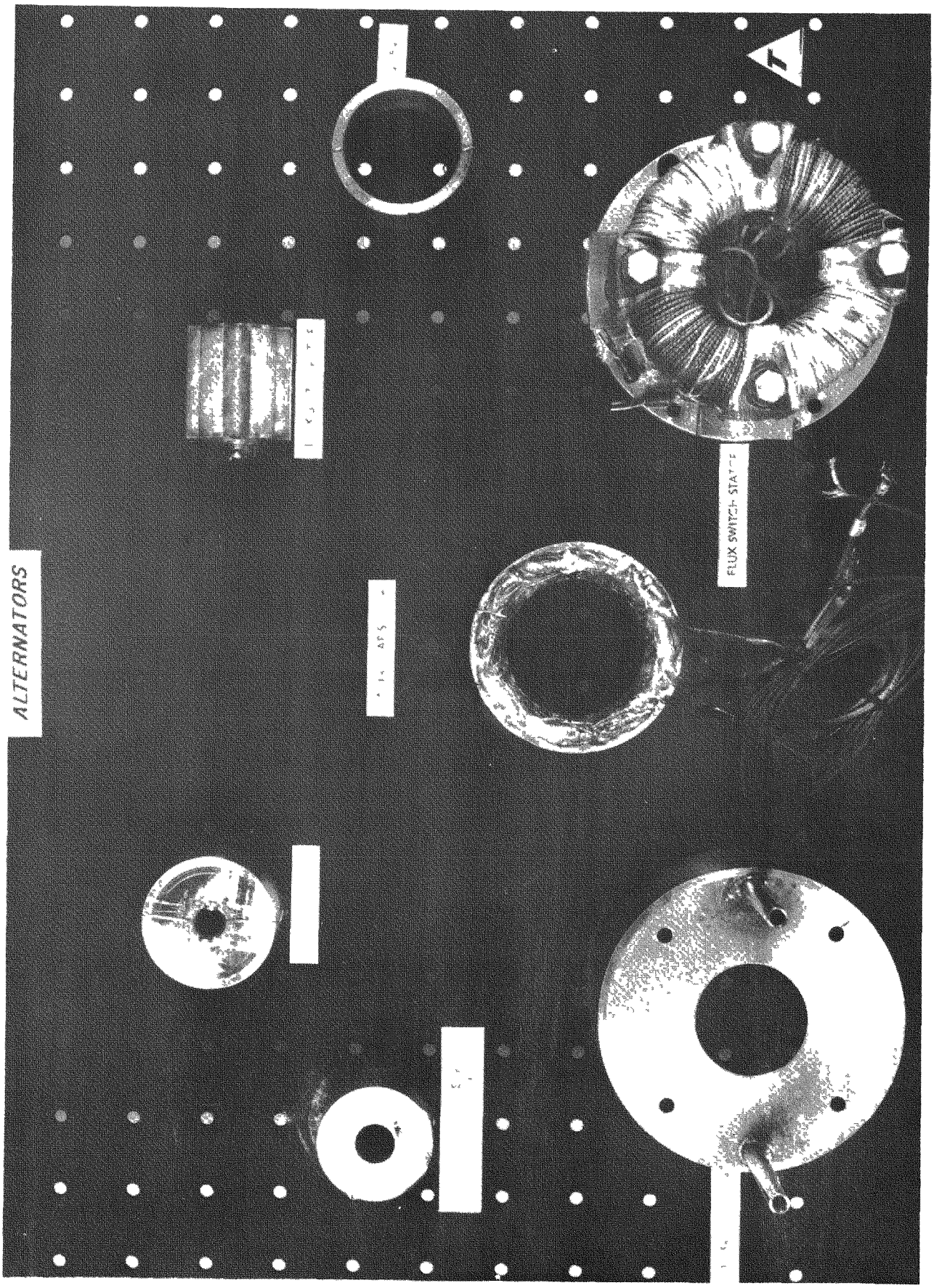

Fig. 25. Alternator Parts

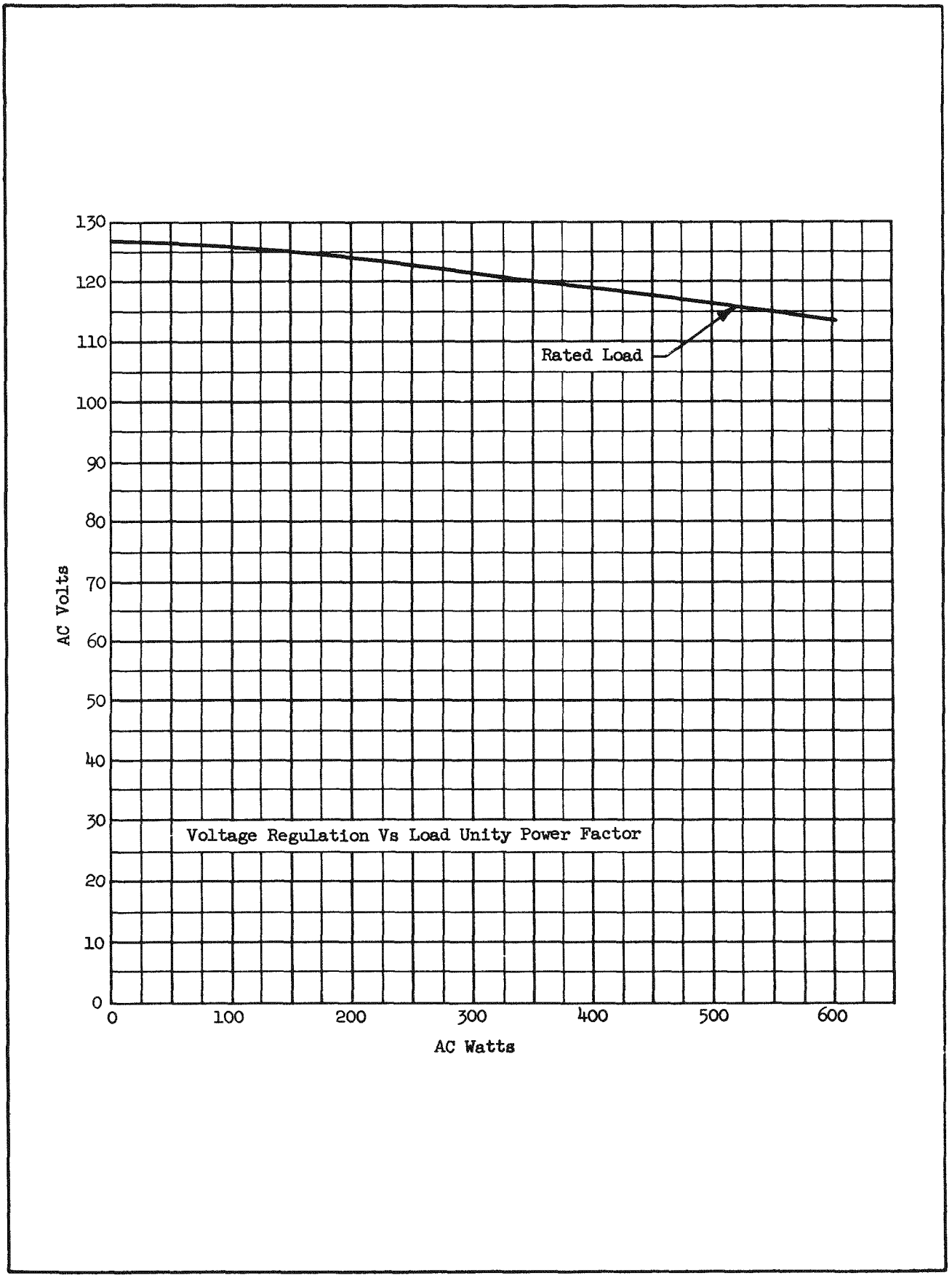

Fig. 26. Radial Gap Alternator

Another method of protecting the windings is the use of a completely closed stator slot lamination. These laminations have been designed and ordered. A stack with this configuration will be fabricated and tested.

Rotors, both with and without shrink rings, have been tested to speeds above 52,000 revolutions per minute, without failure or detrimental effect.

The alternator test rig was also modified to accommodate the radial-gap unit. The shaft was shortened to minimize bearing overhang and subsequent rotor runout.

A study has been conducted to determine the availability of dynamometer equipment for efficiency testing of the alternator. Due to the high speeds and low torques involved, no available commercial dynamometers are deemed suitable for the requirement. The recommended course of action is to build a dynamometer, using a high frequency induction motor. By trunnion mounting the induction motor housing, the alternator torque would be measured.

F. MATERIALS EVALUATION

The metallurgical analysis of the 1010 steel and the stainless Type 446 loops, which were tested for 100 hours at 750 degrees Fahrenheit, has indicated that no significant corrosion or mass transfer occurred. The more significant test data are summarized briefly as follows:

1010 Carbon Steel Loop (100 Hours):

	Boiler	Condenser
Specimen weight before test, grams	210.622	211.245
Specimen weight after test, grams	210.569	211.214
Weight loss, grams	0.053	0.031
Corrosion rate, inches per year	0.0022	0.0032
Change noted by microscopic examination	None	None

Weight loss is considered insignificant

No foreign metal particles were noted in the mercury. Dissolved metals noted in mercury were small quantities of zinc (believed to have been introduced during cleaning) and iron.

Type 446 Stainless Steel Loop (100 Hours):

	Boiler	Condenser
Specimen weight before test, grams	208.813	208.029
Specimen weight after test, grams	208.873	208.062
Weight gain, grams	0.060	0.033

Weight gain is considered insignificant

Some oxidation was noted which may account for the weight gains. No change was noted by microscopic examination. No foreign particles were observed. Dissolved iron appeared in the mercury after the run.

These two 100-hour corrosion tests were used to establish a testing procedure. Evaluation revealed a need for further refinement of the methods of sample preparation, insulation, and instrumentation. Coordination with The Martin Company led to test rig modifications and a revised test procedure. One of the modifications made was the improvement of the loop insulation by installing the loop between two slabs of insulation, as illustrated in Fig. The development of the test procedure and test program were fully coordinated with The Martin Company to insure results consistent with the needs of both Martin and Thompson.

Installation of fittings and air ducts for concurrent testing of eight loops was completed. Test loops of Type 316 stainless steel and Croloy 5 Si have been fabricated and are ready to be tested.

A report has been written, summarizing the reasons for material choices on the TATP unit. An expansion of this effort is also being conducted to define material choice possibilities for the prototype units and the mercury conditions to which the various materials are subjected.

Several silicone rubber and epoxy materials were tested at 550 degrees Fahrenheit and 230 psi pressure in static liquid mercury. None of these materials tested were found to be acceptable for this program. The existence of material limitations was clearly indicated.

Tests were conducted in an effort to find materials satisfactory for protecting silver soldered transducer diaphragms from mercury. No satisfactory materials or coatings were found.

G. CONDENSER

In preparation for the design of the simple condenser model, all analytical work to date was reviewed. These analytical studies included

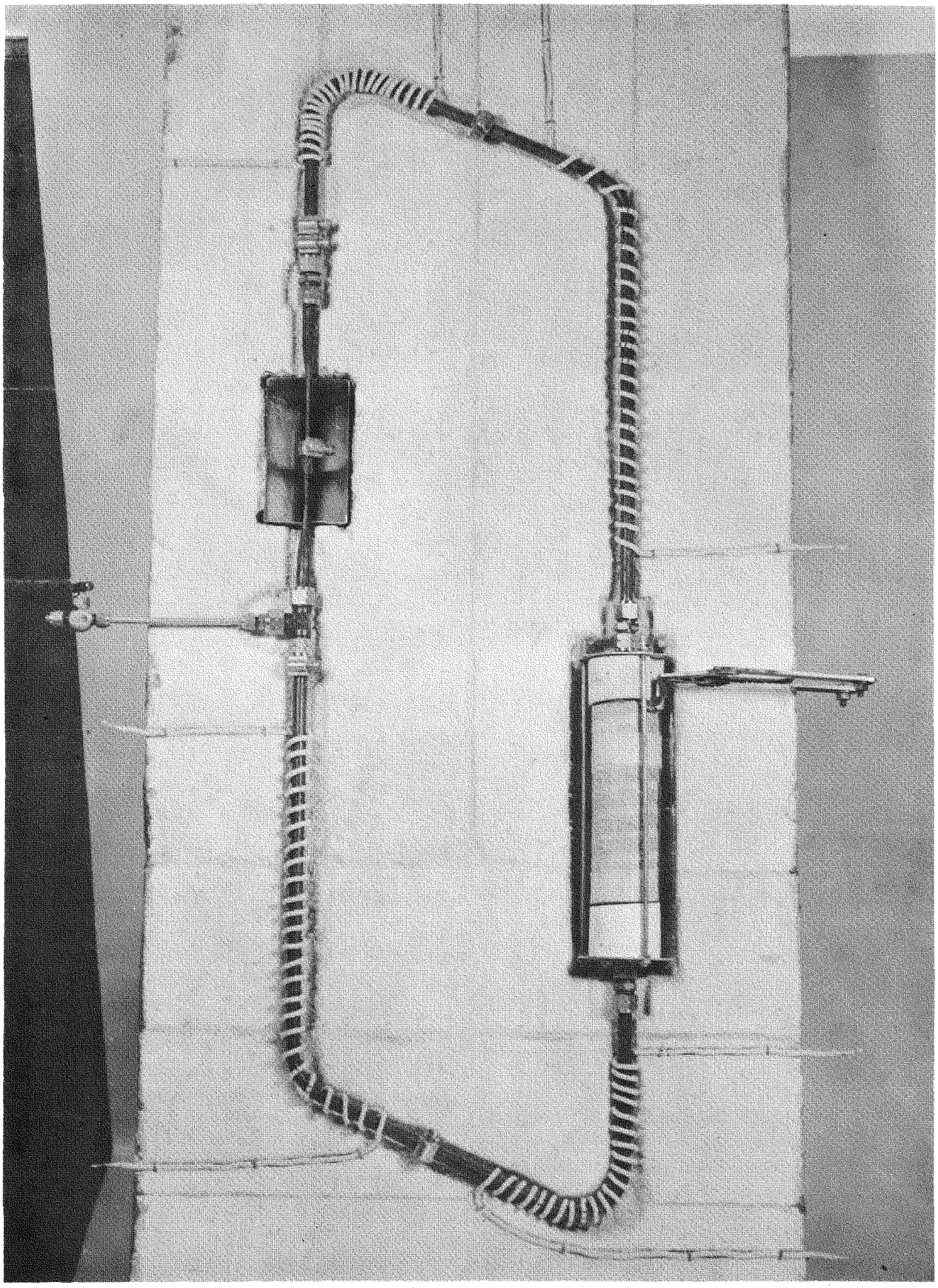

Fig. 27. Materials Test Loop

IBM 650 computer energy and momentum studies for both stratified and fog flow conditions considering fluid phase change for flow through both tubes and flat plate ducts. Pressure drop as a function of heat rejection rate and condenser geometry were evaluated for flat plate designs. A correlation of inventory as a function of condenser geometry was also made. From these studies a simple condenser model and auxiliary test apparatus were designed and fabricated. The experimental test model consists of a rectangular flat plate condenser (3 feet long x 1 foot wide x 1/8 inch thick) with one surface insulated and the other side cooled by forced convection with air. The heat transfer area of the condenser is one quarter of that anticipated for the system condenser, and the convection heat transfer is similar to the equivalent calculated radiation coefficient. The following data can be obtained from the test rig:

1. Air temperature at two-inch intervals in the direction of air flow;

2. Mercury temperature or pressure taps at three-inch intervals in direction of mercury flow;

3. Air flow measured by a sharp edge orifice;

4. Mercury vapor flow measured by a calibrated choked flow nozzle;

5. When the condenser is operated in the vertical position, the liquid level observed by a sight glass;

The purpose of the flat plate condenser tests is fourfold:

1. To determine the effects of condenser heat transfer area, air side heat transfer coefficient, and air temperatures on condenser pressure level;

2. To obtain condenser mercury heat transfer coefficients;

3. To obtain pressure drop over a range of operating conditions;

4. To observe the maximum pressure variations at condenser exit when condenser is operated in various orientations.

All detail drawings for the condenser test model were completed on June 11, 1958. As of June 30, 1958, all test model components were fabricated or received from vendors with the exception of Swagelok fittings and two minor machining tasks on the air duct. Figures 28 and 29 are photographs of the condenser and cooling air channel, respectively.

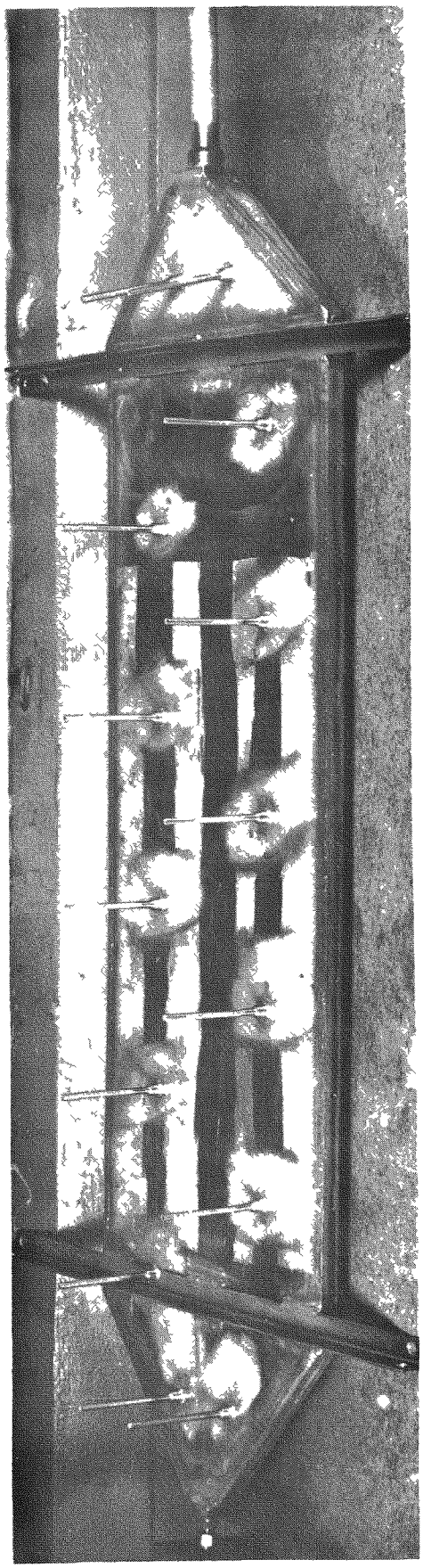

Fig. 28. Test Condenser

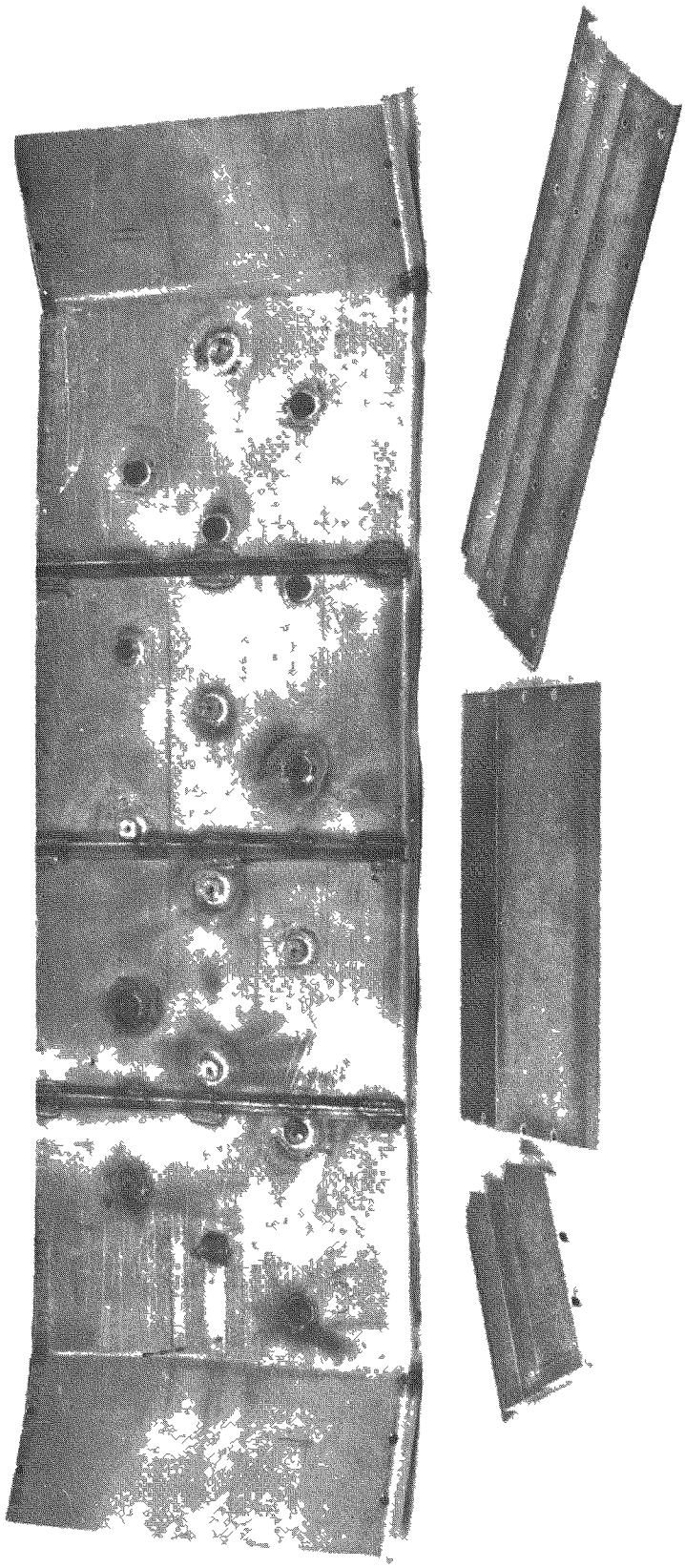

Fig. 29. Cooling Air Channel for Test Condenser

A study of condenser performance when subjected to launch acceleration loads was initiated. The approach used was to modify the momentum equations for stratified flow to include the acceleration force term. The energy, momentum and continuity differential equations in numerical form may be programmed for a digital computer study. The direction of the acceleration forces during launch and at various positions along the vehicle trajectory were also considered and may be incorporated as force vectors to be used to modify the momentum equations. If these analyses were used in a computer study, it may be possible to establish an indication of both pressure drop and mercury inventory at various points along the trajectory for a condenser in which the condensing phenomemon is satisfied by the mathematical model.

General analysis of condenser geometry indicates that for any practical configuration, the pressure drop will be excessive for fog flow. Detailed analysis of a packed bed mercury condenser indicates that low pressure drops are obtainable in a porous bed. An analysis was made to determine the condenser-subcooler demarcation zone in a heat exchanger and to study the stability of the demarcation zone when the condenser is subjected to external forces. It was concluded that the demarcation zone between condenser and subcooler is determined by mercury inventory and flow regime. The zone may be unstable if external forces are imposed. A stable zone is important since an increase in condenser area and corresponding decrease in subcooler area may cause the pump to cavitate due to low pump inlet pressure and high liquid temperature.

H. BREADBOARD TEST PROGRAM

1. Test of TATP

Following the installation of the Turbine Alternator Test Package (TATP) in the breadboard system on May 5, 1958, a series of hot and cold mercury static bearing tests were conducted and the unit was run on nitrogen gas. A maximum operating speed of 20,060 revolutions per minute was attained. Operation on hot mercury vapor was next conducted at rotational speeds up to 17,500 revolutions per minute with 138 psia, 930 degrees Fahrenheit mercury vapor. This test was discontinued due to reductions in bearing socket pressure.

In June, calibration of the turbine nozzle was initiated but discontinued because of a turbine line heater failure. At this stage in the test program, the TATP was received (June 13, 1958) by the test group and installed in the breadboard on June 14, 1958. On June 16, 1958, the installation was completed, the system was checked out, and a cold mercury static bearing test was conducted.

The TATP was set up for hot mercury operation and a hot mercury static bearing test was conducted on June 18, 1958. On the following day, the unit was operated on hot mercury vapor. In this test difficulty was encountered in bringing the turbine up to speed due to excessively tight bearing clearances. A maximum speed of 7200 revolutions per minute was achieved. At this time it was noted that excessive bearing torque was required and the test was discontinued.

The test setup was modified to incorporate the equipment for calibrating the TATP turbine nozzle. A calibration test was conducted on June 24, 1958. This test was limited to 1000 degrees Fahrenheit due to line heater capacity. Analysis of data is still in process.

The test setup was dismantled and a bearing calibration test fixture was installed in the breadboard. This bearing fixture permits checks of bearing clearances. Tests were conducted on June 25, 1958, which verified that the bearing dimensions and clearances on the TATP rotor and bearing sockets gave flows and socket pressures within the limits previously established by the bearing tests.

The TATP was then installed in the test rig for mercury vapor testing. This test was conducted as follows:

Hot Static Bearing Tests were first conducted. With flow to both bearings supply pressures ranged between 238.3 and 245 psig, the socket inlet pressures between 107.5 and 140.1 psig, and the total flows between 9.7 and 12.1 pounds per minute. The mercury supply to each bearing was alternately closed off and data were recorded. With flow to the alternator end bearing only, the socket inlet pressures were between 24.7 and 29.4 psig and the flow was between 7.6 and 8.2 pounds per minute. With flow to the turbine end bearing only, the socket pressures were 22.7 and 30.6 psig, flows were 6.0 and 6.8 pounds per minute. The turbine inlet valve was opened and the turbine speed was raised to 24,000 revolutions per minute. After 15 minutes of stable operation, the speed was raised to 30,000 revolutions per minute. For approximately two hours the speed was then varied between 30,000 and 45,000 revolutions per minute and eight data points were recorded. At 31,000 revolutions per minute the turbine inlet pressure was 128.8 psig and the temperature 1226 degrees Fahrenheit. The exhaust temperature was 501 degrees Fahrenheit at 25.8 inches Hg vacuum. At 40,000 revolutions per minute, the inlet pressure was 180.9 psig at 1248 degrees Fahrenheit, 505 degrees Fahrenheit exhaust, at 25.9 inches Hg vacuum. Turbine interstage pressure data could not be obtained due to malfunction of pressure indication. Total power output data are still being analyzed. To obtain verification of alternator and bearing power consumption, two spin-down tests were made; the first with full alternator load and the second with no alternator load.

Additional static bearing data were recorded to conclude testing.

Over-all results of this test are being evaluated. The major result presently available is verification of turbine mechanical design and freedom from critical shaft speed problems. Demonstration of successful bearing operation under prototype operating conditions is also an important factor.

2. Second Breadboard Test Rig

The components of the second breadboard test rig for which funds were made available were procured.

I. PROTOTYPE DEVELOPMENT

During the last week in June and the first week in July, TATP-1 was installed in the breadboard test rig and operated successfully. The unit was operated at design speed, or above, for one hour. Peak turbine inlet temperature and pressure reached were, respectively, 1290 degrees Fahrenheit and 223 psia. Data reduction has not been completed at this date, and no detailed test results are available.

A description of this test run is also presented in Section J of this chapter.

During the first week of May, the Turbine Alternator Test Package was installed in the breadboard test rig. During cold mercury static bearing tests, bearing pressure changes were noted, indicating the possibility of film buildup on bearing surfaces.

A nitrogen run-up test at ambient conditions was conducted and data were recorded at 7,880, 10,650, 10,310 and 10,340 revolutions per minute. This series of tests was discontinued, however, due to a combination of film buildups and bearing scoring.

During the second week of May, additional precautions were taken in both the laboratory and shop to insure that impurities and foreign materials would be eliminated from affecting future test work. The package was reassembled after ultrasonic cleaning of parts. A hot nitrogen test followed, during which the unit was operated to 20,000 revolutions per minute. Speed fluctuations occurred at this shaft speed and were later attributed to bearing surface contact. Bearing pressures remained constant while the package was heated from 100 to 500 degrees Fahrenheit, indicating that differential thermal expansion had negligible effect on bearing clearances.

After interpreting the expansion effects, it was decided to run the mercury vapor test without making changes to the unit.

The package was heated to 500 degrees Fahrenheit and the bearing mercury temperature was 300 degrees Fahrenheit. The unit started easily at low mercury vapor pressures and was operated for 36 minutes. During this time, data were recorded at speeds of 6,000, 8,000, 14,000 and 17,500 revolutions per minute. An attempt to reach 20,000 revolutions per minute was made, but socket pressures dropped to a low level (50 psig), and it was decided to stop the test after reaching 19,900 revolutions per minute.

During the third week of May, as a result of disassembly difficulties, design changes of the nozzle nut, alternator lead fittings, and alternator and bearing drain fittings were made. The inability of the mercury vapor superheater to supply 1300 degrees Fahrenheit inlet vapor was also investigated.

Inspection of the package showed that the bearing spheres and sockets were scored. Other important diametral fits and clearances remained constant. Thread galling was evident, however, wherever two soft materials were in contact.

The bearing shaft was sent out for tungsten carbide flame-plating after removing score marks. Mated pairs of sockets and shafts of several combinations of materials and finishes were ordered.

During the last week of May, the spare nozzle was prepared for a mercury vapor calibration.

Data reduction was completed of test data from the mercury run of TATP. Analysis of turbine data on the first test was limited because saturated mercury vapor conditions prevailed at the turbine inlet.

The TATP test program was reviewed and a decision was made to use a blue-chip shaft and a set of electrolized chrome-plated sockets. Data obtained on the free running test rig were used as a guide in establishing test conditions.

Data analysis from the first mercury vapor test established axial and radial shaft load, but over-all performance was in question, since flow stability was not achieved. However, because of this analysis, greater radial load requirements were recognized.

Additional capacity from the Sorgel transformers was incorporated into the breadboard test rig to provide superheating requirements for the turbine inlet Hg vapor line.

During the second week of June, TATP schedules and objectives were reviewed and re-established.

Test Package TATP-2 was released for fabrication, to be completed by June 30, 1958. Additional shafts and sockets were ordered; these to cover any successful free-running rig configurations.

Installation of the TATP test package into the breadboard was delayed because of thermocouple fracture. The test was rescheduled and the unit disassembled for thermocouple repair.

During the third week of June, the unit underwent static bearing flow tests. The low flows encountered were attributed to extremely tight radial clearances (0.0001 inch). An attempt to evaluate the effects of bearing pressure fluctuation was discontinued because of condenser inlet valve leakage.

It was decided to conduct a hot mercury test, even though radial clearances were small. Data were recorded at 3000 revolutions per minute with mercury vapor as the working fluid. However, the unit stopped after several minutes. Several starts were made, but the unit came to a stop each time. In the final test a speed of 7300 revolutions per minute was reached, but indications of excessive bearing torque caused the test to be terminated.

No difficulty was experienced in the teardown and inspection of the unit. All parts appeared to be in good condition.

Review of bearing configuration requirements was made and recommended clearances established and agreed upon with the bearing group.

A Plexiglas bearing test flow fixture was designed to evaluate and eliminate bearing flow and clearance difficulties prior to assembly of the actual unit. This bearing test fixture was employed in a static bearing test. Data obtained agreed with previous bearing test rig data, indicating that suitable TATP bearing clearances had been achieved.

A TATP assembly and test schedule was prepared.

Heat losses between the superheater and throttle valve prevented the mercury vapor from reaching the 1300 degrees Fahrenheit necessary for a good turbine nozzle test. This condition was corrected.

The assembly of TATP-1 was completed. This configuration included established clearances of an ungrooved set of sockets and bearings of the most promising configuration to date. This unit was then installed in the test rig and a brief description of operating experience has been given in the first part of this section.

The TATP-2 package is 95 per cent complete on fabrication of parts, and 85 per cent complete on assembly. Completed TATP-2 parts and sub-assemblies are illustrated in Figs. 30 and 31.

J. BEARINGS

As a result of the design and test program conducted during the last quarter of Fiscal 1958, the bearing performance summarized in Table 6 was attained. Although the state of hydrosphere development as the end of Fiscal 1958 does not permit definite conclusions, tests indicate that a nongrooved socket configuration is desirable for maximum radial load capacity. Performance curves are shown in Fig. 32 based on composite data derived from a number of modified and free-running bearing rig tests. These curves are representative of typical hydrosphere bearing performance and are dependent on axial and radial clearances, as well as on capillary sizes.

Several configurations of the hydrosphere bearing, as listed in Table 7 and shown in Fig. 33, were designed, fabricated and tested. Among these were two different types of hydrostatic padded bearings which were expected to demonstrate significant improvements in radial load capacity. Limited tests have shown that the slight improvement in performance over the end-fed hydrosphere is not sufficient to offset the greater complexity of these configurations of the padded type.

The test program outline in Table 8 included a number of partially successful endurance runs. Premature termination of some of these runs resulted from contamination or malfunction of auxiliary equipment. Replacement of suspected contaminant sources and improved purge-and-fill procedures have minimized the first problem. An air turbine drive has been designed to eliminate the second. These problems, coupled with suspected excessive dynamic unbalance and with failure of plating material in the socket have resulted in the bearing failures listed in Table 9. A high speed balancing machine has been designed to permit dynamic balancing of the rotating assembly on the bearings. Electrolized plating of the sockets has been discarded as unreliable.

A hydrosphere bearing, incorporating an extended shaft to simulate the overhung pump shaft, was designed and fabricated. Changes in the pump-bearing concept made testing of this design to determine effect of pump seal leakage impractical. A new design was placed in the Shop, and fabrication is nearing completion.

Because of anticipated Fiscal 1959 requirements, the new bearing rig, originally intended to test single bearings, has been initiated as a dual (free-running) bearing test rig which will incorporate the

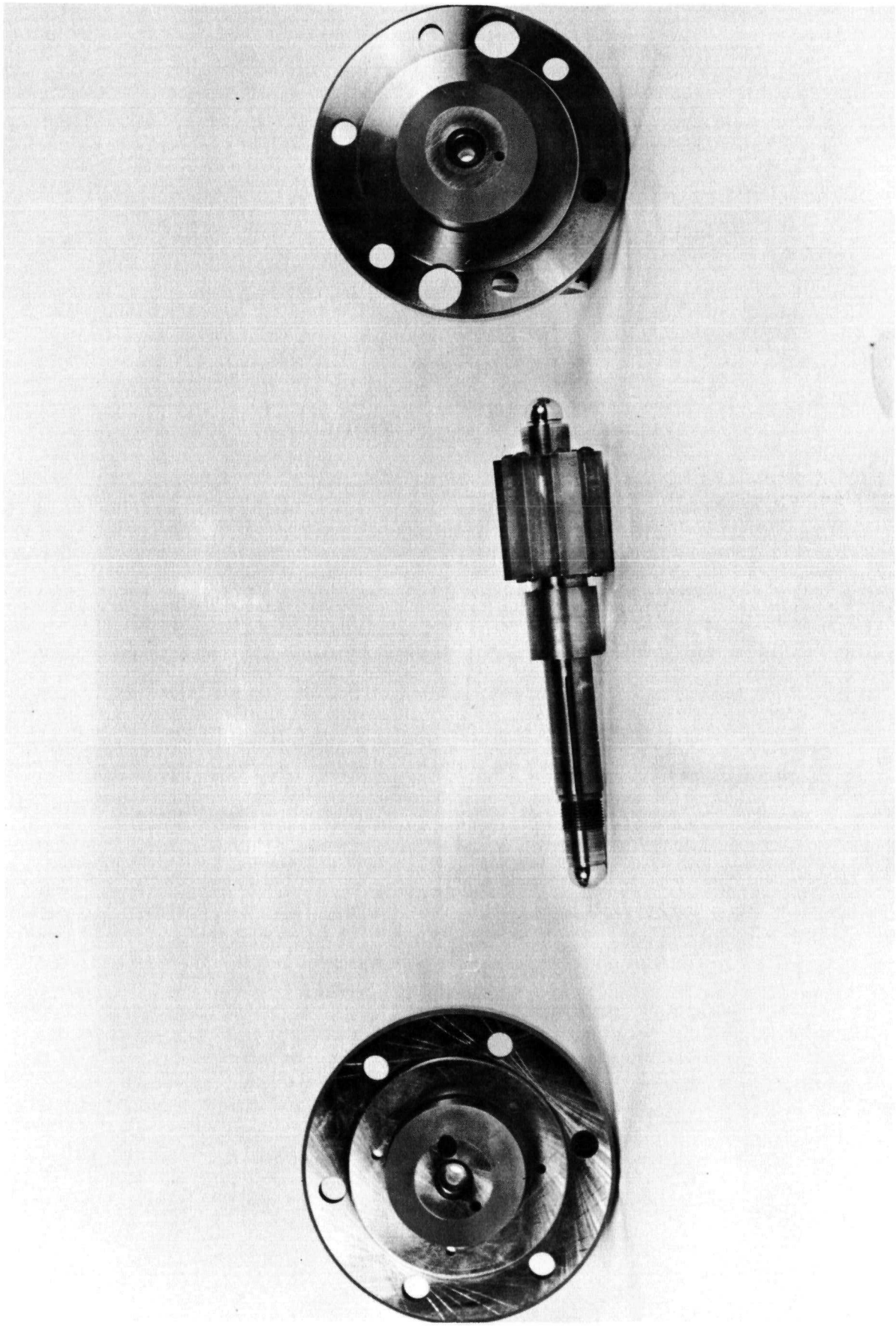

Fig. 30. TATP Number 2 Shaft and Bearing End Caps

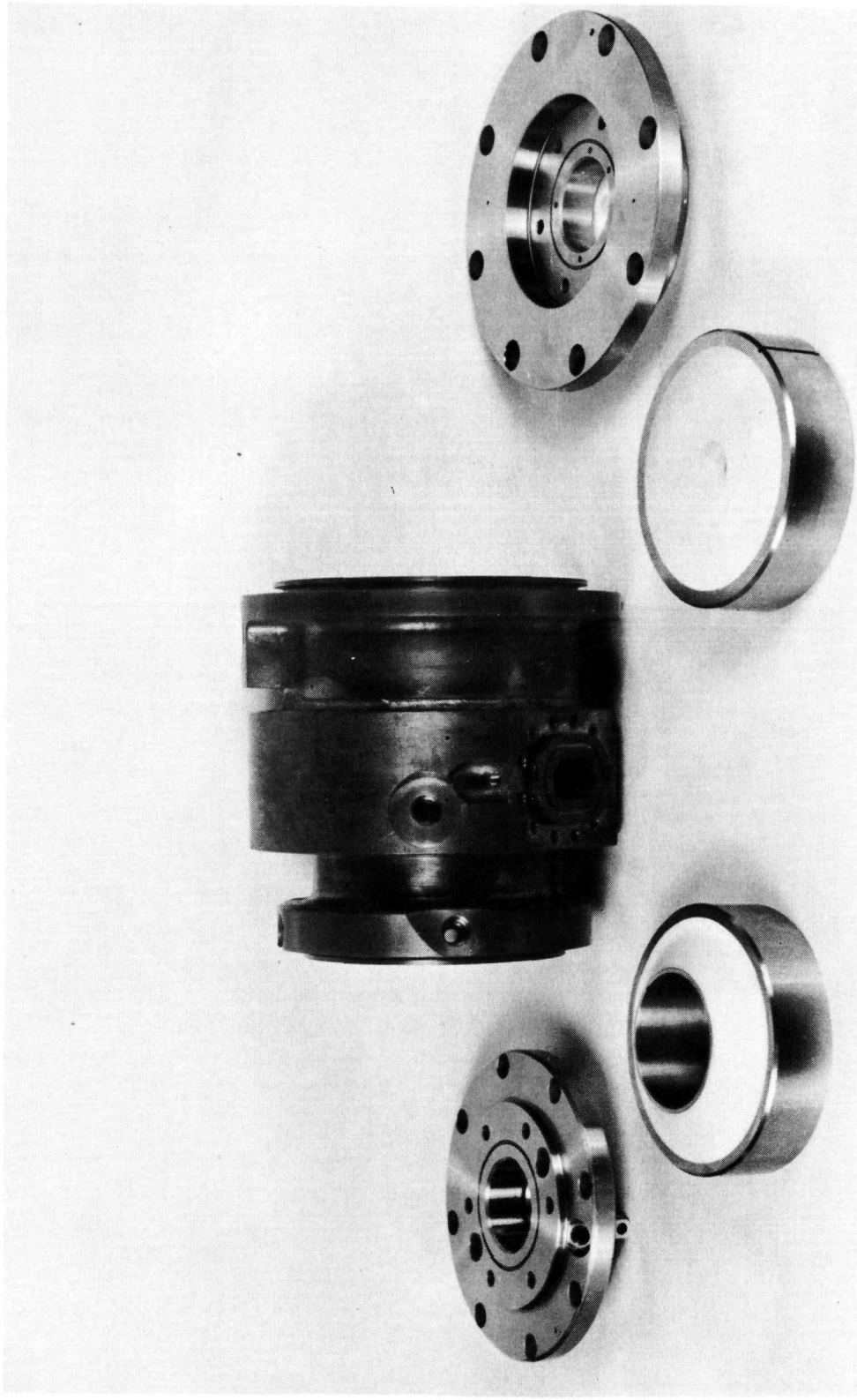

Fig. 31. TATP Number 2 Parts and Sub-Assemblies

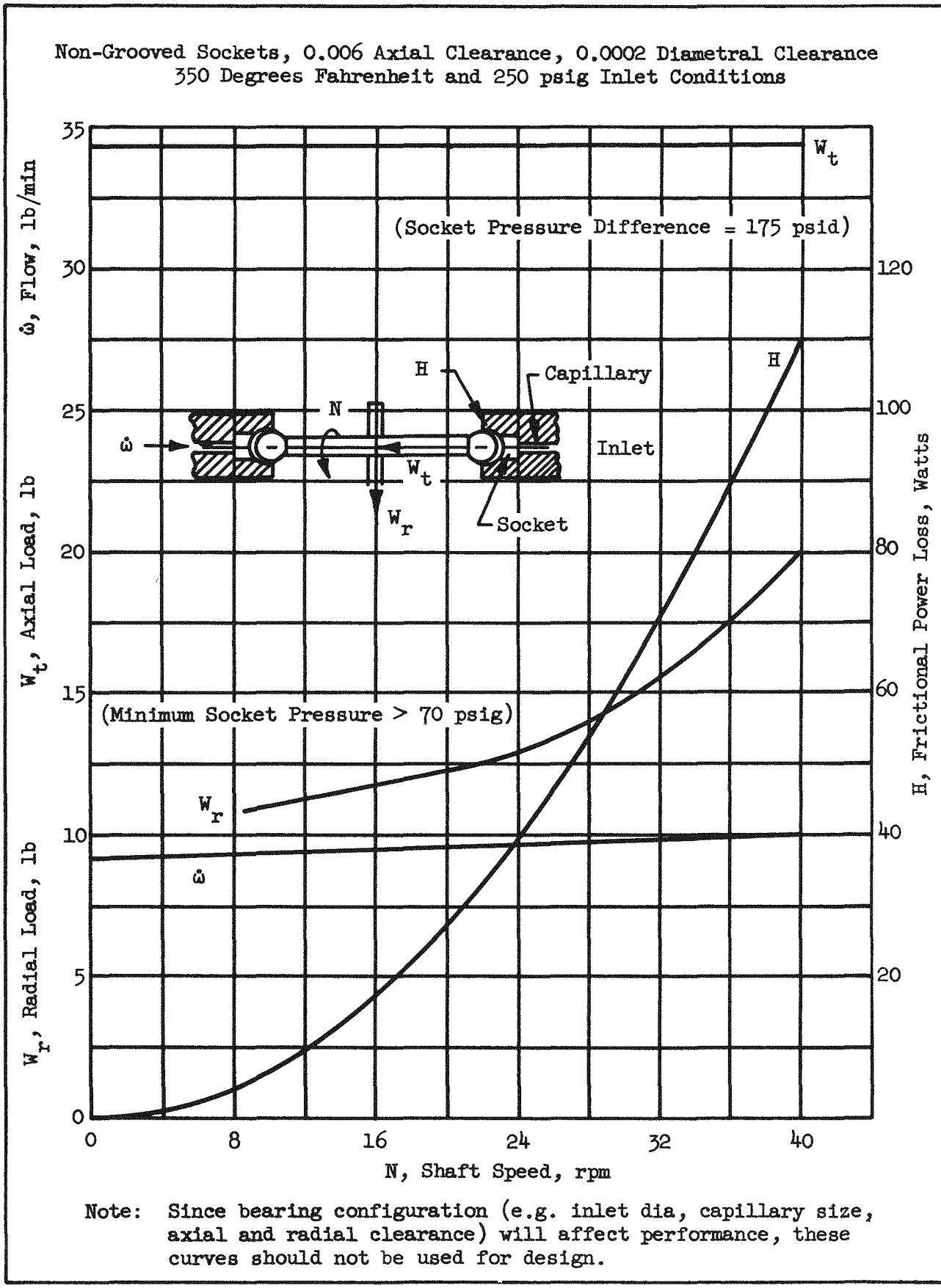

Note: Since bearing configuration (e.g. inlet dia, capillary size, axial and radial clearance) will affect performance, these curves should not be used for design.

Fig. 32. Composite One-Half Inch Diameter Bearing Performance

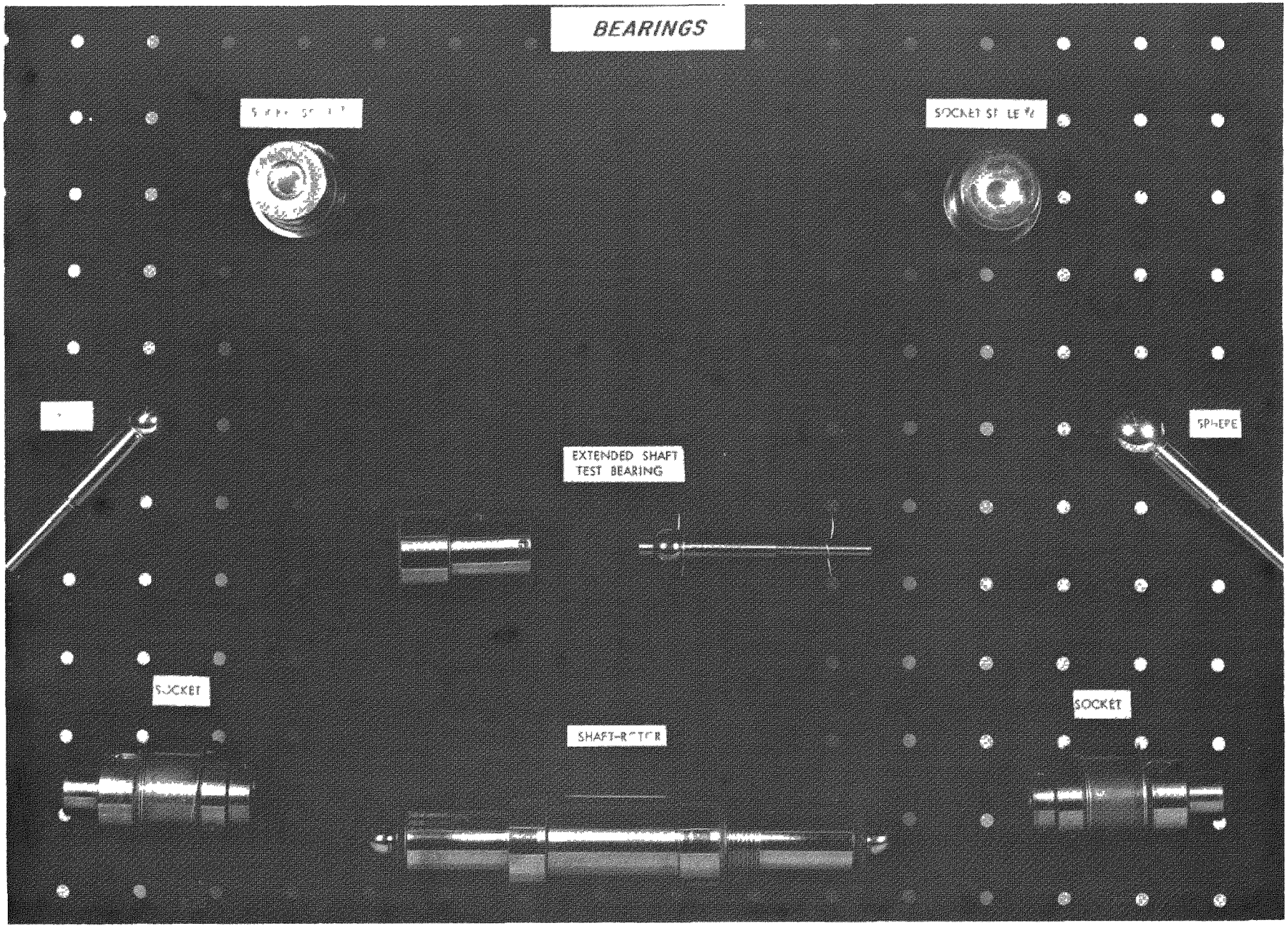

Fig. 33. Various Configurations of the Hydrosphere Bearing

mercury pump, and which will be capable of environmental testing and of testing alternate bearing types. Modifications have been designed and were partially procured to improve the drive and measurements of radial load, torque, and bearing displacement of the modified bearing test rig.

Analysis of short full journal bearings of three different clearance-to-diameter ratios indicated improved radial capacity. Assembly problems relating to alignment capabilities of the present free-running rig have delayed the fabrication and testing of these units.

In anticipation of ultimate unpressurized start-ups and of need for increased resistance to attack by mercury and to scoring, work was initiated to evaluate promising types of anti-friction bearing steels and of cermets. A program has been set up for materials evaluation in Fiscal 1959.

TABLE 6

Bearing Performance

	Specification	Design Objective	Best Single Test[b]	Best Estimated Performance[c]
1	Bearing Size	-	½ inch	½ inch
2	Speed	40,000 rpm	40,000 rpm	40,000 rpm
3	Minimum Axial Load Capacity	32 pounds (a)	20 pounds	32 pounds
4	Minimum Radial Load Capacity	20 pounds (a)	6 pounds	20 pounds
5	Maximum Frictional Power Loss	100 watts	~ 150 watts	~ 120 watts
6	Maximum Flow	10 lb/min	avg. 7 lb/min	~ 5 lb/min
7	Minimum Supply Pressure	250 psig	250 psig	300 psig
8	Maximum Supply Temperature	350° F	175°F	350°F
9	Minimum Life	1440 hours	104 hours	?

Notes:

a. Loads based on predicted system requirements at 8 g acceleration

b. Performance limited by test conditions and recorded values not necessarily ultimate capability. Bearings consisted of unplated "Blue Chip" balls and sockets with concentric radial clearance of 0.0002 to 0.0003 inch and total axial clearance of 0.008 inch. Socket was ungrooved with 30-degree inlet hole. (see Tables 7 and 8) Unit was S/N_9

c. Performance values are based on best currently available MBTR test data. Attainment of this performance in a dual bearing assembly is dependent on solution of design problems associated with dimensional stability and control, mercury cleanliness, materials, capillary size, etc. Improved performance may be attainable with modifications of configuration.

TABLE 7

Hydrosphere Bearing Configurations and Material Combinations

Bearing Size	Material		Concentric Radial Clearance	Socket Configuration			Bearing Serial Number
	Socket	Ball		Inlet (inch)	Groove	Other	
3/4	BC-EP	BC	0	0.53	Standard	Standard Design	F1,8 M11, 18
3/4	BC-EP	Mo	0	0.16	Standard	Standard Design	M12
3/4	BC-EP	Mo arc cast	0	0.53	Standard	Standard Design	M13
3/4	BC-EP	BC-FP	0	0.16	Standard	Standard Design	M14
3/4	BC-EP	BC-FP	0	0.53	Standard	Standard Design	M15
3/4	BC	BC-FP	0	0.16	Standard	Standard Design	M16
3/4	BC	BC-FP	0	0.53	Standard	Standard Design	M17
3/4	BC-EP	BC	0	0.53	Standard	Standard Design	M18
3/4	BC-EP	BC	0	0.16	None	Standard Design	M19
3/4	BC-EP	BC	0	0.53	None	Standard Design	M20
3/4	BC-EP	BC	0.00005	0.31 exit	Padded	1/4 inch diameter pads - 4 - side fed	M24
3/4	BC-EP	BC	0.00005	0.31 exit	Padded	1/16 x 1/4 inch slots - 4 - side fed	M25
5/8	BC-EP	BC	0	0.44	Standard	Standard Design	M21
1/2	BC-EP	BC	0	0.35	Standard	Standard Design	F3
1/2	BC-EP	BC	0.0001	0.35	Standard	Standard Design	F5 M22a
1/2	BC	BC-FP	0.0001	0.35	Standard	Standard Design	F6
1/2	BC	BC-EP	0.0001	0.35	Standard	Tapered Equator	F7
1/2	BC-EP	BC	0.0001	0.25	None	Standard Design	F4

TABLE 7 (Cont'd)

Bearing Size	Material		Concentric Radial Clearance	Socket Configuration			Bearing Serial Number
	Socket	Ball		Inlet (inch)	Groove	Other	
1/2	BC	BC	0.0001	0.25	None	Tapered Equator	F9
1/2	BC	BC	0.0001	0.35	None	Standard Design	M22b
1/2	BC	BC	0.0001	0.35	Wide	0.100 inch wide grooves	M22c
1/2	SS420-Sc	BC	0.0001	0.25	None	Standard Design	F10
1/2	BC-CP	BC-CP	0.0001	0.25	None	Standard Design	F11
1/2	BC	BC-FP	0.0001	0.25	None	Standard Design	F13
1/2	BC	BC-FP	0.0001	0.35	None	Standard Design	F14
1/2	BC	BC	0.0001	0.312 exit	Padded	0.06 x 0.08 inch slots - 4 - ext. shaft	M26
1/2	BC	BC	0.0001	Thin Plate Annulus	None	Extended Shaft	F15
3/8	BC-EP	BC	0	0.27	Standard	Standard Design	F2 M23

Notes:

1. Materials
   BC - 18-4-1 "Blue Chip" High Speed Tool Steel
   EP - "Electrolized" Chrome Plate
   Mo - Molybdenum
   FP - Tungsten Carbide "Flame Plate"
   SS420 - Stainless Steel Type 420
   Sc - "Scottsonizing" Hardened Surface
   CP - Copper Plate
2. Groove - Standard 1/16 Inch Wide to Within 1/16 Inch of Equator
3. Standard Socket Configuration - Hemisphere with Standard or no Grooves
   Single Capillary - End Fed
4. Bearing Serial Number
   F - Free Running Bearing Test Rig
   M - Modified (Single) Bearing Test Rig

TABLE 8

Hydrosphere Bearing Test Time

Bearing Size	S/N	Accumulated Test Hours	Test Rig	Speed Range 1000 (revolutions per minute)	Load Range Thrust (pounds)	Load Range Radial (pounds)	Power Loss (watts)	Flow (parts per million)	Lubricant Supply Pressure (psig)	Lubricant Supply Temperature (degrees Fahrenheit)
3/4	1	20.5	F	6.5 to 43	0 to 21	0 to 5.3	2 to 345	10 to 32.5	50 to 122	70 to 165
3/4	18 to 2	22.5	M	5 to 40	0 to 61	0	6.5 to 567	3 to 9	60 to 160	64 to 580
3/4	11 to 1	6.2	M	5 to 40	0 to 52.5	0 to 17.5	3.8 to 303	2.2 to 7.5	30 to 93	78 to 130
3/4	15 to 2	26.2	M	10 to 40	0 to 85.7	0 to 8	7.8 to 398	1.5 to 7.1	51 to 182	62 to 356
3/4	17 to 2	3.7	M	35	0 to 69	0	92.4 to 276	2 to 4.5	30 to 146	78 to 426
3/4	16 to 1	5	M	5 to 40	0 to 19.4	0	5.9 to 331	1.6 to 3.3	3 to 36	72 to 294
3/4	20 to 4	4.3	M	10 to 40	0 to 79	0	14.2 to 507	5.4 to 15.2	13 to 115	66 to 218
3/8	2	69.5	F	4.2 to 44	1.7 to 10.3	0 to 5.5	N.D.	2.2 to 19.3	43 to 195	70 to 300
1/2	22 to 2	140.5	M	10 to 40	0 to 48.5	0 to 5	2.6 to 57	0.5 to 10.3	0 to 223	64 to 173
1/2	22a to 2	18.4	M	10 to 40	0 to 47	0 to 16	N.D.	0.5 to 6.7	70 to 238	74 to 146
1/2	4	61	F	10 to 40	0 to 25	0 to 5	N.D.	4 to 12	50 to 210	68 to 360
3/4	24 to 5	2.5	M	10 to 30	13 to 50	0	11 to 191	3 to 13	81 to 229	71 to 139
3/4	25 to 6	16.3	M	10 to 40	7 to 31	0 to 12.8	N.D.	1.3 to 12	72 to 148	90 to 177
1/2	5	1.5	F	10 to 34	0	0	10 to 70	10 to 12	120 to 167	76
1/2	6	7.9	F	10 to 35	0 to 6	0 to 4	N.D.	4 to 6	170 to 212	74
1/2	7	16.0	F	30 to 40	0 to 1	0 to 3	N.D.	4 to 8	133 to 190	74
1/2	9	134.2	F	10 to 40	0 to 22	0 to 7	71 to 160	3 to 7	80 to 208	70 to 270

N.D. - Not Determined M - Modified Bearing Test Rig F - Free Running Bearing Test Rig

TABLE 9

Summary - Endurance Tests

Bearing Size	S/N	Test Rig	Run Duration (hours)	Average Speed 1000 (revolutions per minute)	Average Load Thrust (pounds)	Average Load Radial (pounds)	Power Loss (watts)	Mercury Flow (pounds per minute)	Socket Inlet Pressure (psig)	Socket Inlet Temperature (degrees Fahrenheit)	Comments Reasons for Terminating Test Condition of Bearing, etc.
3/4	18 to 2	M	18 to 2	40	35	0	~ 95	~ 5	100	~ 115	Drive motor malfunctioned
3/8	2	F	64.5	30	7	5.3	~ 100	~ 17.5	90 to 170	75 to 340	Initially scored bearings (from previous test) - no change
1/2	4	F	29.5	40	5 to 20.7	2.8 to 3.6	~ 120	~ 11.5	51 to 185	70 to 360	Contamination in test system bearing scored
1/2	22 to 2	M	42	40	7 to 40	3.5 to 5	30 to 58	1.6 to 3.3	17 to 154	~ 95	Purpose of test accomplished no damage to bearing
1/2	22 to 2	M	66.5	40	31 to 40	5	~ 41 to 69	1.7 to 2.4	150 to 190	85 to 280	Drive motor malfunctioned Electrolized plating flaked
1/2	9	F	104	40	20	6 +	~ 150	6.0 to 8.0	80 to 200	~ 175	Purpose of test accomplished No damage to bearings

Notes: 1 M = Modified Bearing Test Rig (1 bearing)

F = Free Running Rig (2 bearings)

VI. TASK VI - GROUND TEST

This test will be the first power test of the complete APU. It is designed to test the APU insofar as possible under actual launch-site conditions.

The chronological outline of procedure as given in the previous quarterly progress report was reviewed, and Items 2 and 3 were changed as follows.

Item 2 - All of the components of the APU will be assembled to form a complete unit or "module". The welds are then checked, and the system leak-tested. The circulation of the biological shield mercury is stopped and the rate of heating of the biological shield mercury is measured. The APU module is then mated to the mock-up of the aft portion of the vehicle.

Item 3 - The mock-up is then lowered into the pit, instrument and working lines installed, and the pit covered.

An analysis was made to determine the addition shielding required for this test in the Martin Critical Facility. A five-foot thick pit cover of ordinary concrete or $2\frac{1}{2}$ feet of ferro-phosphorous concrete is required. Also, there will have to be additional concrete placed on the floor near the pit to keep the dose rates down to tolerance.

The first investigations of the gamma ray spectrograph showed that, using presently developed instruments and technology, the spectrograph could not be located inside the test pit due to the large gamma field present. It was decided to use conventional instrumentation and install it at the end of a 100-foot long columnating beam tube inserted through the critical facility pit. The spectroscope equipment and instrumentation have been specified, and all of the instrumentation except the grey-wedge analyzer has been purchased.

VII. TASK VII - SNAP-III

During this period the conceptual design of the unit was coordinated with Westinghouse, and subcontract arrangements were completed. It was decided that The Martin Company would be responsible for the design and fabrication of the isotope fuel element and electrically heated fuel element, over-all systems integration and testing, and vehicle integration. Westinghouse is to design the thermoelectric element, radiator, power converter, and the excess heat removal system.

A system specification was coordinated with the AEC and Westinghouse and was distributed as MND-P-1283. The outstanding characteristics of the unit are to be:

Power Output - 1 watt

Life - half-life of isotope

Volume - 75 cubic inches

Weight - 10 pounds

Voltage - as required

Heat Rejection - radiation only

Environment - ballistic missile and earth satellite

A. FUEL MATERIAL INVESTIGATION

This subtask was concerned with examining the requirements for the radioisotope fuel for SNAP-III and determining the availability of the best material. While SNAP-III will ultimately be used in space vehicles, the initially produced device is a demonstration model to prove the feasibility of coupling radioisotope heat and thermoelectric conversion materials.

The radioisotopes that were given serious consideration were Polonium-210, Cerium-144, and Curium-242.

Cerium-144 was felt to be unsuitable for the initial unit since the shielding required for a 100 thermal watt source would be unwieldy for a demonstration model. The problems of shielding an operational unit could not be completely analyzed until a specific application or mission were proposed.

Polonium does not form any solid compounds above several hundred degrees centigrade. It would, therefore, probably be unsuitable as a fuel material for an operational SNAP-III unit, due to launch abort hazards. However, its high specific activity, low gamma dose rate and ready availability make Po-210 appropriate for use in the demonstration model.

Considerable time and effort were expended in determining the potential utility and availability of Curium-242 as a radioisotope fuel material. Appendix A includes much of the available information concerning Curium-242 and Americium-241, its source material. It will be noted that Cm-242 has a very high specific activity (120 watts per gram), low gamma radiation, and can be formed into a stable refractory oxide. The disadvantages in the use of this material lie in the unknown status of its availability and the neutron flux from its spontaneous fissioning. However, for the small sources required for SNAP-III, biological neutron shielding can be provided by several inches of a hydrogenous material such as water or plastic. Thus, Curium-242, in the oxide state, would be a suitable fuel for both demonstration and operational units.

The availability of Curium-242 was investigated in two technological areas:

1. Availability of Am-241;

2. Facilities to separate the post irradiation transuranic elements from the fission products.

Visits to the various sites separating Am-241 indicated that this source material would be available in quantities required for SNAP-III. The Martin Company has formally requested the Aircraft Reactors Branch of the AEC to confirm this finding.

However, we have been unable to uncover any existing facility capable of handling the separation of fission products from the post irradiated americium and curium. This is due to the high level of fission product gamma dosage and alpha activity associated with even gram quantities of Cm-242. That such a facility is needed and that it will be built is acknowledged by all interested parties. This unanimity is due to the requirements of the already committed research program to obtain gram quantities of berkelium and californium.

The Chemical Technology Division at ORNL has made a proposal to the AEC to build the facilities and perform the processing necessary for the separation of these high transplutonic elements from large quantities of plutonium and fission products. This program is scheduled (if approved) to be completed in late 1961.

The chemical techniques for performing the desired separation have already been developed. In addition to the ion exchange method utilized at Livermore, solvent extraction techniques have been developed at Argonne National Laboratory for "isolation of individual lanthanides and actinides from their admixture with other members of their groups and for the group separation af actinides from lanthanides," using acid organo-phosphates. This latter process (or the two in combination) holds great promise in obtaining efficient low cost separation for the quantities required.

B. FUEL ELEMENT DEVELOPMENT

This program is aimed at the development of a coating or coatings on a molybdenum fuel container for high temperature oxidation protection of the molybdenum and electrical insulation from thermoelectric elements.

Previous studies of protective coatings on molybdenum have shown that a flame spray-furnace fused coating of Colmonoy No. 5 (79 Ni, 12 Cr, 4 Si,2 B) and an aluminum - chromium - silicon (20 Al, 46 Cr, 32 Si) coating of approximately 0.010 inch thick give excellent protection of molybdenum in an oxygen atmosphere and flowing air at 1832 degrees Fahrenheit (1000 degrees centigrade) for extended periods. However, as these coatings are metal alloys and cannot serve as electrical insulation coatings it is necessary to apply a two-layer coating for oxidation protection and electrical insulation. Therefore, a major part of the development in this period has been devoted to the application of oxide-based electrically insulative coatings on the oxidation resistant coatings.

The following requirements must be met by the oxide coating to be considered for this application:

1. Melting temperature greater than 1832 degrees Fahrenheit (1000 degrees centigrade);

2. Adequate bonding to base coating;

3. Retain bond over broad temperature range;

4. Non-reactive with base coating or with thermoelectric materials;

5. Capable of being applied as thin coating and machined to a close tolerance;

6. Maintain electrical insulating properties to 1832 degrees Fahrenheit (1000 degrees centigrade).

The oxide insulating coatings which were studied during this period were of three types:

1. Self coating technique; i.e., the oxidation protective coating was allowed to oxidize on the surface at elevated temperatures to form a protective oxide film;

2. Wet spraying and fusing of ceramic enamels;

3. Flame spraying of oxides.

Table 10 lists the coatings which have been studied.

TABLE 10

Oxide Based Insulating Coatings

Base Coat	Oxide Coat	Adherence	Electrical Resistance Room Temperature to 900 degrees Centigrade	
Self Coating Oxidized Surface				
Colmonoy No.4	Oxide of Ni-Cr-Fe-Si, B	Fair	*	--
Colmonoy No.5		Fair	*	--
Colmonoy No.6		Fair	*	--
Coast Metals No. 50	Oxide of Ni-Si-B-Fe	Good	High	Low
Coast Metals No. 52		Good	High	Low
Al + Cr-Si	Al_2O_3-Cr_2O_3-SiO_2	Fair	High	Low
Chromized	Cr_2O_3	Fair	*	--
Ceramic Enamel Type				
Colmonoy No.5	A-418 enamel**	Good	High	High
Colmonoy No.6	A-418 enamel**	Good	High	High
Al + Cr-Si	A-418 enamel**	Good	High	High
Coast Metals No. 50	A-418 enamel**	Good	High	High
Colmonoy No.5	A-418 + Cr_2O_3	Good	High	High
Colmonoy No.5	A-418 + Al_2O_3	Fair	High	High

TABLE 10(Cont'd)

Base Coat	Oxide Coat	Adherence	Electrical Resistance Room Temperature to 900 degrees Centigrade	
Flame Spray Oxides				
Colmonoy No.5	Metco Al_2O_3	Poor	--	--
Colmonoy No.5	$Al_2O_3 + Al(NO_3)_3$	Poor	*	--
Colmonoy No.5	Rokide Al_2O_3	Good	High	High

* Discontinuous coating which gave electrical insulation in localized areas.

** Enamel contains Cr_2O_3, Al_2O_3, SiO_2, ZnO_2, B_2O_3, etc. Enamel is soft at elevated temperatures.

The most promising coating of those listed in Table is aluminum oxide coating applied by the Rokide flame spray. This aluminum oxide is produced by heating the tip of a solid alumina rod to its fusion temperature in an oxy-acetylene flame and projecting the molten particles at a high velocity against a surface to which they will adhere and solidify.

The enamel type coatings containing excess alumina and chromia also appear to have favorable properties for this application. The A-418 enamel which has a high expansion coefficient to match stainless steel also bonds well to the Colmonoy coatings.

It is planned to continue the study of the Rokide alumina coatings and other oxide coatings that may be applied by the Rokide process, such as zirconium silicate and zirconium oxide and the A-418 enamel with Al_2O_3 and Cr_2O_3. Thermal conductivity and electrical resistivity of the coating will be determined, as well as other physical properties which may be required.

C. THERMOELECTRIC GENERATOR DESIGN

1. Thermal Design of Generator

In the initial design of the generator the thermoelectric material was to be indium arsenide and copper, operating at a hot junction of

700 degrees centigrade and a cold junction of 400 degrees centigrade. This yielded a theoretical over-all efficiency of approximately 1.1 per cent. An analysis of a generator employing the more efficient zinc antimonide-indium antimonide is presented in this section.

The following assumptions are employed in the generator design:

1. The hot junction temperature

   T_h = 450 degrees centigrade (723 degrees Kelvin);

2. The area available for radiation of heat at the cold junction is 50 square inches. (The remaining 50 square inches are for the excess heat dump.);

3. The effective parameters for the ZnSb leg are:

   $\bar{\alpha}$ = + 158 v per degree centigrade

   $\bar{\rho} = 2.1 \times 10^{-3}$ ohm-centimeter

   $\bar{k} = 2.5 \times 10^{-2}$ watts per centimeter degree centigrade

   These values were measured on a "good" pellet with a gradient of 400 to 32 degrees centigrade. The values are only weak functions of temperature and are assumed constant with temperature;

4. The parameters of InSb are given by Figs. 34 and 35. Table 11 summarizes data from these curves.

TABLE 11

Parameters of InSb

Temperature (degrees centigrade)	$\mu \alpha$ v Per Degree Centigrade	$\sigma = \frac{1}{e}$ ohm^{-1} Centimeter^{-1}	k Watts Per Centimeter Degrees Centigrade
150	- 220	0.68×10^{3}	0.125
200	- 205	1.00	0.113
300	- 170	1.54	0.096
400	- 147	2.0	0.086
500	- 126	2.36	0.080

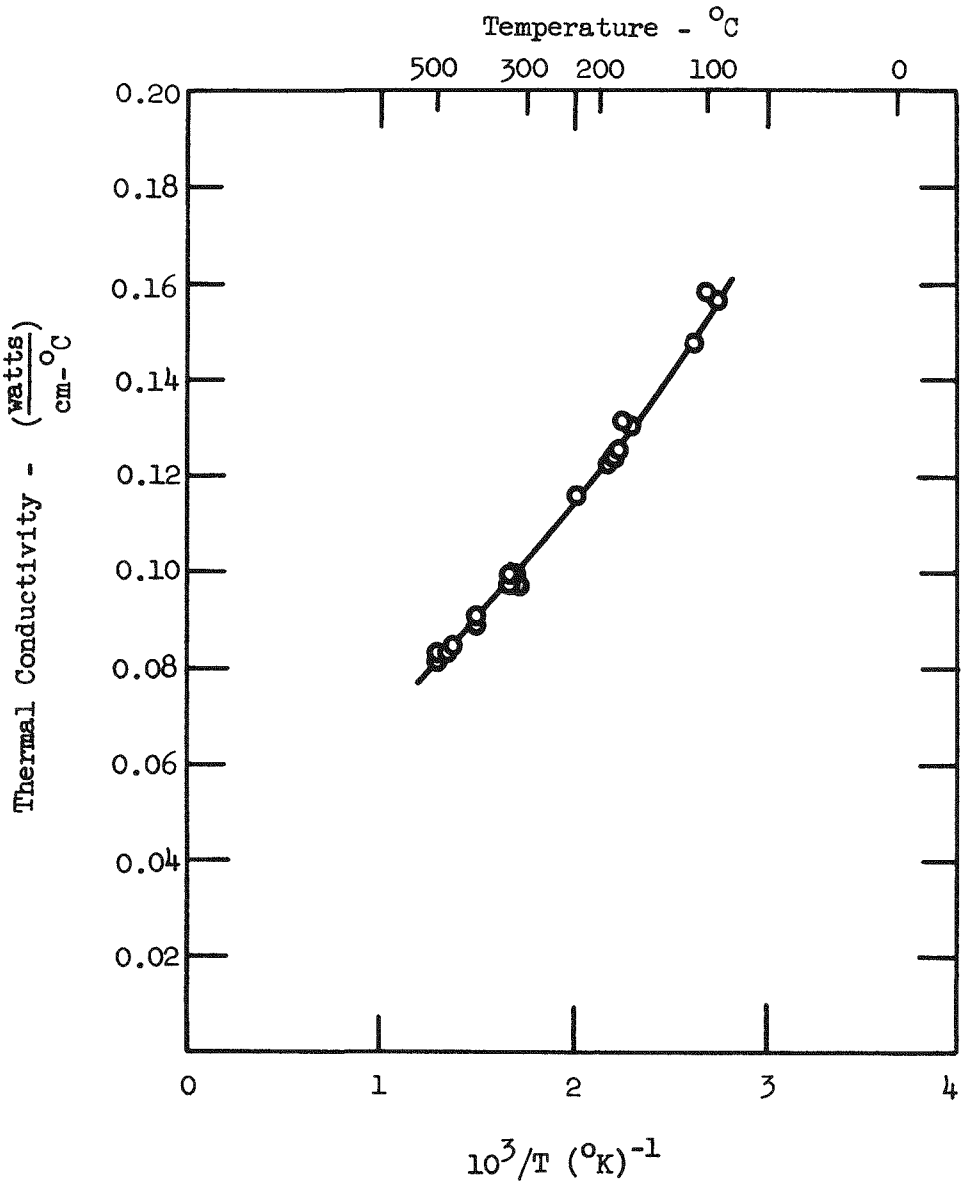

Fig. 34. Thermal Conductivity of InSb versus 1/T

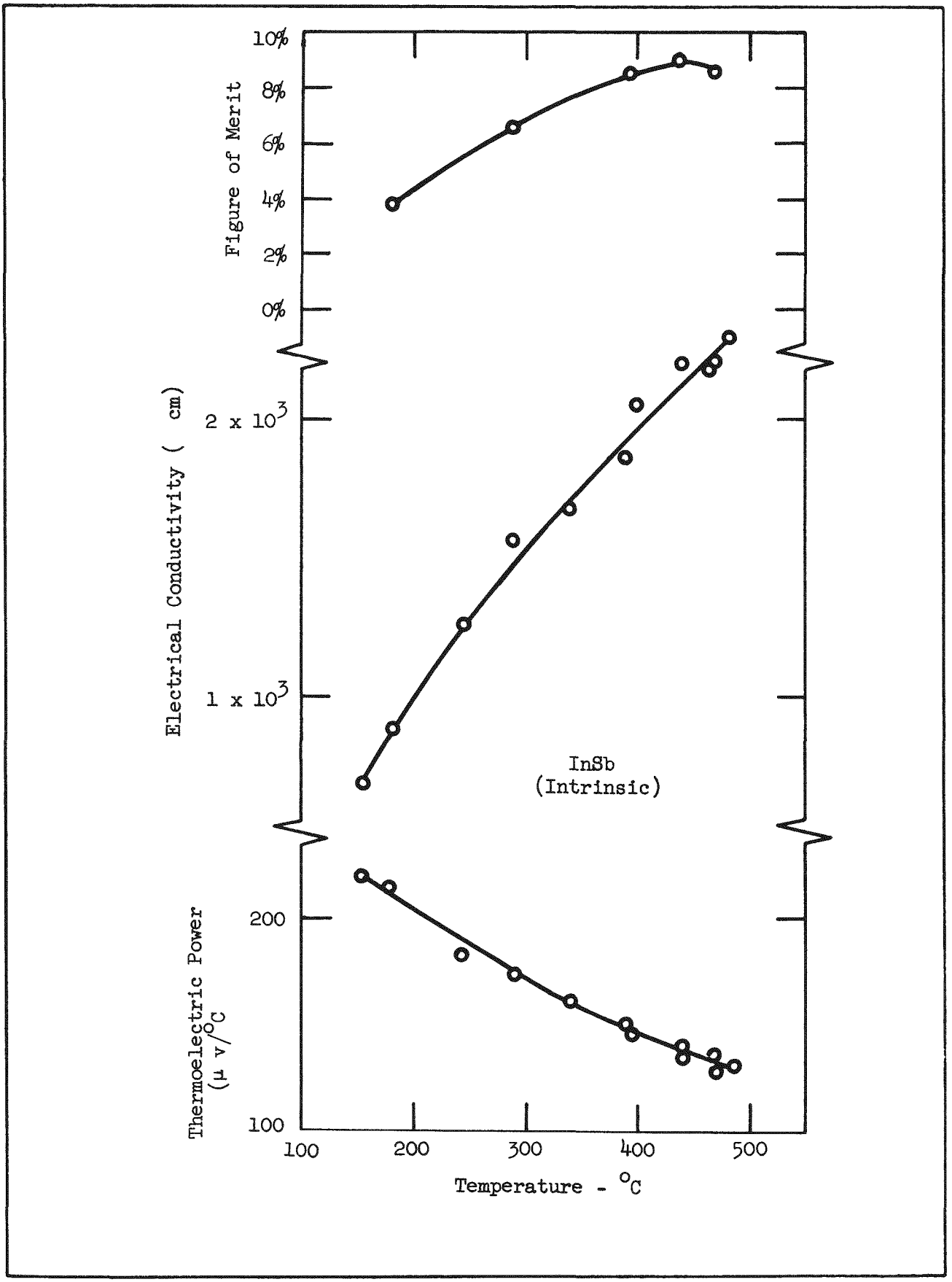

Fig. 35. Parameters of InSb

5. The emissivity of the radiating surface is 0.8. The procedure will be to calculate the effective figure of merit of a couple. This is given by

$$M_{eff} = \frac{T_h}{4} \frac{(\bar{\alpha}_1 - \bar{\alpha}_2)^2}{\left(\sqrt{\ell_1 \bar{k}_1} + \sqrt{\ell_2 \bar{k}_2}\right)^2}$$

where (1) = ZnSb and (2) = InSb. We have the (1) parameters already, but the (2) parameters must be calculated from the data of Table 17. We have

$$\bar{\alpha}_2 = \frac{1}{\Delta T} \int^{\Delta T} \alpha_2 (T) \, dT$$

$$\bar{\rho}_2 = \frac{1}{\Delta T} \int^{\Delta T} \rho_2 (T) \, dT$$

$$\bar{k}_2 = \frac{1}{\Delta T} \int^{\Delta T} k_2 (T) \, dT.$$

The interval ΔT is the interval between the cold junction temperature and T_h = 450 degrees centigrade. ΔT is taken in steps of 100, 200, and 300 degrees centigrade, that is, T_c = 350, 250, and 150 degrees centigrade.

Graphical integration of plots of these functions results in the data in Table 12.

The variations of parameters with temperature tend to compensate in the figure of merit so that the M_{eff} is not a strong function of temperature.

TABLE 12

Effective $\bar{\alpha}$, $\bar{\rho}$, $\bar{k}$ as a Function of ΔT Below 450 Degrees Centigrade

T	$\bar{\alpha}$ μ v Per Degree Centigrade	$\bar{\rho}$ ohm Centimeters (times 10^{-4})	$\bar{k}$ Watts Per Centimeter Degree Centigrade	M_{eff} (per cent)
100	147	4.98	0.0865	8.78
200	159	5.65	0.0912	8.7
200	173	6.63	0.0985	8.39

Calculating the thermocouple efficiency from the expression

$$\frac{1}{Tc} = 1 + \frac{1}{2M} + \sqrt{\frac{1}{2M}\left(-\frac{\Delta T}{T_h} + 2 + \frac{1}{2M}\right)}$$

Finally, the over-all efficiency ϵ in Table 13 calculated from $\epsilon = \epsilon_{Tc}\ \epsilon_c$ is tabulated, where $\epsilon_c = \frac{\Delta T}{T_h}$

TABLE 13

Over-All Efficiency ϵ

ΔT	$\epsilon_c = \frac{\Delta T}{T_h}$	$\bar{\epsilon}_{Tc}$ (per cent)	ϵ (per cent)
100	0.138	7.50	1.03
200	0.277	7.52	2.08
300	0.415	7.33	3.04

To calculate the generator fuel requirement for different load powers as a function of ΔT, in order to select the maximum ΔT, and hence, the best possible efficiency, is now desired.

A calculation for 1.5 watts in the load is given in Table 14. The inverter is assumed 75 per cent efficient requiring two watts at the generator terminals.

TABLE 14

Calculation for Two Watts of Generator Power

ΔT	Input = $\frac{\text{Two Watts}}{\epsilon}$	Watts Per Square Inch = $\frac{\text{Input}}{\text{50 Square inches}}$	ϵ (per cent)
100	194 watts	3.88	1.03
200	96.3	1.93	2.08
300	65.8	1.32	3.04

We have plotted in Fig. 36 the values of ϵ_c, ϵ, and watts per square inch as a function of ΔT (and, hence, T_c). The lower T_c, the more efficient the generator, but also, the smaller the radiated watts per square inch. The two-watt generator curve is shown to be below the radiation curve up to ΔT = 240 degrees centigrade or T_c = 210 degrees centigrade. To allow some margin, we would consider T_c = 250 degrees centigrade.

A calculation for 2.5 watts out of the generator yields a curve which never goes below the radiation curve; hence, this power cannot be generated with the 50-square-inch area restriction.

A calculation for 2.25 watts yields one point at T_c = 250 which just touches the radiation curve.

We conclude that the upper limit of power which can be generated within the assumptions of the exercise is

$$\frac{P_L}{2.25 \text{ watts}} \qquad \frac{P_Q \text{ input}}{108 \text{ watts}} \qquad \frac{\text{per cent}}{2.08}$$

Since we have not taken account of other thermal losses, the actual limit is probably closer to

$$\frac{P_L}{2 \text{ watts}} \qquad \frac{P_Q \text{ input}}{96.3 \text{ watts}} \qquad \frac{\text{per cent}}{2.08}$$

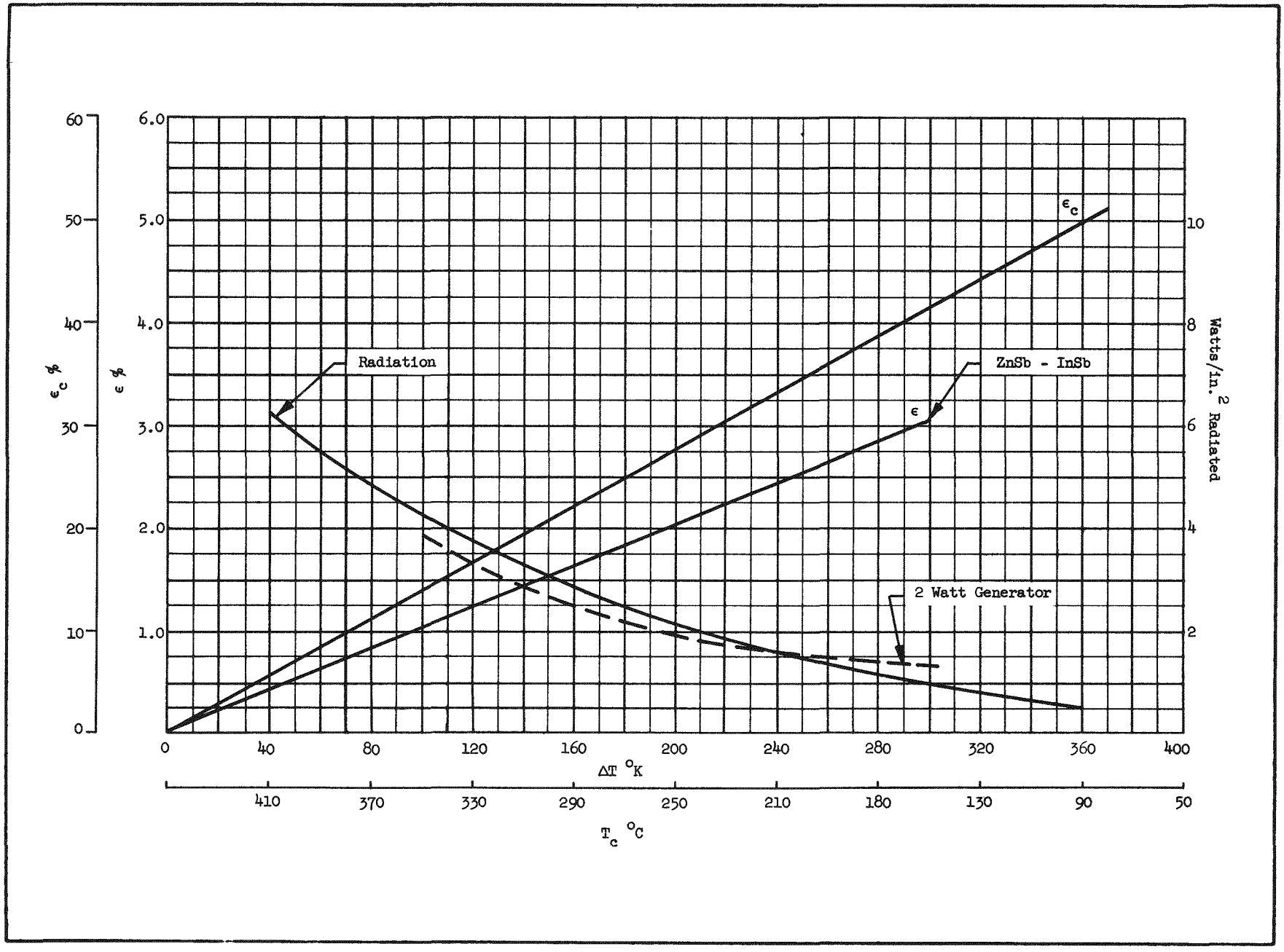

Fig. 36. Curve A SNAP III

D. JUNCTION CONTACT PROGRESS

Heat from the radioisotope source will be conducted to the thermoelectric hot junctions with a low temperature drop by means of a controlled close spacing (less than 0.001 inch). This gap will be filled with helium gas to aid in the heat transfer.

At the cold junction,heat must be transferred from the thermoelectric material to the radiator. Tests which have been run indicate that anodized aluminum or Martin Hardcoat surfaces held firmly together by a shrink fit provide a low resistance path for heat transfer between surfaces without electrical continuity between them.

The test pieces were made to simulate the heat transmitting junction between the cold end of a thermocouple element and the radiating outer shell of a generator. The test apparatus was set up so that the heat flow across the interface and 0.040 inch of aluminum could be measured. The measurements therefore indicate a temperature much greater than that across the very thin aluminum oxide interface. However, they do give a measure of the magnitude of the temperature difference which could be expected with this specific geometry. The following curve shows the measured temperature difference for various heat flow rates.

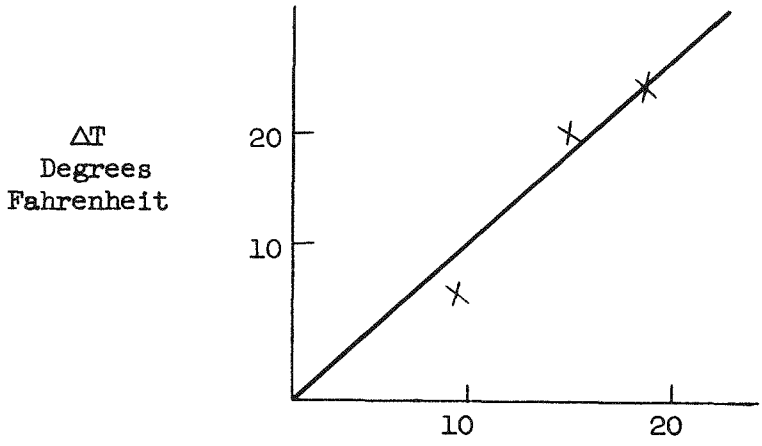

At the design condition the heat flow rate for each couple of the generator is about six watts, hence ΔT is about five degrees Fahrenheit. The tests which have been run also confirm the reliability of the anodized surfaces as an electrical insulator for this application. After a number of heating cycles, the electrical resistance between the pieces showed no adverse change.

E. THERMAL INSULATION

The design of this generator requires an embedment material which can be used to fill the interstices of the thermoelectric (T/E) elements, withstand the high temperatures, and have a low thermal conductivity to minimize heat leak around the T/E elements.

A sample quantity of fibrous potassium titanate has been obtained from DuPont. A thermal conductivity versus temperature curve is shown in Fig. 37.

An upper bound for the heat leak with this material can be estimated as follows:

$$Q_{\text{heat leak}} = - \frac{2 \pi k h \Delta T}{\ell n \frac{v_o}{v_i}}$$

Where we assume the configuration of two concentric cylinders with the

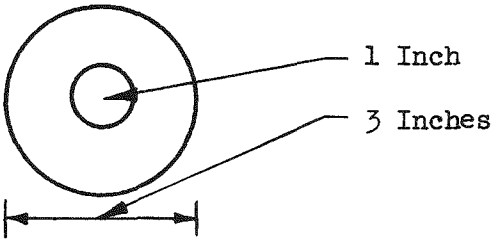

thermal insulation between the cylinders. The inner temperature is 700 degrees centigrade and the outer is 400 degrees centigrade set by the fuel and T/E system. We take

$k = 3 \times 10^{-4}$ watts per centimeter degree

v_o = outer radius 1.5 inches

v_i = inner radius 0.5 inch

$\ell n\ v_o/v_i = \ell n\ 3 = 1.1$

h = 10 inches; the height of the generator

$$Q_{\text{heat leak}} = \frac{2 \times 3.14 \times 3 \times 10^{-4} \times 10 \times 2.54 \times 300}{1.1}$$

= 13 watts.

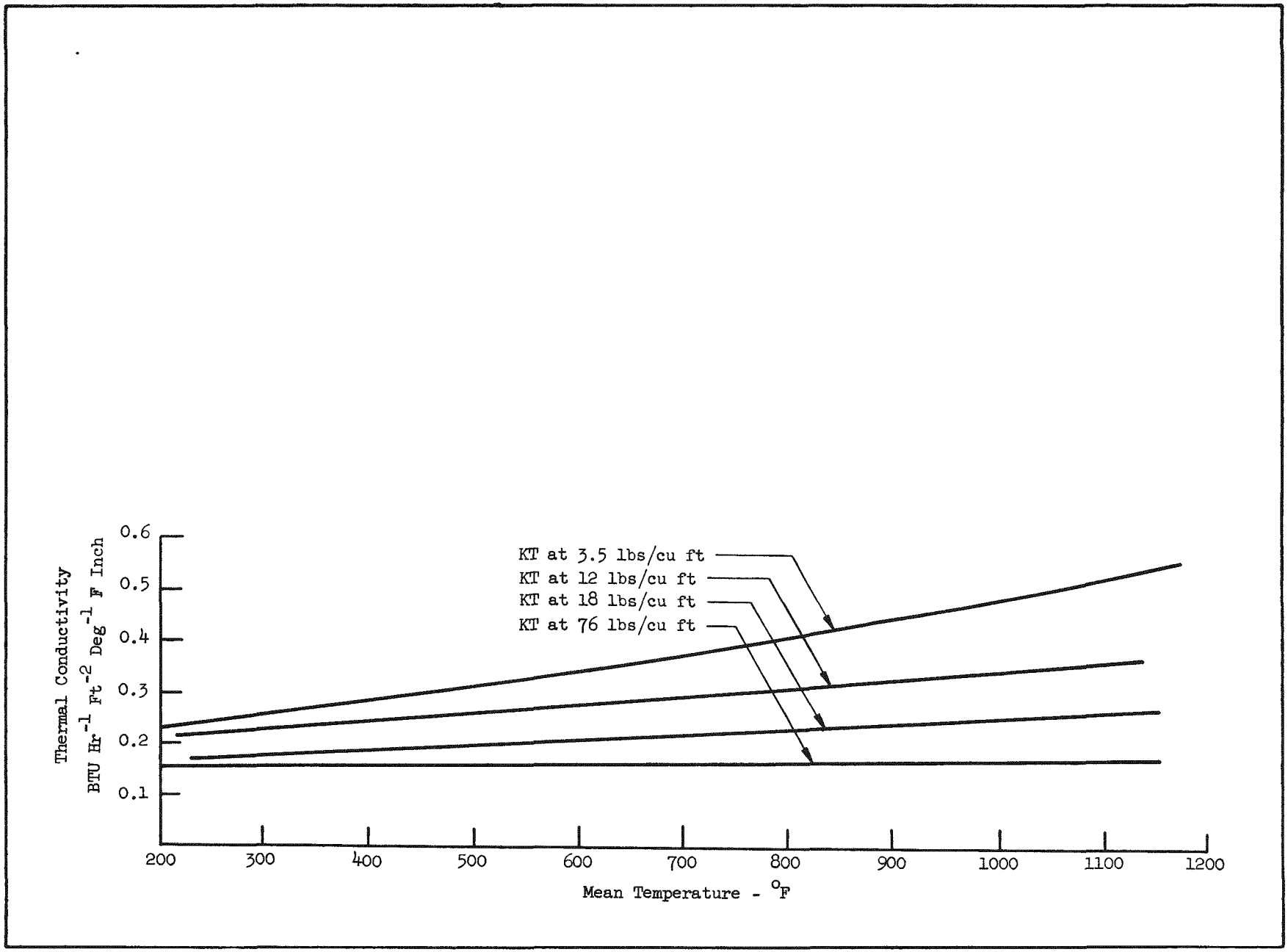

Fig. 37. Thermal Conductivity versus Temperature

But only half of the radiating area is used for the T/E system, hence the heat leak is 6.5 watts. The total T/E source power is 300 watts, or the heat leak is two per cent of the total power. If this can actually be attained in the practical generator, it will be quite satisfactory.

Fabrication experiments and test work on this material have been initiated.

APPENDIX A

INFORMATION PERTAINING TO THE USE OF CURIUM-242 FOR PRODUCING HEAT

Curium-242 is an artificially produced transplutonium element. It is made by neutron irradiation of Americium-241, which results from the beta decay of Plutonium-241. The reactions involved are:

$$Pu^{241} \xrightarrow[14\ yr.]{\beta} Am^{241}(n,\gamma)\ Am^{242} \xrightarrow[16\ hr.]{\beta} Cm^{242} \xrightarrow[163\ days]{\alpha} Pu^{238}$$

Plutonium-241 is formed and recovered along with Plutonium-239 when Uranium-238 is irradiated. The formation of transplutonium elements is illustrated in Fig. A-1.

Since the amount of Cm^{242} which can be produced depends primarily upon the supply of Am^{241}, it was necessary to determine the sources of americium. Some americium and curium are present in the wastes when plutonium is first recovered. The most abundant source would be from reprocessing plutonium which has been allowed to decay for several years. Future sources of these transplutonium elements will be from power breeder reactors and plutonium fueled power reactors. It is assumed that burn-ups in these reactors will be much greater than are allowable in the production reactors at Hanford and Savannah River.

Nuclear data pertaining to production of Cm^{242} from Am^{241}:

During the irradiation of Am^{241}, several processes compete for the Cm^{242} as it is formed. A breakdown of these processes is as follows:

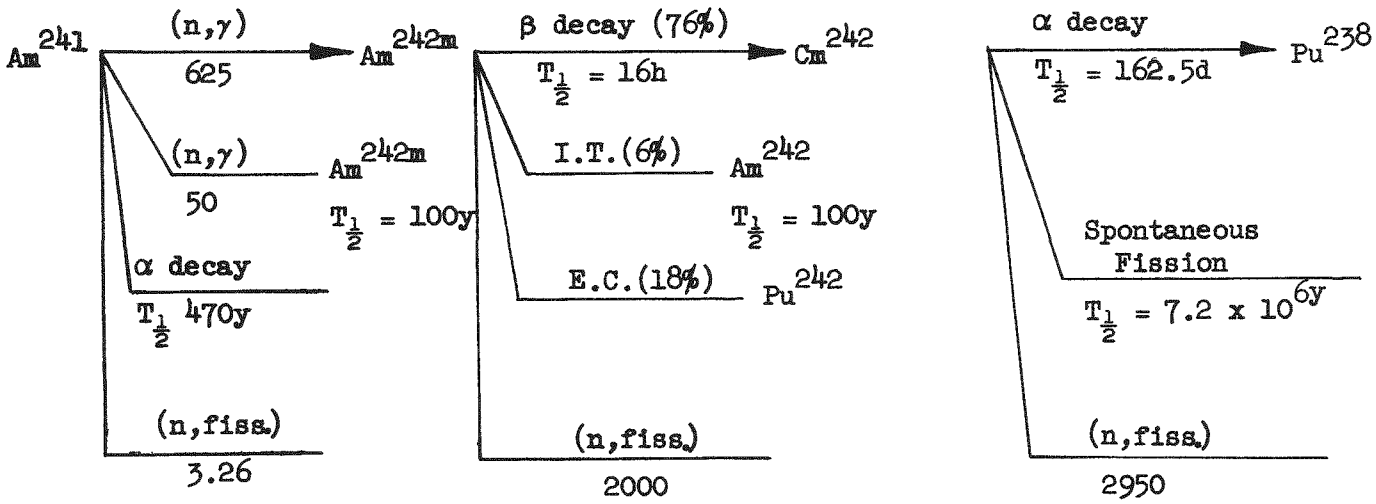

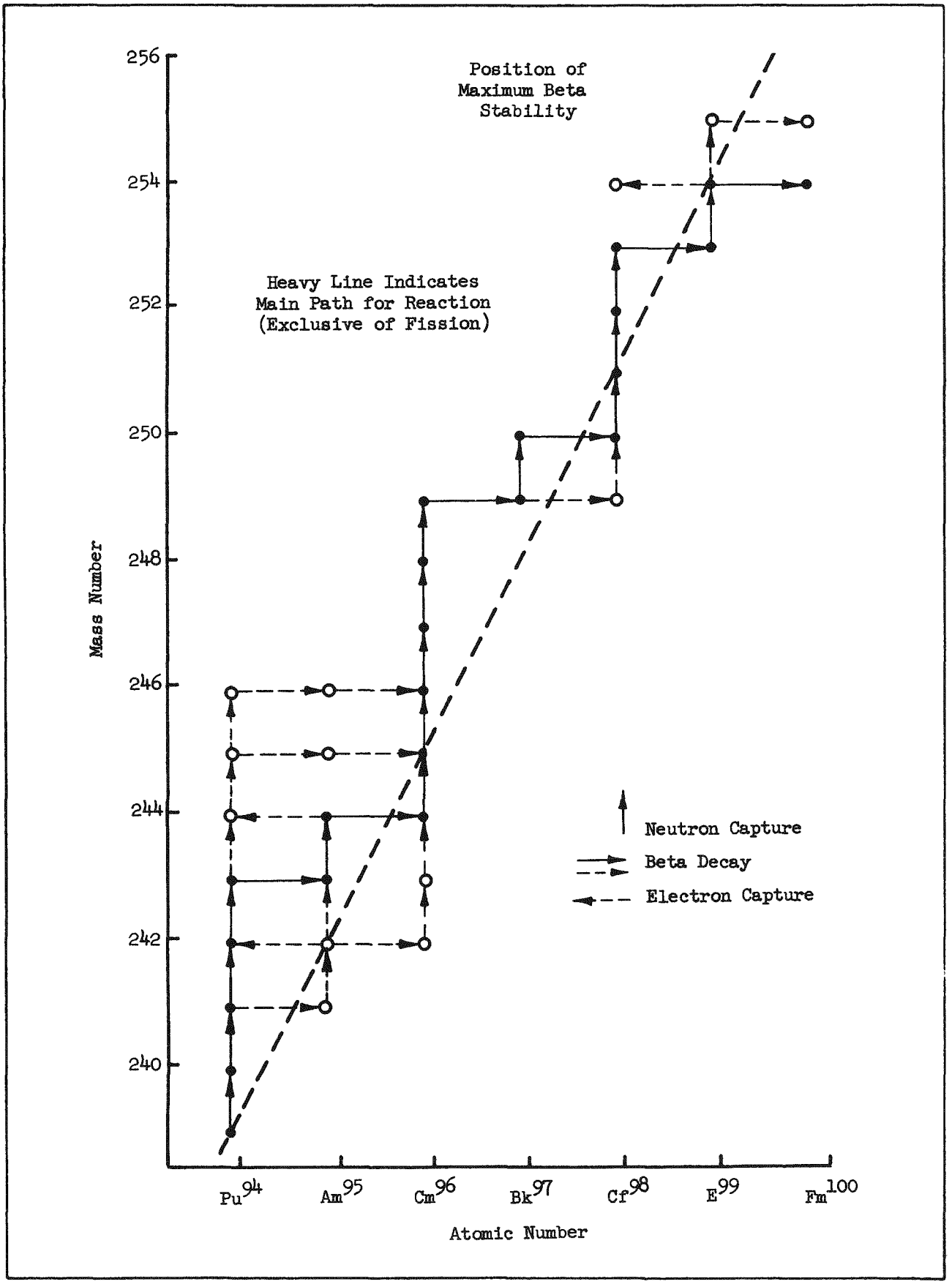

Fig. A-1. Formation of Transplutonium Elements

The cross-sections and half-lives shown under the lines indicating the reactions taking place were obtained from BNL-325 and the new nuclear data section of Nuclear Science Abstracts.

More than half of the Am^{241} is consumed during irradiation to obtain a good yield of Cm^{242}. Consequently, calculations pertaining to the formation of Cm^{242} must include this burn-up of the target material. If A is allowed to represent the amount of Am present at any time during irradiation, the rate of change in the amount is expressed by:

$$\frac{dA}{dt} = - \lambda_A A - \sigma_a \Phi A \qquad (1)$$

where λ_A = decay constant of Am^{241} (sec^{-1}) this is negligible when compared with $\sigma_a \Phi$

σ_a = total absorption cross section of Am^{241} = 678 barns

Φ = thermal neutron flux neutron cm^{-2} sec^{-1}

A_o = amount of Am^{241} at start

This equation readily yields the following solution:

$$A = A_o e^{- \lambda^*_A t} \qquad (2)$$

$$\lambda^*_A = \lambda_A + \sigma_a \Phi$$

t = time of irradiation-second

If B represents the amount of $Am^{242\ m}$ which decays into Cm^{242}, the amount present at any time during irradiation is found by solving the equation

$$\frac{dB}{dt} = \sigma_A \Phi A - \lambda_B B - \sigma_B \Phi B - .24\ \sigma_A \Phi A \qquad (3)$$

σ_A = 625 barns (cross section for producing $Am^{242\ m}$)

λ_B = 1.2034×10^5 sec^{-1} (decay constant for $Am^{242\ m}$)

σ_B = 2000 barns (absorption cross section for $Am^{242\ m}$)

The first term on the right is the amount produced, the second is the amount lost by decay to Cm^{242}, the third is the amount lost by neutron capture, and the last term represents the amount of $Am^{242\ m}$ which is lost through isomeric transformation and electron capture.

Equation (3) is readily solved to give:

$$B = \frac{.76\ \sigma_A \Phi A_o}{\lambda^*_A - \lambda^*_B} \left(e^{-\lambda^*_A t} - e^{-\lambda^*_B t} \right) \qquad \lambda^*_B = \lambda_B + \sigma_B \Phi \tag{4}$$

If C is allowed to represent the amount of Cm^{242} present at any time during irradiation, the rate of change in the amount present is given by:

$$\frac{dC}{dt} = \lambda_B B - \sigma_c \Phi C - \lambda_c C \tag{5}$$

σ_c = 2950 barns (absorption cross section of Cm^{242}).

$\lambda_c = 4.922 \times 10^{-8}$ sec^{-1} (decay constant for Cm^{242}).

The solution of Equation 5 is found to be:

$$C = \frac{.76\ \lambda_B\ \sigma_A \Phi A_o}{\lambda^*_A - \lambda^*_B} \left[\frac{e^{-\lambda^*_A t} - e^{-\lambda^*_c t}}{\lambda^*_A - \lambda^*_c} - \frac{e^{-\lambda^*_B t} - e^{-\lambda^*_c t}}{\lambda^*_B - \lambda^*_c} \right] \tag{6}$$

$$\lambda^*_c = \lambda_c + \sigma_c \Phi$$

The decay schemes of Am^{242m} and Cm^{242} are:

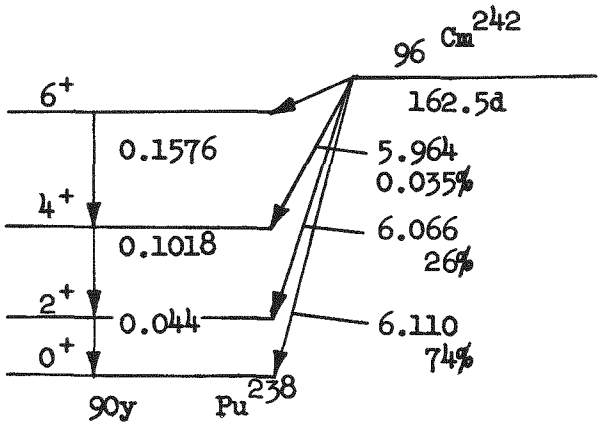

Decay Scheme Cm^{242}
(Ref. 1)

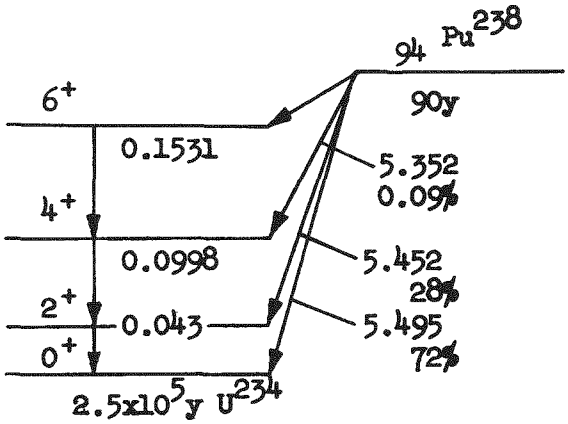

Decay Scheme Pu^{238}
(Ref. 1)

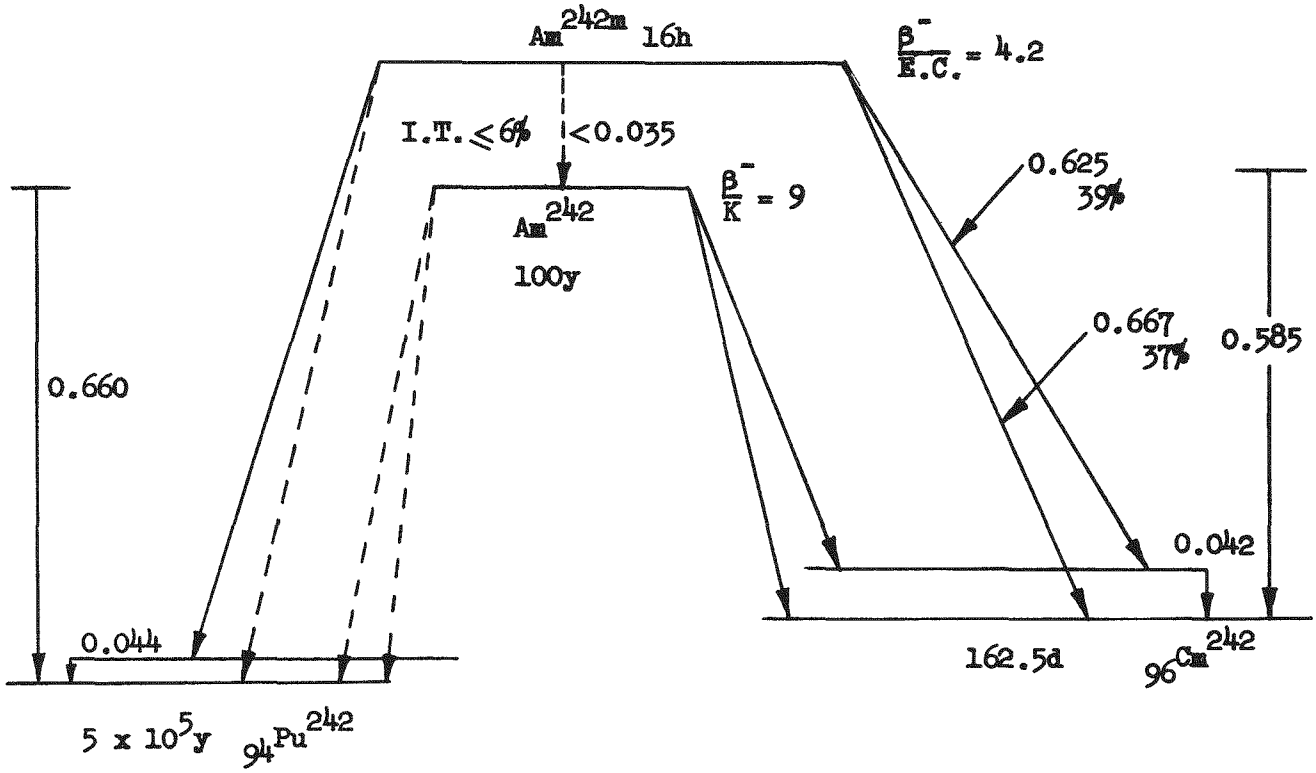

Decay Scheme of Am^{242} (Ref. 2)

Alpha Emission

Specific power	120 watts per gram	
Specific activity	3.33×10^3 curies per gram	
	27.75 curies per watt	

Gamma emission associated with alpha emission is negligible.

Neutron Emission

Half life for spontaneous fission	7.2×10^6 years	(Ref. 3)
Average number of neutrons from spontaneous fission	2.65 ± 0.09	(Ref. 4)
Neutrons per second per gram from fission	1.97×10^7	
Neutrons from (α,n) reaction (about equal to neutrons from spontaneous fission)	1.97×10^7	(Ref. 5)
Total neutrons per gram	3.94×10^7	
Average kinetic energy of fission fragments per fission	184.9 Mev.	(Ref. 6)
Specific power from spontaneous fission - based upon the kinetic energy of the fission fragments only. The energy from prompt fission gammas, beta particles and gammas from fission products amounts to less than 10 per cent of energy available in U-235 fission. These quantities were not included since the power from spontaneous fission is negligible in comparison with power from alpha emission.	2.25×10^{-4} watts per gram	

Shielding Requirements:

The radiations resulting from alpha decay do not constitute a shielding problem. The self-absorption of the heat source is sufficient to reduce the radiations way below accepted radiation levels.

The radiations resulting from spontaneous fissioning, however, present a minor potential hazard. For a power level of 100 watts, preliminary calculations indicate that two to four inches of water will be required to reduce the fast neutron dose rate to a level which would allow a person to work continuously in the vicinity of the heat source. No shielding would be required to protect equipment located near the source.

The dose rate from gamma radiation, at three feet from the source, due to spontaneous fissioning has been calculated to be 0.0133 milliroentgen per hour per watt.

Fission products resulting from spontaneous fission are roughly the same as for thermal neutron induced fission in U-235, (Refs. 7, 8). Due to the low wattage resulting from spontaneous fissioning, many thousand hours of operation would be required to build up fission products to the point where it would be necessary to account for them in shielding calculations.

For similar reasons, capture gamma rays and activation gamma rays may be neglected during the early stages of assembly and operation of the heat source.

The effect of spontaneous fissioning on initiation of a rapid chain reaction has not been examined. It is not expected to present a problem, but this aspect should be investigated thoroughly.

Chemistry of Americium and Curium:

Americium and curium are members of the actinide series (5f, inner transition) of elements. Americium and curium occupy positions in the actinide series analogous to europium and gadolinium, respectively, in the lanthanide (4f) series. Strict application of the analogy between the 4f and 5f elements is primarily useful in comparison of properties of the (III) oxidation states, and is an uncertain guide for prediction of valance state stability. The (II) and (III) states of europium are well known but there is no reliable evidence for ionic compounds containing Am(II); and the existence of Am(III), Am(IV) Am(V), and Am(VI) has been established. Gadolinium has the III oxidation state only, and although Cm III is the only valance state known in aqueous solution, there is positive evidence for Cm(IV) in the oxide. (Ref. 9).

Oxidation states Am II, Am IV and CmIV exist as subnormal oxidation states. The subnormal states are characterized by the presence of non-bonding 6d electrons and cannot exist in solutions. The corresponding compounds are apt to show pronounced metallic character. (Ref. 10).

An excellent separation of curium from americium may be achieved by oxidation of the Am(III) to Am(VI) in acid solution by $S_2O_8^{--}$ and precipitation of the unoxidized Cm(III) by F^-.

Chemical Compounds (Ref. 10)

Oxides

The hydroxides of these elements tend to precipitate in a gelatinous form. The dried hydroxide or oxalate is frequently used as the starting material for the preparation of other compounds. Most compounds of these elements when heated to over 500 degrees centigrade in air, containing moisture, will hydrolize or decompose to the oxide. The formulae for the normal oxides are Am O_2 (black) and Cm_2O_3 (white).

Am_2O_3 may be prepared by gentle decomposition of the oxalate in a vacuum. Americium sesqui-oxide (Am_2O_3) is easily re-oxidized to AmO_2 when it comes in contact with air. Curium sesqui-oxide may be oxidized to a compound that is very close in composition to CmO_2 by heating gently in ozone or oxygen.

Fluorides:

The fluorides may be obtained by the action of gaseous hydrogen fluoride on the oxalate, dried hydroxide, or oxide at approximately 500 degrees centigrade. If a reducing agent such as hydrogen is present, the product will frequently be a fluoride of lower oxidation state if such exists; if oxygen is present a higher fluoride may be obtained.

The trifluorides and tetrafluorides of these elements are non-hygroscopic, high melting solids. The pink fluoride AmF_3 is formed by the action of hydrogen fluoride on the oxide at 500 degrees centigrade. The trifluoride is converted to AmF_4 by use of a fluorinating agent such as free fluorine or cobaltic trifluoride.

The trifluorides have low solubilities (Ref. 11).

Chlorides:

The oxides or oxalates of these elements react with carbon tetrachloride vapor at elevated temperatures to form the chlorides. Trichlorides are formed from AmO_2, Am_2O_3 and Cm_2O_3. The chlorides of americium are pink; those of curium are white. The tri-chlorides sublime at 700 to 800 degrees centigrade, the tetrachlorides at 400 to 500 degrees centigrade and the higher chlorides may be volatile at 200 degrees centigrade.

The trichlorides and tetrachlorides may be partially hydrolized by the action of water vapor at low concentrations. CmOCl is formed from the trichloride.

All the chlorides and oxychlorides are hygroscopic to varying degrees. On exposure to moist air they form various chloride hydrates which decompose to the oxides when heated.

Bromides and Iodides:

The oxides react with aluminum bromide and iodide to form these halides. The tribromide and trioxide are formed from the oxide. The tribromides and triiodides volatilize at 700 to 800 degrees centigrade, the tetra bromides distill at 400 to 500 degrees centigrade.

Sulfides:

When the oxides are heated to high temperatures in a stream of hydrogen sulfide containing carbon disulfide vapors, various sulfides and crysulfides are found. Americium oxide yields the sesquisulfide by this procedure at 1200 to 1400 degrees centigrade.

Miscellaneous Compounds:

Reference 2 does not give specific Am and Cm compounds of the following types but reports componds for other heavy elements. Am and Cm compounds could probably be produced by similar techniques.

Carbides:

The oxides of these elements react with carbon at temperatures above 2500 degrees centigrade to form carbides. These preparations are made by heating the oxide in a graphite crucible in a hydrogen atmosphere. Carbides also result when metal preparations are carried out in graphite crucibles.

Nitrides:

Neptunium nitride was prepared by the reaction of neptunium hydride with ammonia gas.

Silicide:

The silicide may be formed by the reaction of calcium silicide or silicon metal on the oxide or fluorides of these elements. The compounds Pu Si_2 and Np Si_2 have been identified.

Metals:

The metals are prepared by the reaction of barium vapor with the tri- or tetrafluoride at 1200 to 1400 degrees centigrade in a vacuum.

Properties of Americium Metal:

The metal is malleable and silver gray in color. It is indexed as double hexagonal close packed, a = 3.642 $\pm$ 0.0005 A, c = 11.76 $\pm$ 0.01 A, with an atomic radius of 1.82 A. The experimentally determined density is 11.7 $\pm$ 0.3 grams per cubic centimeter and the density calculated from x-ray crystallography is 11.87 $\pm$ 0.05 grams per cubic centimeter. The melting point is uncertain, the metal begins to soften at about 850 degrees centigrade with incomplete melting at 1200 degrees centigrade. The vapor pressure in this range of temperatures is given by:

$$\log p = 7.563 - \frac{13,162}{T}$$

If a value of Cp of vaporation of -2 cal mol^{-1} deg^{-1} is assumed, the following equation is obtained,

$$\log p = 11.092 - \frac{13,700}{T} - \log T$$

The free energy of vaporization is then given by:

$$\Delta F = 62,690 - 50.76T - 2.303\ (-2)\ T \log T$$

Other reported thermodynamic quantities are:

$$\Delta H_{1273} = 60.2 \text{ k cal-mol}^{-1}$$

$$T_B = 2880^{\circ}K$$

$$\Delta H_{2880} = 57 \text{ k cal mol}^{-1}$$

$$\Delta S_{2880} = 20 \text{ cal mol}^{-1} \text{ deg}^{-1}$$

Properties of Curium Metal:

The metal is silvery and resembles plutonium metal in its malleability.

The density is reported as seven grams per cubic centimeter.

Toxicology of Curium and Americium:

These elements are among the most toxic materials known (Ref. 12). They are deposited in the bone material, probably in the blood vessel channels, as contrasted with plutonium which is deposited on the surface of the bone (Ref. 13). Experimental work on rats indicated "the tolerance values for Am should be essentially the same as those for plutonium". (Ref. 14).

PERMISSIBLE CONCENTRATIONS

	AIR		WATER		
	Am^{241}	Cm^{242}	Am^{241}	Cm^{242}	Ref.
Occupational or restricted area	8×10^{-11}	5×10^{-10}	4×10^{-4}	2.7×10^{-3}	15
Civilian or non-restricted areas	3×10^{-12}	1.8×10^{-11}	1.3×10^{-5}	1×10^{-4}	15

All values are microcuries per milliliter.

Total Body Burden (Microcuries)	Am^{241}	0.056	Ref. 16
	Cm^{242}	0.05	

REFERENCES

1. Asaro,F.,and I. Perlman, Phys. Rev., 94, 381 (1954).

2. Hoff,R. W. et.al., Phys. Review, 100, 1403 (1955).

3. Hollander, J. M.,I. Perlman, and G. T. Seaborg, Rev. Mod. Phys. 25, 469 (1953).

4. Hick, Ise, and Pyle, Phys. Rev. 101, 1016, (1956).

5. Personal Communication: W. T. Crane, Univ. Cal. Rad. Lab.

6. Leachman, R. B., Phys. Rev. 101, 1009, (1956).

7. Steinberg, E. P., and L. E. Glendenin, Phys, Rev. 95, 431 (1954).

8. Cuninghame, J. G., J. Inorg. and Nuclear Chem., 4, No. 1, 1 (1957).

9. Penneman R. A., and L. B. Asprey; "A Review of Americium and Curium Chemistry" Geneva Conference Papers Vol. VII, p. 355 (No. P/838).

10. Fried, Sherman and Zachariasen, W. H.; "The Chemistry and Crystal Chemistry of Heavy Element Compounds." Geneva Conference Papers Vol. VII, p. 235 (No. P/730).

11. UCRL-2547, Feay, D. C. "Some Chemical Properties of Curium (1954).

12. ANL-5584, Therapy of Radioelement Poisoning

13. RL-28.5.135, Summary of the Research Progress Meeting.

14. LA-1309, W. Langham, et.al; "The Relative Physiological and Toxicological Properties of Americium and Plutonium."

15. Federal Register, Vol. 22, No. 19, Jan. 29, 1957 p. 553.

16. National Bureau Standards Handbook 52, p. 16